An Intrepid Tour of the Complex Fractal World
using Dark Heart Package 2.17 for Mac

Updates and **downloads** at: http://dhushara.com/DarkHeart/ under the GPL

Chris King

Contents

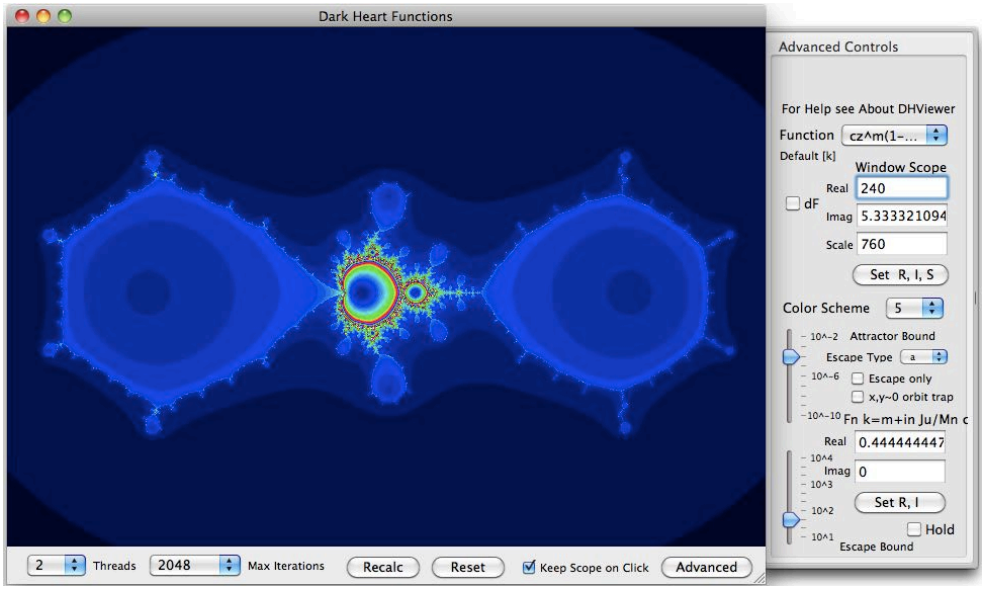

Fig 1: Parameter plane of the Function $f(z) = cz^4(1-z)^5$

Introduction

The Dark Heart Viewer Package contains two key complex function fractal viewers, **Dark Heart** and **Riemann Zeta**, which are both a pleasure to explore and are also professional research tools for exploring virtually every conceivable complex function in the universe, along with their fractal dynamics.

At first sight, it shows you a portrait of a function that is to be explored in 4-D colour and when you click the screen switches to a Mandelbrot parameter plane view. You can then scale this by dragging rectangles to explore ever-diminishing parts of the fractal and click again to see the Julia set of the point chosen. Clicking again will switch between these two views and reset will take you back to the function. But the real interest begins when you select advanced controls and a drawer pane opens which expands the application into a research tool which can be used to investigate a vast variety of polynomial, rational and transcendental functions leading all the way to Riemann's famous zeta function and the full spread of esoteric zeta and L-function at the cutting edge of mathematical research in the Riemann Zeta Viewer.

There are several colour schemes which are designed not just to be beautiful to watch, but to provide focused research investigations, by highlighting by colour specific periodicities, distinct attractors, irrational flows and other features key to investigating particular examples. The packages also provide saving and loading of images and parameters so an exploration can be recreated exactly and a suite of application scripts which enable the generation of movie image sequences for any process the mind can imagine. The help menu documentation enables you to check all the details of operation easily while using the app.

An Intrepid Tour of the Complex Fractal World

The easiest way to show what the package can do is to show you how it can represent key features of complex fractal dynamics in both a visually exciting and mathematically significant way. So let's go back for a minute to where this all began.

In the early 20th century Julia and Fatou investigated the complex sets that arise when a function, say $f(z) = z^2 + c$, is iterated over and over again $z \to z^2 + c \to \left(z^2 + c\right)^2 + c$ for some fixed number c. For large z the points would expand to infinity. For small z, they seemed to settle into an attracting pattern, but what happened in between? What about the points that couldn't decide which way to go? Julia realized that the critical point, where the slope of the function is zero, was pivotal in determining the form of the Julia set, which he also recognized was a type of self-similar fractal like the Koch flake.

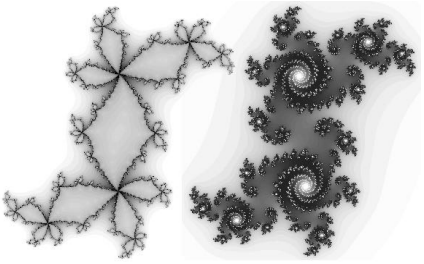

It was only when computer graphics came along, that we began to appreciate that, on the boundary was a chaotic set - the Julia set - which had a variety of fractal forms, on which the dynamics was wildly unstable. The left-hand Julia set J_c shown here is the boundary between the points on the outside heading to infinity and those on the inside together forming the set of ordered basins of attraction, in this case heading into an attracting period 4 pattern of four periodic points, both regimes of the rule of order forming the Fatou set. The dark boundary is where chaos rules! The one on the right where, we can see the top and bottom halves are disconnected and so on ad-infinitum, so the whole set is completely disconnected Cantor dust.

Chaos has three manifestations: (1) the *butterfly catastrophe* - arbitrarily close points iterate exponentially away from each other - making the process unstable and computationally unpredictable, like weather can be, (2) dense collections of repelling periodic points, and (3) *topological transitivity* - every small pair of open sets getting mixed so one iterates over the other.

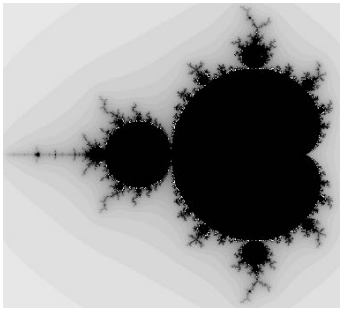

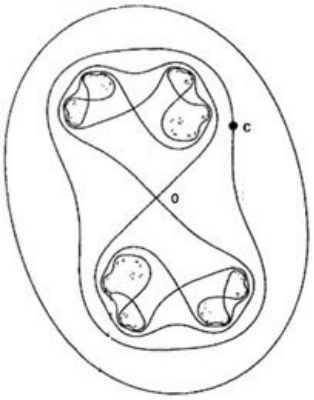

A deep and puzzling question then arose, which proved to have a stunning answer. Some of these sets were topologically connected, as is the one on the left, but others were fractal dust, sometimes in complicated swirls, as the one on the right. This question looks at first sight impossible to solve for such a fractal set. Mandelbrot used Julia's insight about critical points to investigate c values where the Julia set is connected, using the critical point, where the function was neither shrinking nor growing - as on on a mountain top or in the bottom of a lake in topography, in this case $z = 0$. The idea is that these are the last points to escape to infinity, so if they don't escape, the Julia set must have encircled them. So instead of applying the above iteration to all z for a fixed c, we start with the critical point and apply the iteration to each c in turn $0 \to 0^2 + c \to c^2 + c \to (c^2 + c)^2 + c$. Mandelbrot, working at IBM, decided to make an atlas of the *c* values of all the connected Julia sets, and discovered the Mandelbrot parameter plane M - the set of *c* where J_c is connected, is also a fractal, through which we can graphically compute the answer to the topological chaos of J_c. Furthermore this atlas is universal to all quadratic functions since any quadratic iteration can be shown by scaling and translation to be conjugate to that of $f(z) = z^2 + c$. M is sometimes called the most complex mathematical object in existence, because its dynamics are not simply self-similar, but vary so that they represent in one fractal, the dynamics of all quadratic Julia sets.

We can prove this connection in the following way. For very large z values, z^2 dominates *c* and maps a large circle onto an even larger one. Take a great circle big enough that z^2 dominates, so that all the points are escaping to the super-attracting fixed point at infinity and step it backwards. Instead of squaring, we are now taking two square roots, so we either get a circle winding twice around itself, a figure 8, or two separate circles, just as we see in the boundaries of level sets using Dark Heart. However, if we reach a figure 8, we have a double root, which is also the critical point $z = \pm 0$ since a double root is also critical and $f(0)=c$ so *c* lies on the image of the figure 8 i.e. the first image circle escaping to infinity, so The Julia set is disconnected and we are outside M. The inverse images of each figure 8 will now be a pair of figure 8s, with graduated pairs of circles between, resulting in an infinite disconnection so the Julia set is totally disconnected fractal dust forming a Cantor set. If there are topological circles all the way down and there is no figure 8, we never reach the circle containing *c* so it is captured inside a connected Julia set and *c* is in M. M itself can also be

shown to be connected by considering the fact that its own level sets are all topological circles, because it contains precisely the *c*-values where the Julia level sets are all circles.

We can also see why the Mandelbrot set has dendrites. One-dimensional real number quadratic iterations can also have chaotic dynamics. These *c* values result in connected Julia sets lying along the *x*-axis corresponding to points on the period 2 dendrite, where the critical point iterates to chaos, or lands on repelling periodicities on the Julia set itself, which, although still connected, now has no internal basins (5, 18 in fig 3). The same situation pertains for every periodicity around M, resulting in a principal dendrite for each period bulb. Once we exit the bulbs and enter the dendrites, these periods become repelling and the critical point may become eventually periodic to a repelling periodic orbit at the tips and branching points of each dendrite, called Misiurewicz points. We can solve for these, e.g. for $M_{2,1}$, we have $(c^2+c)^2+c=c^2+c$, giving c = 0 and -2 at the tip of the period 2 dendrite.

Inside each period-n bulb, we have attracting periodicities. There is a central super-attracting point, where $f_c^{(n)\prime}(z_i) = f_c'(z_1)\circ\cdots\circ f_c'(z_n) = 0$ for any point on the period-n cycle. But this means that one of the derivatives $f_c'(z_i)$ has to be zero, so $z_i = 0$ the critical point. Hence the critical point is periodic with period n at this c value. Hence there is a point c in each bulb where $f_c^{(n)}(0) = 0$, resulting in an equation of degree 2^{n-1}. For example for period 3, we get $(c^2 + c)^2 + c = c(c^3 + 2c^2 + c + 1) = 0$, giving 0 for the period 1 heart -0.1226 ± 0.7449*i*, for the two period 3 bulbs above and below and -1.7549 on the small satellite Mandelbrot on the main dendrite on the negative x-axis.

We can also see why the Mandelbrot set is surrounded by an infinite number of satellite copies of itself. Consider points around -1.7549. These behave under the third iterate when renormalized by rescaling, just as $f(z)$, acts on M. We can see this by examining the Taylor series as follows:

Since $f_c^{(3)}(z) = f_c^{(3)}(0) + \frac{1}{2}f_c^{(3)"}(0)z^2 + O(z^4)$. There are no z or z^3 terms since f is an even function.

Applying the scaling $k = \frac{1}{2}f_c^{(3)"}(0)$, we have $kf_c^{(3)}\left(\frac{z}{k}\right) = \frac{1}{2}f_c^{(3)"}(0)f_c^{(3)}(0) + z^2 + \cdots = f_{g(c)}(z) + O(z^4)$

where $g(c) = \frac{1}{2}f_c^{(3)"}(0)f_c^{(3)}(0)$, since we are now simply squaring and adding $g(c)$, so it's locally a scaling of $f(z)$, by $|g(c_0)|$ and rotation by $\arg(g(c_0))$ since to first order $g(c) = g(c_0) + g'(c_0)(c - c_0) + \cdots$.

The periodicities associated with the bulbs on the Mandelbrot set add fractional rotations as mediants $\frac{p}{q} + \frac{r}{s} = \frac{p+r}{q+s}$. Mediants correctly order the fractional rotations between 0 and 1 into an ascending sequence providing a way of finding the fraction with smallest denominator between any two other fractions. A way of seeing why this is so is provided by using a discrete process to represent the periodicities or fractional rotations. For example if we have 2/3 =110 and combine it with 1/2=10 by interleaving, we get 11010, or 3/5 so between period 2 and 3 we find a period 5 bulb. Because the periodicities grow exponentially on the boundary of M, particularly around parabolic periodic points at the base of the main cusp or those on bulbs, (see left) whose Julia sets have fractal dimension converging to 2, the boundary of M has a space-filling fractal dimension 2, as its local dynamics corresponds to that of the associated Julia set.

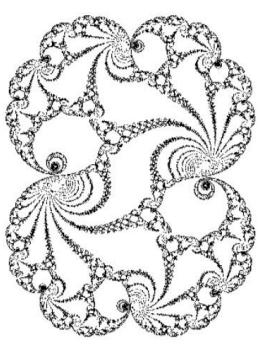

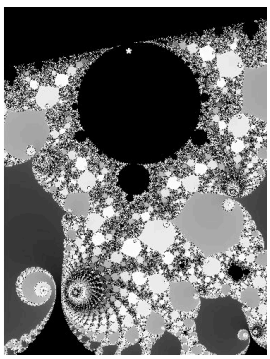

To derive the cardioid boundary of M , we set $z = f(z) = z^2 + c, |f'(z)| = 1, f'(z) = 2z = e^{i\theta}$, giving $c = z - z^2 = \frac{e^{i\theta}}{2} - \frac{e^{2i\theta}}{4}$. For the period 2 bulb we can solve for $f^{(2)}(z) = (z^2 + c)^2 + c = z$ to get the cardioid again plus $c = -1 + \frac{e^{i\theta}}{4}$ the circular period 2 bulb.

Points on the boundary have more enigmatic behavior. Here

the fixed or periodic point becomes neutral and at least two different outcomes can happen. For rational $\theta = p/q$ the neutral fixed or periodic point has both attracting and repelling arms, forming q quasi-attracting petals on the Fatou set, separated by *q* repelling arms on the Julia set and *c* is in the Julia set, as in the illustration above with the critical point orbit neutrally approaching the fixed point on the petals.

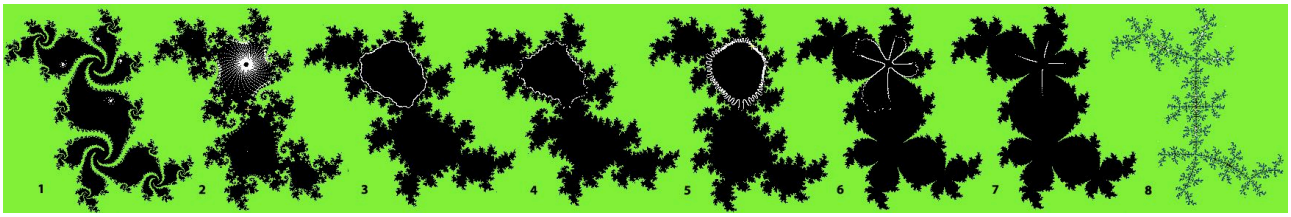

Fig1b: Critical point orbits using Wolf Jung's Mandel application (Jung 2014) included with the package. Left to right: Period 4 attractor, a nearby period 1 orbit near a high attracting period bulb, a golden ratio Siegel disc with the critical orbit traversing its boudary, one radian digitated Siegel, a Liouville number neighbouring a higher period parabolic point, 'digitated Siegel' near period 4, period 4 parabolic orbit and a fractal strange attractor in the repelling Julia set on the dendrite at the limit of period 4 doubling. One can see in example 6 how the dynamics evolves. The critical orbit running close to period 4 at first converges towards the neutral point, but because it is slightly off period, as the parabolic approach stagnates, moves laterally until it approaches the repelling arm of the Julia set on the boundary, where it is very rapidly hurled up into the next period 4 pseudo-petal in an intermittency crisis. This implies the neutral point is already in the Fatou component. **Mandel comes with a swathe of facilities complementary to the Dark Heart viewer,** with an extensive set of help tutorials.

For irrational values the situation is still not completely resolved. Golden numbers like the golden ratio $\gamma = \frac{-1 \pm \sqrt{5}}{2} = 0.618, -1.618$, avoid becoming mode-locked to a dominant periodicity because their distance from any fraction of a given denominator q exceeds a certain bound: $\left| g - \frac{p}{q} \right| > \frac{\varepsilon}{q^2}, \ \varepsilon \sim \frac{1}{\sqrt{5}}$. The golden numbers can most easily be described in terms of continued fractions, which, when truncated represent the closest approximation by rationals: $n = k_0 + \cfrac{1}{k_1 + \cfrac{1}{\ddots}} = [k_0, k_1, k_2, \ldots]$. Rotation angles with bounded k_i (golden numbers end in 1's), and hence far from rational values, have neutral fixed points lying in the inner basin of the Fatou set with an irrational flow called Siegel discs, with the critical point orbit on the boundary.

But there are other irrational values with large or unbounded k_i which lie very close to rational numbers, so that for every n there are p, q such that $0 < \left| x - \frac{p}{q} \right| < \frac{1}{q^n}$, including Liouville numbers, such as $\sum_{k=1}^{\infty} 2^{-k!} =$ 0.7656250596 defined more generally by $\sum_{k=1}^{\infty} a_k b^{-k!}$ where an infinite number of the a_k's are non zero, and those of sequences like 0.01001000100001000001… and 0.10001000000000000001… which are associated with Cremer points where the irrational value cannot be linearized into an irrational rotation and form invariant sets called "hedgehogs" containing Cantor combs of radial hairs (Shishikura 2014) reminiscent of the exponential fronds of fig 8. These Julia sets remain enigmatic and uncharacterized.

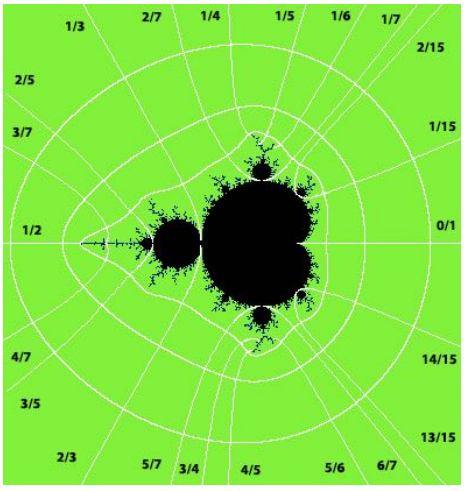

Fig 1c: External rays and potential levels displayed using Wolf Jung's **Mandel** application (2014) included in the Dark Heart package.

Douady and Hubbard discovered a number of intriguing relationships depending on the critical point that index the features of the bulbs and their dendrites in terms of the critical points. Because the Mandelbrot set is connected, with a simply connected complement, the complement can be mapped to the complement of a unit disc. E can

thus define the external angle, the angle of the ray from the unit disc that corresponds to each ray from M, just like the rays of an electric field emerging from M. There are intriguing ways to calculate these angles for the bulb cusps and key points on the dendrites. If we consider a critical point in either a periodic orbit or an eventually periodic orbit, we can encode the dynamics as a binary 'decimal' setting a 0 for each iterate in the upper half of the local traverse of the 0/1 and 1/2 rays, which are asymptotic to the positive and negative real axis. When we expand this decimal as a power series it gives the external angles of the cusps of the bulbs and dendritic Mandelbrot islands and the Misiurewicz dendrite tips and branching points. Rays emerging from period n cusps and dendritic islands all have external angles fractions of the form $\frac{k}{2^n-1}$ because of the repeated binary decimal associated with their periodicity, associated with each step in the period squaring and hence doubling the angle. E.g. $\overline{00\cdots01} = \sum_{i=1}^{\infty} 2^{-in} = \frac{2^{-n}}{1-2^{-n}} = \frac{1}{2^n-1}$. Furthermore these lead to every odd denominator fraction as a result of Euler's generalization of Fermat's little theorem $a^{\varphi(n)} \equiv 1 \bmod n$ where a, n are coprime and $\varphi(n)$ is the number of integers less than n co-prime to n. For example for 9 we have 1, 2, 4, 5, 7, 8 give $\varphi(9) = 6$, so $\frac{1}{9} = \frac{7}{63} = \frac{7}{2^6-1}$ and $\frac{1}{9}$ is actually an external angle of a period 6 dendritic Mandelbrot. By contrast, those from eventually-periodic Misiurewicz points have even denominators because the non-periodic initial iterations cause an irreducible power of 2 in the denominator.

$$0 \to -2 \to \bar{2},\ or\ \frac{1}{2}\left(\frac{1}{2^1-1}\right) = \frac{1}{2}$$

For example the ray to $M_{2,1}$ at c = -2 gives .

There are many processes which represent chaos in the real world such as the dynamical crisis, or *verlust*, of rabbit populations, where we have a function $f(x) = cx(1-x)$ representing exponential breeding cx in a finite pasture (1-x). This gives all manner of periods 2, 4, 8 etc. as the growth rate c increases through boom and bust due to overpopulation and starvation then entering chaos and other strange periods. Once we put this process into complex numbers, we get another Mandelbrot set (illustrated in fig 10b bottom left) and a collection of Julia sets, showing that these different real phenomena are all part of one complex process.

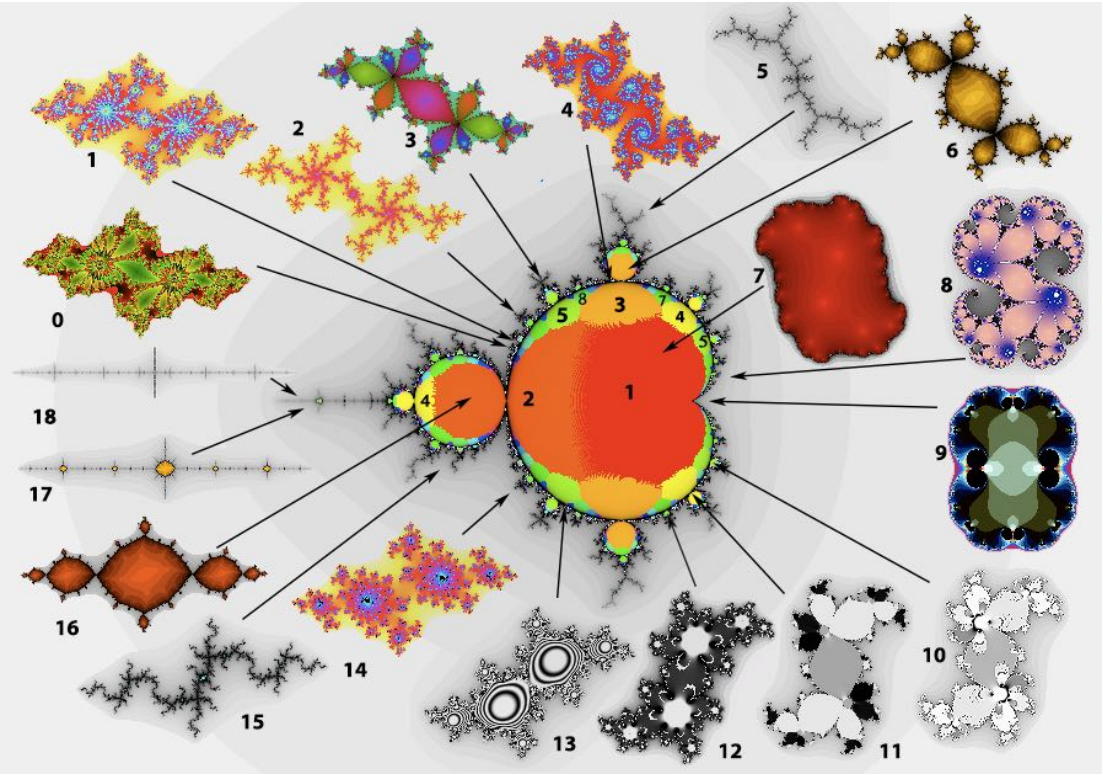

Fig 2: Diverse Julia sets and the period highlighted Mandelbrot parameter plane of $f(z) = z^2 + c$.

Classical Quadratics

So now let's have a look at how Dark Heart handles the diverse Julia sets of the classical Mandelbrot set, which have proved surprisingly difficult to capture due to their varied forms and unstable dynamics.

Julia sets come in diverse forms. They can consist of a single connected internal basin of attraction (7) have an infinite number of internal basins (3, 6, 16) and semi-dendritic (15, 17) which are generated from satellite Mandelbrots). Julia sets can be dendritic and have no interior basins but still be connected (1, 2, 17). They can be totally disconnected fractal dust (4, 14). They can also display behavior on the boundary between these states. For example a point right at the base of a bulb (8, 11) is called parabolic because it is bifurcating between periods (e.g. 1 and 5 for 11) and instead has neutral points surrounded by petals drawing towards the points and radiating arms on the Julia set repelling away. In between all the bulbs in golden mean type locations, which avoid all the periodicities associated with the fractional rotations of each bulb, are Julia sets with a neutral irrational rotation (13) called Siegel discs. Between these cases are emigmatic irrationals close to rationals whose dynamics have not yet been classified. (10, 12) show hybrid irrationalstates close to parabolic (11). One can also find parabolic Julia sets right on explosive bifurcation such as on the cardioid cusp (9).

Dark Heart Julia Journeys around the Mandelbrot Set: https://www.youtube.com/watch?v=BIFh3LoXSH8

Originally different techniques were developed to handle these cases. The simplest algorithm is the level set, where we colour the exterior by how many steps it takes to escape a large circle, leaving the interior and boundary filled dark. This doesn't work well either for complex dendritic sets which needed another technique called the distance estimator. Nor did it work for parabolic sets which required inverse iteration. Howeer these techniques are focussed on the quadratic and don't easily generalize to all functions.

Dark Heart viewers use a modifed level set algorithm which works for any kind of function and has several colour schemes suited to highlight all these types of Julia set and in addition to portray internal periodicities by colour (mode 1 in 6, 7,16,17), capture the dendrites and fractal dust using non-linear colouring schemes (modes 1 and 4 in 1, 2, 4, 5, 15,17,18), distinguish multiple attractors if they exist and to sample irrational flow velocities and highlight parabolic petals (mode1 in 10-13). One can also follow the way periodic lobes are mapped by colour (mode 3 in 5) and distinguish multiple attractors in rational functions such as Newton's method. The default (mode 0) is a useful general exploratory mode with non-periodic sinusoidal colouring.

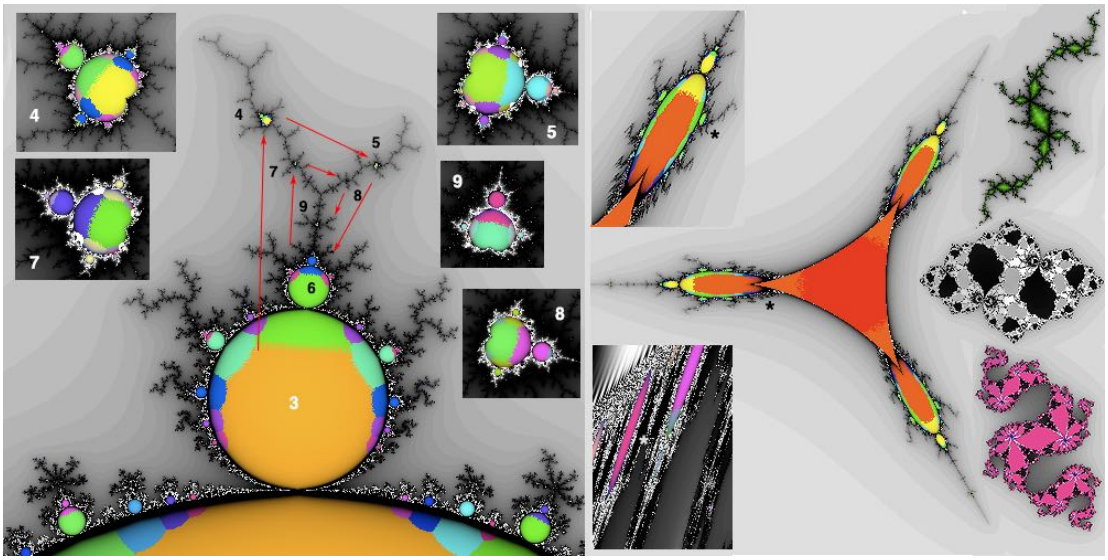

Fig 3: Left: Winding sequence of dendritic satellites and sub-bulbs of Mandelbrot period 3 increases in steps of 1. Right: Mandelbar of $f(z) = \overline{z}^2 + c$ is symmetric by rotation by 2π/3, since if $\omega = e^{2\pi i/3}$ then $\overline{\omega} = \omega^2$ and so $f_{\omega c}(\omega z) = \omega f_c(z)$ and by induction all iterates are rotations of the original. It has Julia sets distinct from those of fig 2. A topological space is locally connected if every neighbourhood (open set of a point in the space) has a connected sub-neighbourhood. The regions in the lower inset indicate that the mandelbar is not locally connected.

The view of the Mandelbrot set is also coloued to highlight the dendrites which connect the main body to all of the Mandelbrot satellites, demonstrating that the quadratic mandelbrot set is connected, despite having fractal dimension 2 the highest the 2-D complex plane can accommodate. The interiors are coloured by incipient periodicity, which begins to track as period say 3 within the period 1 bulb as we approach the period 3 bulb because the algorithms finds the third iteration close enough at the cutoff. Colors indicate the periodicities of the regions as follows: **1 2 3 4 5 6 7 8 9 10 11 12 13 14 15 16 17 18**. Because the process

stops after a finite number of iterations, the colors of sub-bulbs permeate the edges of the main bulb because the dynamics of the base period is beginning to subdivide, although in limit, the whole bulb is the base period. Hence the entire central bulb is period 3 with neighbouring sub-bulbs of periods 6, 9, 12, 15 & 18, that is 2, 3, 4, 5 & 6 times the base period of 3. Between the smaller period 6 and 9 bulbs is an even smaller one of period 6 + 9 = 15 and so on. The arrows indicate base periods on the Mandelbrot satellites on the dendrites going up in steps of 11 i.e. 3 4 5 6 7 8 9, each in turn having sub-bulbs of *n* times their base period *n* = 2, 3, 4 ...

This makes it easily possible to see the relationships in the periodicities. Starting from period 2 to the left we have period 3 at the top and bottom and successively 4, 5, etc. as we move towards the cardioid cusp as the rotation under iteration goes through 1/2. 1/3 etc of a revolution on each bulb. At the same time, between each pair of bulbs there is a fractional rotation that works by mediants - *p*/*r* and *q*/*s* become (*p*+*q*)/(*r*+*s*) so between 2 and 3 is a 5 and so on. We can also see how the periods multiply on sub-bulbs as oscillations of the base frequency.

In fig 3 we can see how the colouring can also enable us to chack the base periodicities of satellites and hence to see how each of these correspond to a cycling series of locations where each has a period a constant step up, forming a cycle of periods surrounding the base dendrites. The settings colour periods up to 35, making it easy to explore fine grained details and understand their dynamics on blow-up.

Higher Degree Atoms

In Dark Heart viewer, we can alter the settings for this function to portray any function of the form $f(z) = z^k + c$ by setting R,I to be e.g 3,0 instead of 2,0. We can then see each of the germ periodicities for multiple roots of higher degree clones of our original function, each of which is analogous to the quantum wave functions of an atom because each integer power winds precisely one revolution more around the origin. These form the root possible single critical point kernels which appear in all more complicated examples to follow and they represent the only kinds of solutions we can have, except for an exponential plateau and the inversions of these solutions in the presence of singularities, such as those caused by negative powers of z. In fig 4 are shown each of these along with the period 6 Julia sets of a period 3 sub-bulb of a period 2 bulb on each set to show their dynamics are essentially similar except for the *k*-fold geometry. All of these have well-defined boundary curves of their central region, so Dark Heart has a script which can generate interesting movies of the changes in the Julia sets as we move around the boundary, or out of the cusps.

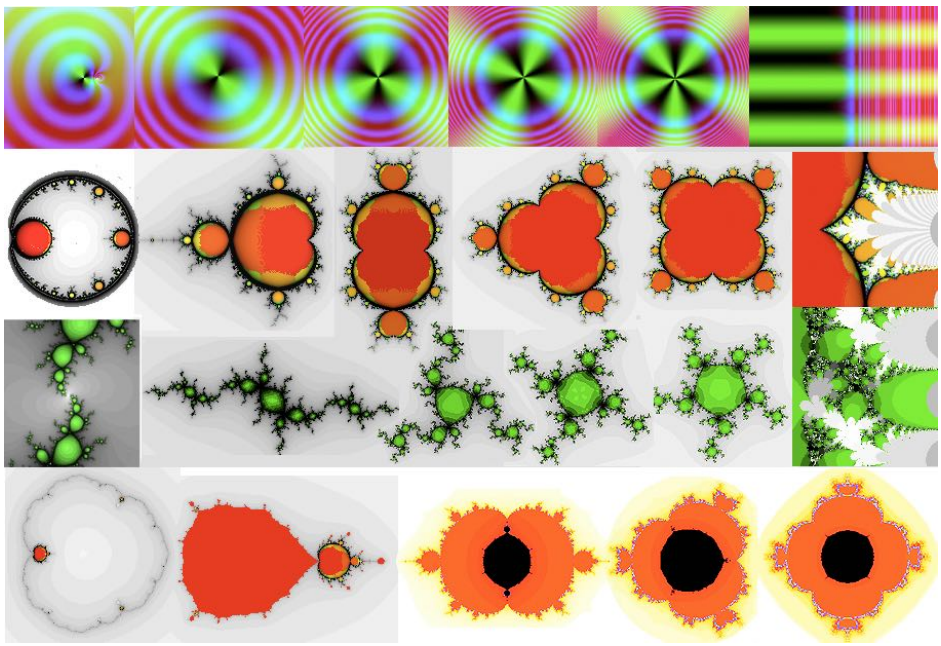

Fig 4: Elementary higher powers and their functions and parameter planes.

In fig 4 rows 1-3; we have the function, Mandelbrot and Julia views of $f(z) = cz^2 / (1 - z)$, $f(z) = z^k + c$ *k* = 2-5 and $f(z) = e^z + c$ show the principal power atoms forming the stable critical points of a diversity of

functions with main body boundaries following well-defined curves. To derive these, we set $z = f(z) = z^k + c,\ f'(z) = kz^{k-1} = e^{i\theta}$, giving $c = z - z^k = k^{-\frac{k}{k-1}}\left(ke^{\frac{i\theta}{k-1}} - e^{\frac{ki\theta}{k-1}}\right)$. Thus we can see the central basin is always a dark "heart" having *k*-1 cusps, with bulbs having *k*-2 cusps, supporting *k* revolutions as we move around the boundary, counting the base journey, equalling the *k*-fold winding of the function, illustrated in row one. Row 4: Mandelbrot views of second order atoms which arise in a region in which two or more dark hearts of critical points overlap giving full continuity (next section). Left to right: $f(z) = cz^3/(1-z)$, $f(z) = cz^2(1-z)$, both of which have a hidden infinite dark heart due to a second critical point a $z = 0$ mapping to 0, and $f(z) = (z^k - 0.1z)(z + c)$ k = 2-4 (black inner bodies with full continuity) consist of a fractal curve with quadratic cardioids emerging from the cusps and fractal symmetries of the order *k*, rather than the *k*-dimensional bulbs and well-defined body boundary curves of the upper sequence. The last 3 have outer bodies in the *k*+1 form but bulbs in the *k*-form due to the *c* parametrization.

Transitions between parameter planes: https://www.youtube.com/watch?v=rQ3kK58VvsI

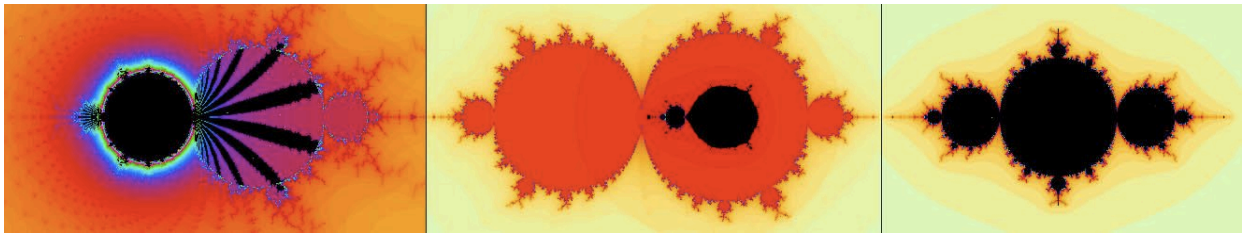

Fig 4b: The parameter planes of $c(z+k)z(z-1)$, passing (a) $cz(z-1)^2$, (b) $cz^3(z-1)$ and (c) $c(z^3-z)$

The parameter planes in fig 4b display radically different dynamics. While in (c), both critical points give the same parameter plane, resulting in first order bulbs although there are two separate criticals, in (b) there is a second order dark heart rocky coastline parameter plane where both criticals give rise to connected dynamics enclosed in a first order plane with double bulbs. By contrast, in (a) there is a unique crisis around the double zero $z = 1$, again giving a zero derivative and hence a critical that maps to 0, inducing an infinite parameter plane, but coinciding with the multiplicative idenity for *c*. In this case, every neighbouring value of $k = -1$ has a finite parameter plane with a rotational connectivity crisis caused by the Julia sets forming two sets of 'spokes' with an infintessimal hub winding around the two closely spaced zeros, resulting in alternating connections and disconnections, as we move *c* across the fractal bulbs, resulting in the fractal banded arms in each bulb. In the limit as *k* approaches -1, the combined plane still has first-order bulbs, because all adjacent *k*-values have a finite parameter plane for the near-vanisihng critical $z \sim 1$.

Cubic Chaos: Multiple Criticals and Interference

The above functions don't really give us any kind of generalized higher degree Mandelbrot set because they all have degenerate critical points. To see what really goes on in higher degrees, we need to explore more general polynomials. While with quadratics, the family $f(z) = z^2 + c$ forms a complete parameter space of all quadratic Julia sets under equivlence by affine transformations, cubics require two free complex parameters to do so, meaning we need an effectively 4-dimensional parameter space. We also have two interacting critical points, so new phenomena arise. There are two approaches to this problem.

The one used predominanly in dark heart is to choose a parametrization with one complex variable, such as the cubic $f(z) = z^3 - z + c$, which has a pair of distinct critical points spaced apart and examine the combined behavior of the two critical points for this parametrization. We shall examine this first. The alternative is to form 'slices' of the 4D parameter space involving a single complex parameter which fixes the behaviour of one critical point and examines the variations in the other. We will give two examples later.

We can make the same arguments for cubics and higher polynomials that we made for the figure 8 in quadratics, showing that each critical point is measuring the connectedness of the Julia set, which is fully connected only if neither can escape. If the cubic has distinct critical points, a great circle where

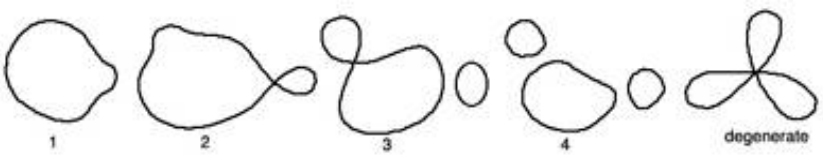

z^3 dominates will either have entirely simple closed curve inverses, as in the connected quadratic case, or it will reach a local figure 8 where there is a double root, which must also be one of the critical points as the slope is also zero, therefore this critical value will escape and we have a disconnection. In general were will also be a second inverse image where there is a second figure 8 of the other critical point resulting in a further disconnection to fractal dust. In the degenerate case such as $f(z) = z^3+c$ where we have coincident critical points, we will have a triple point, resulting in the escape of the other critical and a complete disconnection.
We now have to contend with the fact that we don't have just one parameter plane, but two overlapping ones, one for each critical point and we going to see that each is measuring the connectedness of the Julia setwhich can now become disconnectd and/or scrambled chaotically in two different ways by the oscillations of the cubic iteration. Dark Heart deals with this by calculating the critical points and iterating the function over each parameter plane and presenting a superimposd prolile of the two so we can select any point and see the consequences in terms of connectivity and winding. Only in the black central region in fig 5 will the Julia set be entirely connected. You can also view each one separately by checking dF and using the derivative portrait zeros to locate and select the critical point using hold.

Fig 5 (1,12) shows a variety of new features which enter into the chaos with $f(z) = z^3 - kz + c \;\; k = 1$. The double parameter plane now has both black regions where the Julia set is connected, orange regions where there is a fractal disconnect in one of the factors and a light yellow exterior where both are disconnected. Julia sets above illustrate (1) a single disconnection with the other factor of period 9, (2) a connected set with two different periods, (3, 4) two sets in the right hand cleft with rapidly changing dynamics between the two, (6) a doubly connected Julia set of period 3 at a Mandelbrot satellite on the rocky coastline of the black set and (7) a set on the edge of the lower cleft dendritic on one factor and disconnected on the other.

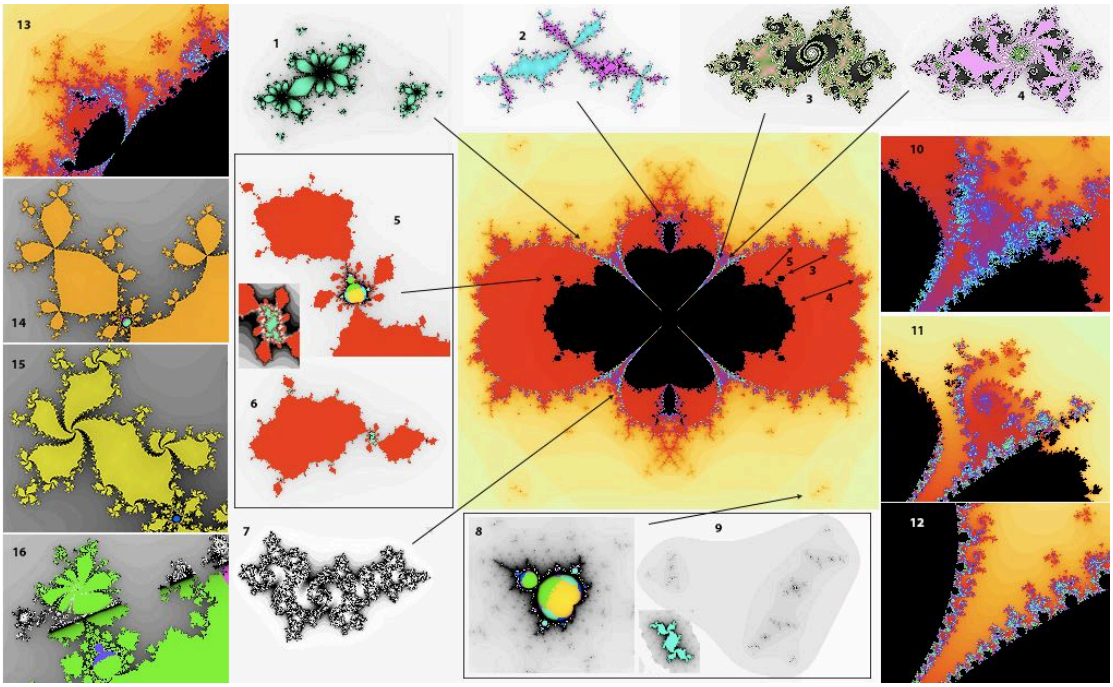

Fig 5: Dynamics of the function $f(z) = z^3 - kz + c$.

Journey in and out of the Cubic Mariana Trench: https://www.youtube.com/watch?v=xuPm4ooVZOE

But two major new features also arise. The first is interference between the dynamics of the two critical points. In each of the 'Mariana' trenches formed by the four deep cusps the higher and higher periodicities of each are being perturbed by the other, fragmenting the bulbs of each and leading to a newly chaotic dynamic, reminiscent of the mode-locking perturbations that have thrown all the asteriods in any sort of periodic relationship with the orbit of Jupiter into the other planets. In (10-12) we can see blow-ups of the two separate parameter planes which not only show chaos in superposition but each on its own is responding to the perturbations of the other. This results in extremely small changes in the *c* values strongly altering the relationship between the periodicities in the Julia sets.

Also the Mandelbrot satellites are no longer confined to dendrites but can also be connected through solid regions on the inner boundary where the bulbs are replaced by rocky coastline dark hearts, as on the dendrites of the quadratic case, except now attached to the main body via the cusps. (13-16) for k~0.2 show the erosion of higher period bulbs as k increases, with concretion of dendrites to periods 3, 4 and 8 due to a dominant periodicity on one critical point as for period 1 in (5,6). Below is a movie link showing how the period 3 bulb of $f(z) = z^3 + c$ becomes bifurcated to form the outer period 3 bulb and the inner period 3 dark heart illustrated in (5) and how dendritic cubic satellites become both rocky coastline hearts and Mandelbrot islands disconnected from the main body, so that neither cubic parameter plane is now a connected set. The collapse of dendrites to dark heart rocky coastlines and islands happens because the one-dimensional chaos is disrupted by perturbations of the other critical point, causing it to either converge to the dominant periodicity leading to rocky coastline dark hearts, or diverging it to two dimensional repelling chaos resulting in true dark heart islands.

Period 3 Separations of the Cubic Mandelbrot Set: https://www.youtube.com/watch?v=3IXcYmU0szU

The above movie shows how these phenomena arise, as we move from $f(z) = z^3 + c$ to $f(z) = z^3 - z + c$, each of which is shown in figs 4 and 5. The period 3 cubic double bulb and its satellites separate, with (a) the left lobe in the movie becoming the dark hearts on the rocky inner coastline of the distant critical point and (b) the right lobe becoming the outer bulbs of the nearer critical point. The same picture applies to the cubic satellites on the dendrites, the right set splitting to become (a) the dark hearts on the smaller fractal period 1 rocks of the inner coastline defined by the distant critical and (b) the dark heart islands of the nearer critical with the the left set splitting with one set (a) descending to the adjacent rocky coastline of the distant critical as the left lobe did, and the other (b) continuing as outer bulb dendritic satellites. The dark hearts of each critical point, being nuclei of attractive winding periodicities, are atomically robust to interference from the other critical point and pass unaltered through such changes, while their associated repelling dendrites become perturbed and undergo bifurcation through an irrational flow to a base period Julia component. The fractal rocks on the coastline associated with each dark heart thus originate from the concretion of dendrite webs that have become frozen to the main body attracting period of the other (adjacent) critical point.

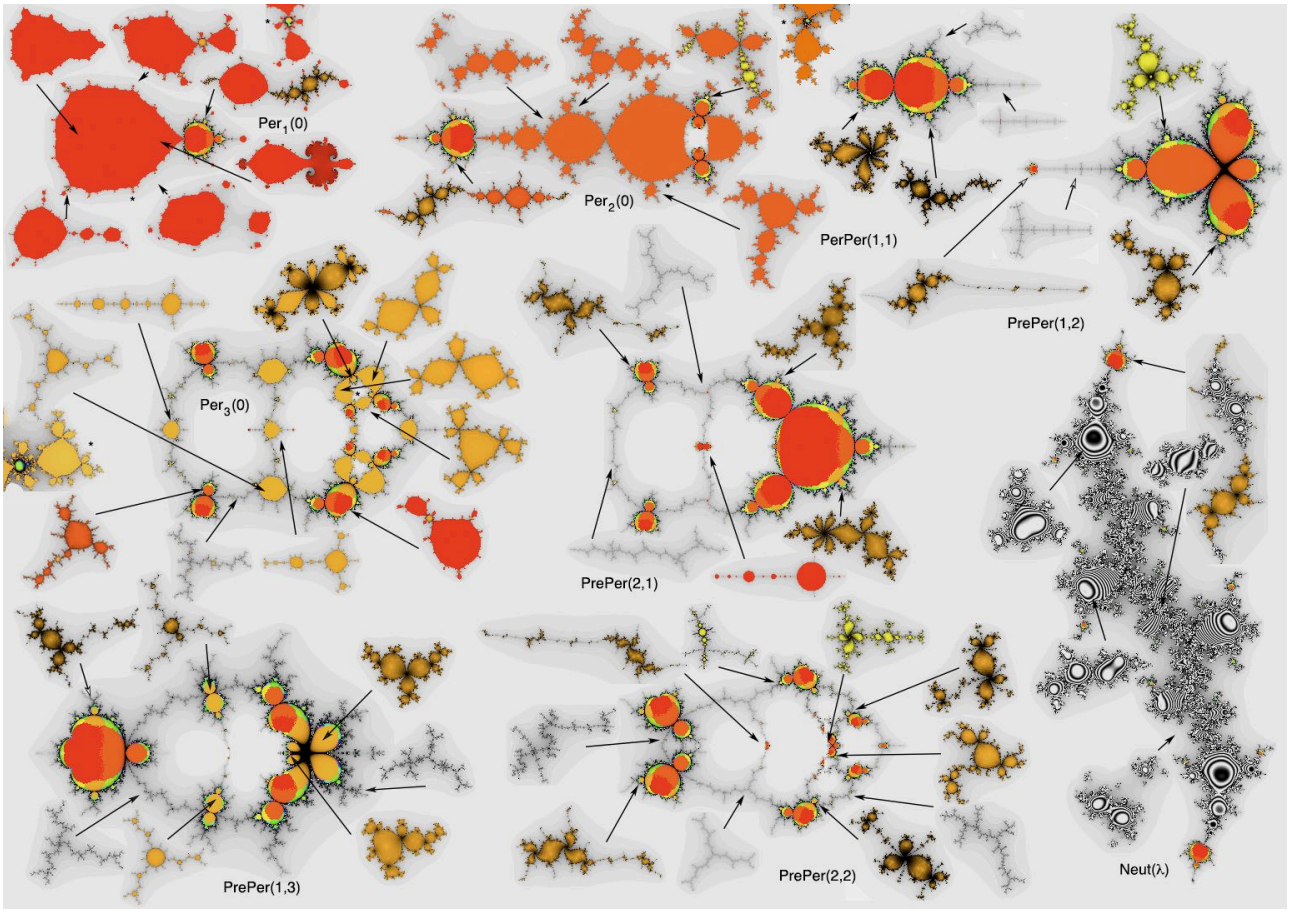

Fig 5b: $Per_1(0)$, $Per_2(0)$, $Per_3(0)$, colour coded by period, the Neut(λ) plane of Siegel discs, and five pre-perodic parameter planes with example Julia sets.

Now let's turn to the 'slice' method of investigating higher degree Julia sets favoured by classical research. In figure 5b are shown slices of the 4D so-called cubic connectivity locus which fix one critical point to periods 1, 2 and 3. These are highlighted in mode 1 to emphasize their local congugacy with the dynamics of the Julia sets. We can easily confirm that the illustrated function $f(z) = cz^2(1-z)$ has a superattracting fixed critical at 0, (derivative 0 with period 1 hence $Per_1(0)$), causing all its Julia sets to have period 1 for this critcal while the dynamics of the other critical at 2/3 can vary. We can likewise confine one critical point to be period 2. We set the two critical points to be 0 and c so we have: $f'(z) = az(z-c)$ $f(z) = \frac{a}{3}z^3 - \frac{ac}{2}z^2 + b$. Now let's stipulate that $0 \to 1 \to 0$, giving $0 \to 1$ $b = 1, 1 \to 0$ $0 = \frac{a}{3} - \frac{ac}{2} + 1$, $a = \frac{6}{3c-2}$, $f_c(z) = \frac{a}{3}z^3 - \frac{ac}{2}z^2 + 1 = \frac{2}{3c-2}z^3 - \frac{3c}{3c-2}z^2 + 1$. This has the parameter plane shown top right in fig 5b. The selected Julia sets for several values of c show that one critical point component of the dynamic is period 2 while the other can take any configuration, from period 3 through Cantor dust to compound period 2 configrations. As shown lower left in fig 5b we can do likewise for period 3 by sending $0 \to c \to 1 \to 0$, resulting in the parametrization $f_c(z) = \frac{(c^3 - c + 1)}{c^2(c-1)}z^3 - \frac{c^4 - c + 1}{c^2(c-1)}z^2 + c$, giving rise to a spectrum of locations, all of which have one critical point inducing period 3 dynamics. In fig 5b are four preperiodic parameter planes. For example, PrePer(2,1) with $0 \to c \to 1 \to 1$, has parametrization $f_c(z) = \frac{(c^2 - 1)}{c^2}z^3 - \frac{c^3 - 1}{c^2}z^2 + c$. Complexity increases rapidly, so $0 \to c \to 1 \to d \to 1$ in PrePer(2,2) with $f_c(z) = \frac{cs - c + c^2 + c^3 - s + 1}{2c^2(c-1)}z^3 - \frac{c^2 - cs - 3c + c^3 + c^4 + c^2 s + 2}{2c^2(c-1)}z^2 + c$, $s = \sqrt{c^4 + 4c^3 - 2c^2 + 1}$ gives rise to branch cuts and multiple parameter planes. These cases give rise to Julia sets with dendrites, tails and geometrical doublings.

Dark Heart also includes the period 4 case $0 \to c \to 1 \to d \to 0$, which is right on the limits of computability, generating a 42 page formula in Mathematica after Matlab froze (http://dhushara.com/DarkHeart/Period4.pdf), which, after computational streamlining, results in four multiply-split parameter planes, generating a comprehensive collection of period 4 coupled Julia sets. In fig 5c is shown the superimposed parameter planes with selected Julia sets. The equations of the splits cannot be computed as they are of degree greater than five.

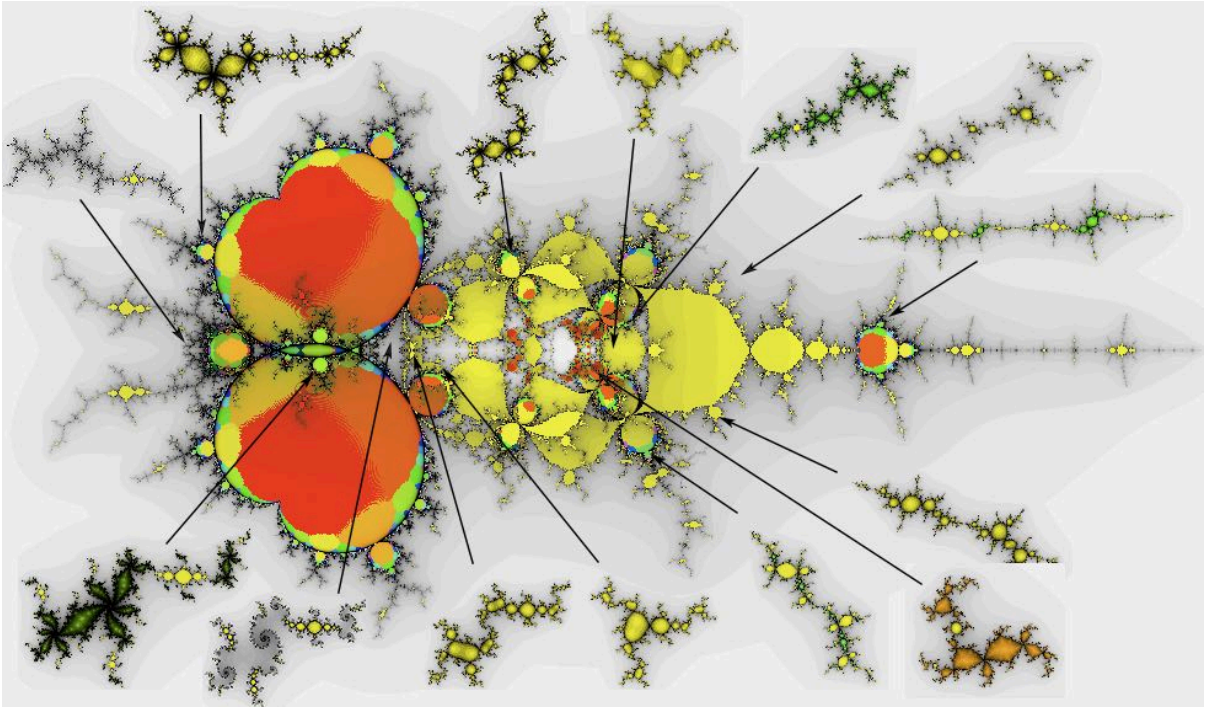

Fig 5c: Four parameter planes of $Per_4(0)$ superimposed, with a selection of Julia sets.

On the right of fig 5b is $f(z) = z^3 + cz^2 + \lambda z,\ \lambda = e^{2\pi i\gamma},\ \gamma = (\sqrt{5}-1)/2$ (golden mean), which forces one critical point to give rise to the neutral point rotation of a Siegel disc, while the other can vary, as illustrated in the various Siegel disc Julia sets. Rational values can also be chosen for gamma, resulting in parabolic examples. Again this parameter plane has domains conjugate to Siegel discs. In the case gamma is a Cremer point, this parameter plane is connected but not locally connected (Buff & Henricksen 2001), due to it being quasi-conformal with quadratic Julia sets of the form $f(z) = z^2 + \lambda z$.

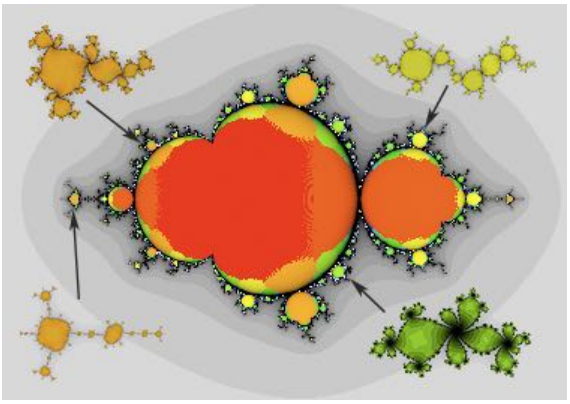

Fig 5d: The quasi-degenerate slice $f_c(z) = cz^2(z-1) + 2/3$ has the critical point at 0 mapped into the other at 2/3, resulting in a parameter plane with bulbs having 'quartic' double cusps.

Higher Polynomials

Dark Heart includes a series of higher degree functions which can be modified in the advanced settings to both change the degree and alter the separations between critical points, leading to a huge diversity of examples. Application scripts are also provided which can portray any polynomial up to degree 5 either in terms of its coefficients by solving for the critical points, or by setting the positions of each of the four critical points and calculating the coefficients. Several of the examples in advanced settings with symmetries can go to higher degrees and also have negative powers, leading to infinite singularities.

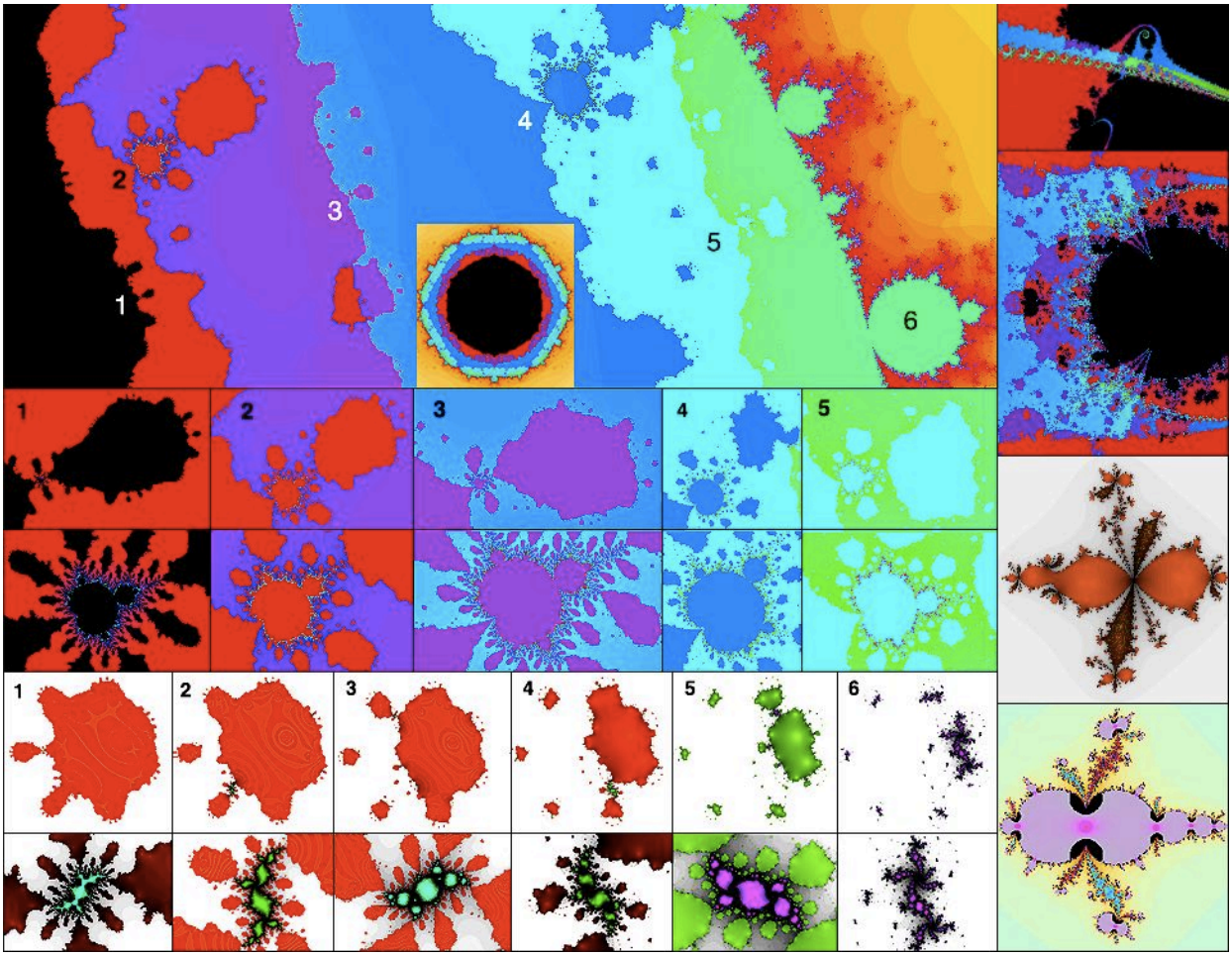

Fig 6: Dynamics of higher degree polynomials illustrating overlapping parameter planes, graded disconnections and multiple Julia dynamical systems.

In fig 6 is shown the graded parameter planes of $f(z) = z^7 + 0.4z + c$, with a cascade of 5 dark hearts in successive rocky coastlines, ending in a quadratic bulb illustrating six stages in the fragmentation of a degree seven Julia set, with the seventh stage being a disconnected Cantor dust. On the right are blow-ups of $f(z) = z^4 - z + c$ (see fig 6b), showing multiple interference zones with two Julia sets below, each of which show the interaction of four dynamical systems. For example, in the lower one, we have three periodic systems in green red and pink and a Cantor dust disconnection of the multiple 'violins'.

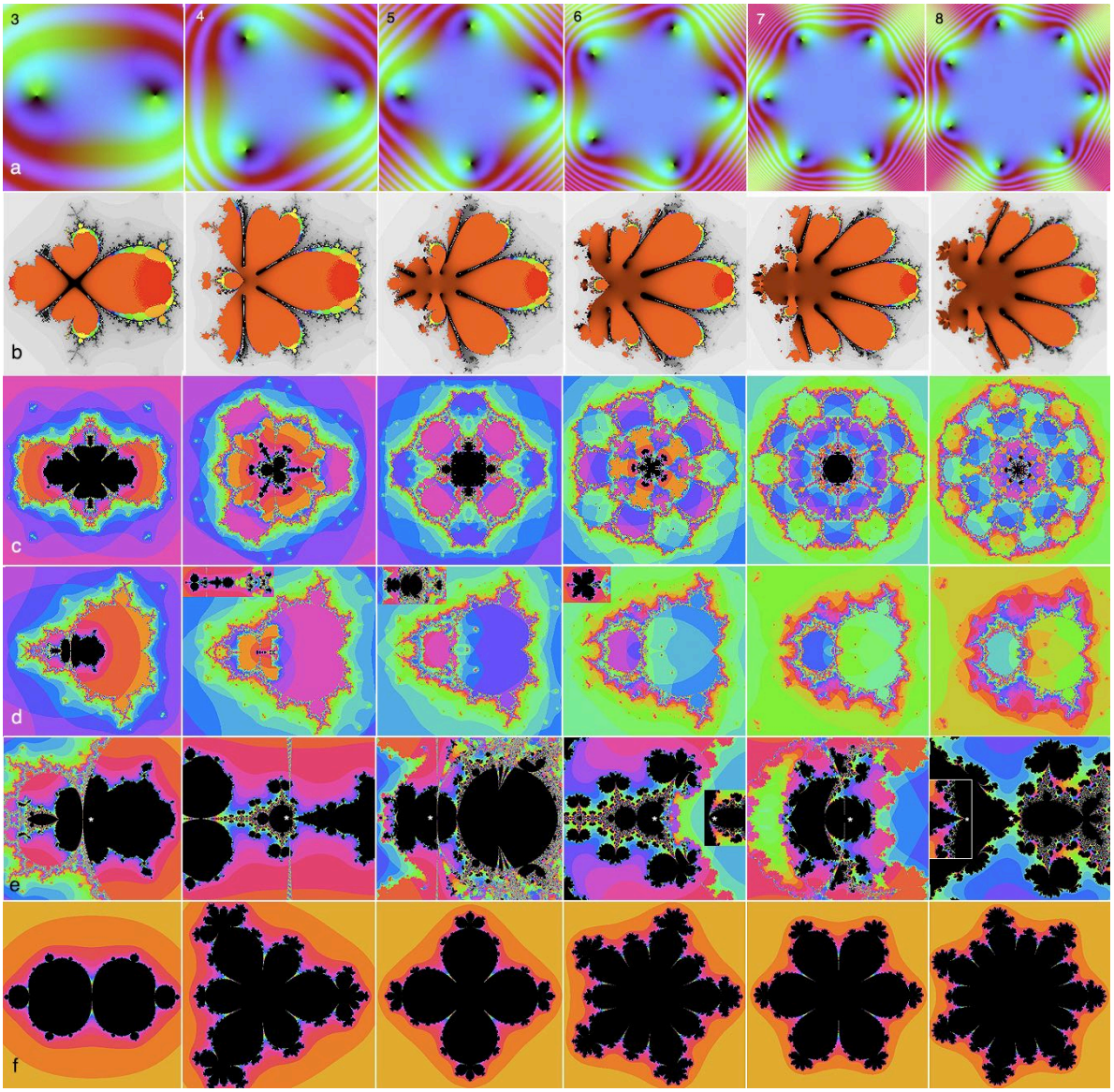

Fig 6b: Symmetries in polynomial dynamics of $f(z) = z^k - z + c$ for k = 3-8.

In fig 6b, we explore the effects of symmetry, the use of moduli spaces and the dynamics of odd and even powers. The polynomials $f(z) = z^n - nz$ are unique in that they give rise to symmetric parameter planes. For n = 1, for every k the functions $f(z) = z^k - z + c$ have parabolic Julia sets at the origin, with multiple cusps and petals, in bifurcation between periods 1 and 2. We can see this because $|f'(z)| = |kz^{k-1} - 1| = 1$ for $z = 0$, so 0 is on the boundary of the period 1 basin. In (a) the positions of the critical points show that for even k, the odd number of k-1 critical points means that none are diametrically opposite one another, while in the odd case the even k-1 criticals are opposite. This leads to completely distinct Julia dynamics, in which for odd k we have k-1 petals, but for k even, we have 2(k-1), as illustrated in (f). We can see why this is this in (b) when we examine the individual parameter planes of each critical point for even k and find they have an intact period 2 basin opposite the main period 1 basin, ecause there is no diametrially opposite critical point the the rotational interference of the others tend to cancel, while the odd k have rocky coastlines there due to interference from the antipodean critical, as we noted for k = 3 in fig 5. In the even case, this causes the central (black) region where the Julia sets are fully connected (c) to be 'stellated' and split by multiple cusps from the adjacent period 2 basin. In the odd case we have a central region punctuated only by the global cusps of the remote period 1 basin, which we can see intersecting for k = 3, but gradually become invisible for higher powers.

We can explore this further, by explitiong the symmetry of the functions by a rotation by 1/(k-1) of a revolution when the overlapping parameter planes are combined, as shown in (c). We can thus introduce a mapping to another C-plane, where $C = c^{1/(k-1)}$, to form the **moduli space** of equivalence classes of c under the rotational symmetry, as illustrated in (d). In particular, this transformation is a Mobius transformation $m(z) = (pz + q) / (rz + s)$, which conjugates with the polynomial function, so we can generate its own

parameter plane which looks like a set of overlapping dark hearts, using colour mode 3 with orbit trap. The quotient plane perfectly represents all the possible Julia sets up to rotation by 1/(*k*-1) of a revolution, but it also involves scaling by powers, so that for higher values of *k* the black fully connected region (inset for *k* = 4-6) becomes shrunken and distorted about the origin, while preserving the fractal structures and topological dynamics. When we examine the cases in (d), we see that for even *k*, the origin is always at a cusp in a dark heart region, while in the odd case we find a central region penetrated only by the universal vertical cusps of the remote period 1 basin, leading to the differing dynamics.

Separations of $f(z) = z^k - nz + c$ for *k* = 3, 4, 5: https://www.youtube.com/watch?v=8P6EOxT65sU

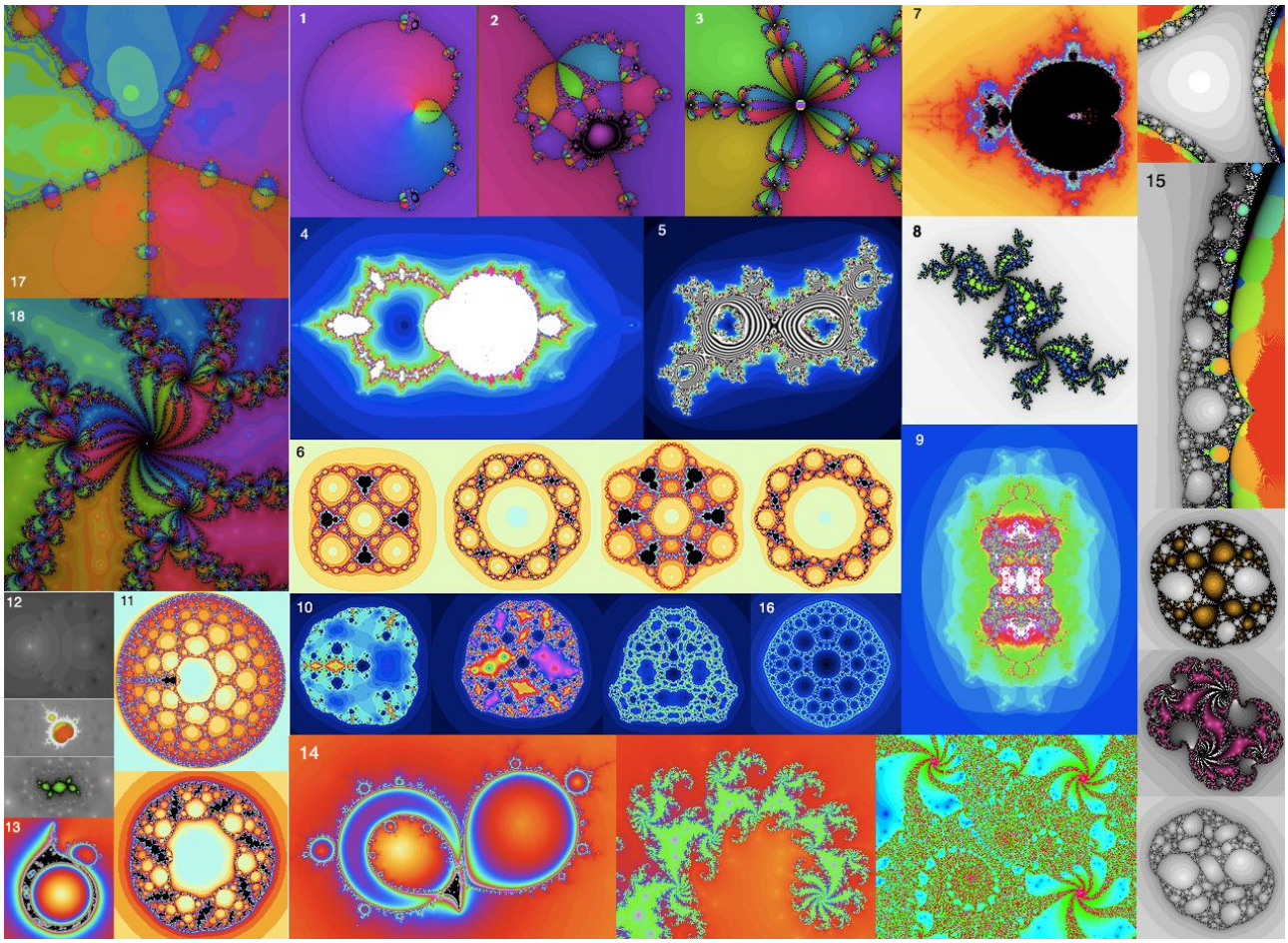

Fig 7: Varieties of rational function dynamics

Rational Functions and Infinities

There are also an intriguing array of rational functions which have infinite singularities as well as critical points which disturb the dynamics in sometimes unpredictable ways and which provide new interesting dynamical examples. A famous one is Newton's method in which we find the zeros of a function by iterating from a start point *x* , going up to *f*(*x*) and then down the slope *f*'(*x*) to the point $x_1 = x_0 - \frac{f(x_0)}{f'(x_0)}$. Virtually always, this closes in on the zero but not every time. There is a chaotic set of points that can't decide what to do and we can explore it for the complex cube roots of unity. It turns out that we can describe any cubic in the form $f(z) = z^3 + (c-1)z + c$. Dark Heart applies this generalized to $f(z) = z^k + (c-1)z + c$ to get Newton's method for the complex *k*-th roots of unity. In fig 7 the parameter plane of Newton on the fifth roots of unity is shown (1), iterated from the repelling critical point at 0. This puts the origin on the chaotic Julia set, but other *c* values not on the Julia set mostly iterate into one of the five attracting roots. (2) shows a parameter plane blow up with a degree-4 Mandelbrot kernel, and (3) the Julia set of the iteration for *c* = 1, to the fifth roots. This provides a unique fractal 5-colour mapping problem in which every point on the boundary of each region is simultaneously touching all of the other four regions because each is an intersection point of all regions.

In (4) is the parameter plane of $f(z) = cz^2(z-k)/(1-kz)$, $k = 4$, which for golden mean rotations in the left sector, provides the Herman ring - a unique example of an annular irrational flow in the Julia set (5). Notice also that the left hand portion of the parameter plane surrounding the singularity has both inward and outward-pointing bulbs, leading to inversions of the Julia set dynamics.

In (6) parameter planes and Julia sets for $f(z) = z^m + cz^{-n}$, $m,n = (5,3),(6,3)$ provide an example of symmetries generated by each of the two powers. In the (5,3) case there are 5-1=4 baby dark hearts. Each of the intervening 4 concentric domains has 5+1 outer sub-domains and 3-1=2 inner sub-domains adding to the 5+3=8 fold rotational symmetry of the Julia sets with 5 outer and three inner sub-domains.

Filigree journeys around z^3+n/z for small n: https://youtu.be/sCubplja0nU

Another intriguing phenomenon is the way a singularity can introduce fractal perforations in an existing iteration. In (7) the parameter lane of $f(z) = z^2 - 0.01/z + c$ shows the dark heart perforated in the centre by the effect of the singularity, which has also fragmented the critical points into a closely spaced set of 3, generating overlapping parameter planes. A Julia set from the period 3 bulb (8) shows internal perforation by a latticework of 'holes' with multiple dynamical systems in the interior due to the multiple critical points. In (9) the iteration $f(z) = z^3 - 0.1/z + c$ shows an almost completely scrambled parameters plane generating the diverse Julia sets shown in (10). (11) Shows $f(z) = cz^2(1-z)^{-9}$ and a Julia set of period 3, with similar power-based symmetries to (6). (12) shows the ghostly outlines of the repelling version of Newton's method $x_1 = x_0 + \dfrac{f(x_0)}{f'(x_0)}$, dominated by escaping points, leaving only isolated regions of connectivity, with a Mandelbrot island of base period 2 and a period 6 Julia set. (13, 14) show parameter planes and Julia sets of $f(z) = (z + rc + s + 1/z)/c$ using the Milnor C-script and function. (15) Shows the parameter plane and Julia sets of $f(z) = 1/(z^2 - c^2) + c$. (16) Shows the Julia set of $f(z) = z^2 + (1/16)z^3$ is a Sierpinski carpet. (16,17) Julia sets of $c(z+0.5/z^2)$ and $c(z+1/z+2)+1$ (Mandel1.txt) showing internal dynamics and fractal tilings of the complex plane in mode 3 showing how the attractors separate the plane into fractal tilings.

Both cubic polynomials and quadratic rational functions have two critical points, where the derivative is zero or infinite, leading to a 4D moduli space (2 complex parameters), under equivalence by Mobius transformations, to completely describe the Julia sets of every function. However, as with the cubic case, we can form a **slice** consisting of functions fixing the behavior of one critical point, to form a 2D parameter plane constituting a section through the higher dimensional space, in which the remaining critical point is set free and we can study the dynamics of the Julia sets.

The critical points can have one of four behaviors *adjacent* if they both fall into the same attracting set, *bi-transitive* if each falls into the others basin, *capture* if one falls into the periodicity of the other and *disjoint* if they have entirely separate basins of attraction. The *k* periodic regions of the infinite component differ in their behaviours. For example the main light-coloured bulb in $Per_2(0)$ has *adjacent* behaviour. Each successive period 2 generation daughter reverses between this and *bi-transitive*.

We thus fix the period of one critical and find a parametric class of functions all of which preserve the periodicity. In fig 7b are shown representative parameter planes $Per_k(0)$ k=1-4 for the sections fixing the periodicity of the critical point $z = 0$, corresponding to the following four parameterizations:

$$f_1(z) = z^2 + c,\ f_2(z) = c/(z^2 + 2z),\ f_3(z) = (z^2 + c^3 - c - 1)/(z^2 - c^2),\ f_4(z) = (z^2 + (c - 1 \pm \sqrt{5c^2 - 6c + 5})(1 - c^2)/2 - 1)/(z^2 - c^2)$$

The first is chosen to be the quadratic Mandelbrot set because it has fixed critical point zero and a super-attractor at infinity (the north pole of the Riemann sphere), leading to an infinite period one basin (enclosing the northern hemisphere) surrounding the Julia set. In the period two case, $0 \to \infty \to 0$. In period 3, $-c \to \infty \to 1 \to -c$ using $f_c(z) = \dfrac{z^2 + a}{z^2 + b}, -c \to \infty \Rightarrow b = -c^2, 1 \to -c \Rightarrow -c(1+b) = 1 + a$, giving the above equation, with critical points at 0 and infinity. This provides symmetric Julia sets rather than the asymmetric model based on $f_c(z) = 1 + a/z + b/z^2$.

The symmetrical period 4 case is special because it has a square root in the c parameter defining f, which leads to a double split parameter plane, generating the two parameter planes shown in the third row of fig 7b forming a “fermionic” loop where one cycle through the elliptical cut in the centre of the each plane takes you to the complementary plane. Together these planes cover all the period 4 locations on the classical Mandelbrot set, as shown on the left. There is also a topological homology between the Julia sets generated by Medusa and those generated by the fermionic plane, as shown in the second and fourth rows of fig 7b.

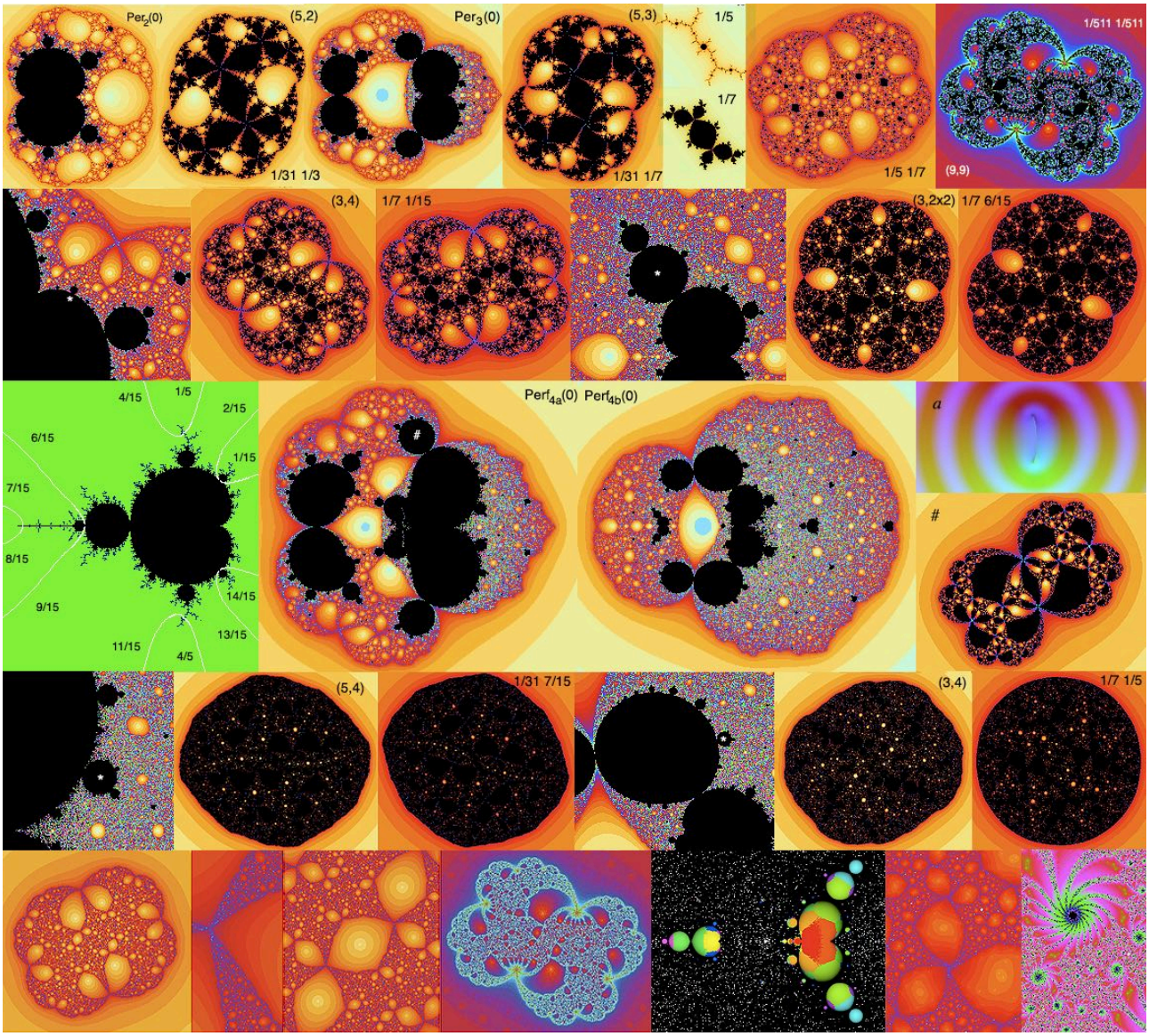

Fig 7b: Top row: Periodic 2 and 3 slices and Julia set matings. Right: Two Medusa matings. The lower three rows show the split “fermionic” parameter plane $\text{Perf}_4(0)$, with Julia sets at the starred locations, showing topological homology with the corresponding Medusa matings confirming the techniques give conjugate dynamical systems. Bottom row: Medusa portraits of 1/4 1/7, with dendritic tree detail, 1/7 1/4 and 1/4 1/511. Right: slice of PrePer(2,1) with example Julia sets.

Each parameter plane gives rise to complementary Julia sets, in which a new phenomenon, called **mating** appears. You can think of a quadratic rational function as the quotient of two quadratics, one of which has dynamics which is dominant near zero with the other dominant near infinity. Because the complement of a connected Julia set is a topological disc, two connected Julia sets can be entwined together on opposite hemispheres of the Riemann sphere. Consequently they can form complementary Julia sets “mated” together. Almost any pair of connected Julia sets can be so mated except for those in conjugate limbs of the Mandelbrot set. Thus we can see that the boundary of a mated Julia set is penetrated by periodic basins, as well as having periodicities of its own, just like the period 2, 3 and 9 basins in the first row. The cubic Newton’s method map is likewise the limit of a mating between two polynomial Julia sets of z^3-z and z^3+az^2. Any two quadratic Julia sets can be mated via a rational function provided they aren’t in conjugate domains of the Mandelbrot set, when the two cannot form a Riemann sphere, so cannot mate in $\mathbb{C}$.

The **Medusa** algorithm to find a rational function, which mates two rational Julia sets of any pair of external angles p/q and r/s, (Boyd & Henriksen 2012) uses the combinatorics of a spider consisting of a set of periodic points and external angle rays in the orbit of the critical point *c*. John Hubbard designed the Medusa algorithm, based on topological theory of Thurston and the foundational theory of polynomial matings. A medusa consists of two spiders forming northern and southern hemispheres of the Riemann sphere sewn together along the equator. This makes it possible to define a convergent sequence of coefficients (a_n, b_n) defining in limit a rational function $f(z) = (az^2 + 1 - a)/(bz^2 + 1 - b)$ mating the Julia sets defined by the two external angles. It may diverge or remain unstable for some fractional angles. As shown in fig 7b many Medusa matings are visually and topologically identical to those of slices, but some are surprisingly different because Medusa throws up an equivalent or shared mating, such as the period 4 "Eye of Sauron" denoted with a # in fig 7b, which is equivalent to 1/15 7/15 linking the period 4 bulb to the dendritic Mandelbrot on the negative x-axis, although it doesn't look like it. **Mandel** included with Dark Heart can show spiders in action.

Medusa can also generate matings involving dendritic Julia sets by using external rays with even fractions, as shown in fig 7c. Notice that 1/7 1/4 has an unbounded Julia set because the point at infinity is on a dendrite. One can generate sets like 1/4 1/7 by selecting an appropriate *c* value in $Per_3(0)$. To generate sets like 1/7 1/4, we need to construct a pre-periodic parameter plane, such as the pre-periodic slice PrePer(2,1) $f_c(z) = 1 - 8\frac{c-8}{c+8}\left(\frac{1}{z} - \frac{1}{z^2}\right)$, $0 \to \infty \to 1 \to 1$, in fig 7b, which, as noted above, results in the point at infinity being in the chaotic repelling domain, since pre-periodic iterations arrive at Misiurewicz points on repelling dendrites. The complement of the finite attracting Fatou component defined by any period bulb is thus entirely Julia, with all other points in the parameter plane leading to chaos, rather than escape to infinity in the super-attracting basin of infinity. The Julia/Fatou portraits thus extend all the way to infinity.

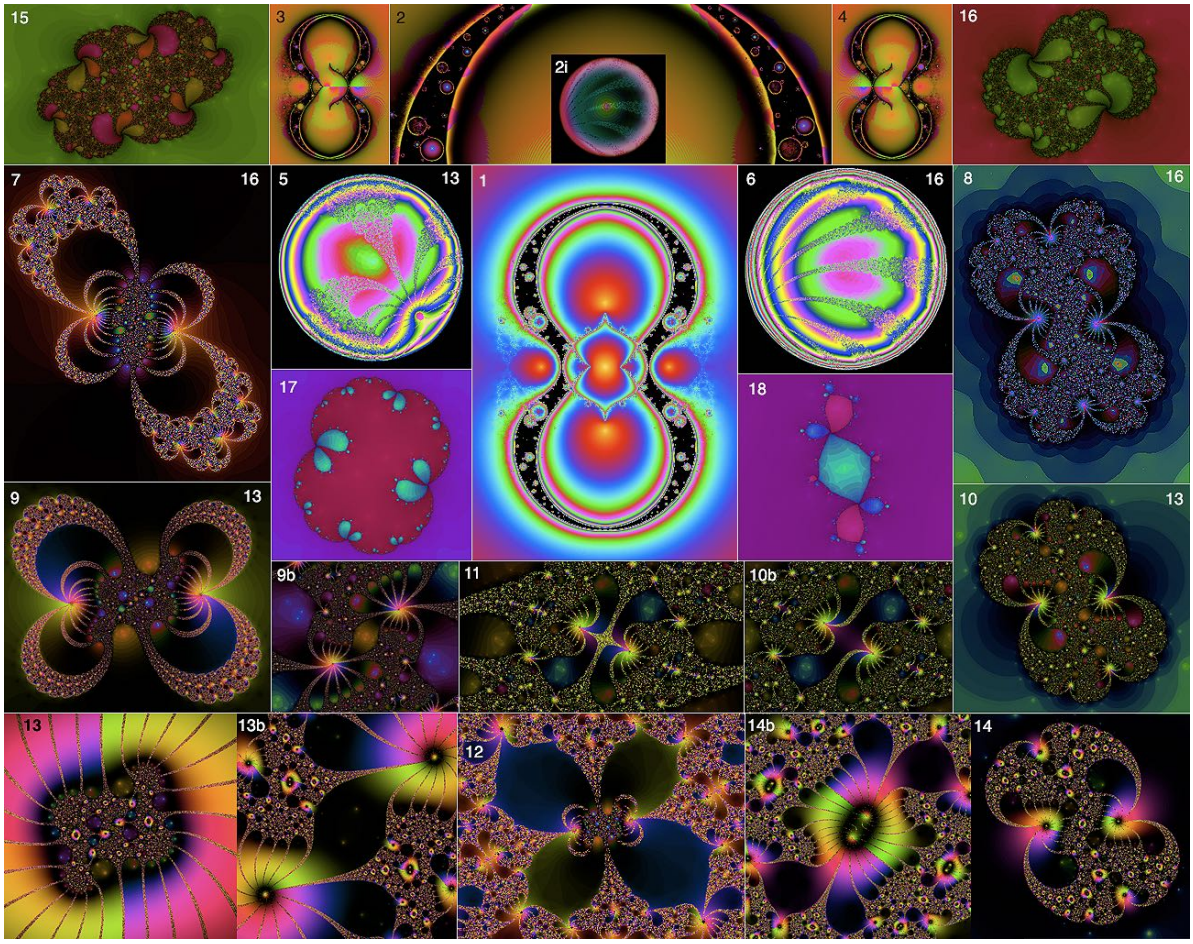

Fig 7c: Dynamics of the function $f_c(z) = \frac{z^2 - c^3}{z^2 + c}$ with both finite and infinite critical points.

The function $f_c(z)=\frac{z^2-c^3}{z^2+c}$ in fig 7c demonstrates the dynamics when we have to take account of both the critical points with zero derivative and those with an infinite derivative. Here we have $f_c'(z)=2(c-c^3)z/(z^2+c)^2$, $f_c'(0)=0$, $f_c'(\pm(-c)^{1/2})=\infty$ and since $\pm(-c)^{1/2}\to\infty\to 1$, we can effectively use 0 and 1 as the critical points. Moreover, we can see by swapping 0 and ∞ by $z\leftrightarrow c^2/z$ in both the domain and range that $c^2/f_c(c^2/z)=c^2\frac{(c^2/z)^2+c}{(c^2/z)^2-c^3}=\frac{c^6+c^3z^2}{c^4-c^3z^2}=-\frac{z^2+c^3}{z^2-c}=-f_{-c}(z)$, so the parameter plane of ∞ is simply the parameter plane of 0 flipped in the c direction. This results in the combined plane shown in (1), with the two individual planes in (3,4). The combined plane forms a symmetrical figure 8 with pairs of bulbs running in two series (2) in the interior of the black chaotic region, which consists of points which fail to head to any attractor from either critical point.

Close inspection however reveals that, the two, apparently symmetrical sides differ. Superimposing the left and right for the period-16 bulb (2i) shows that, although these overlap, there are key differences. The expanded superimposed period 13 and 16 bulbs (5,6) have clear patterns indicating critical point interference. Intriguingly for the period 13 and 16 cases, the bulb of 0 intersects both with regions of identical asymptotic period in the bulb of ∞, and with c values where ∞ is pre-periodic, or chaotic, and hence in the Julia set.

Note the two critical points differ fundamentally in their behavior, because one is a zero of the derivative, which is not a solution of the numerator and the other is simply a solution of the denominator. This means that the Julia sets on either side have distinct dynamics.

In the above cases, when a c value is chosen, where both criticals have the same asymptotic period, as in (7,8 c = ±0.995627+1.937037*i*) and (9,10 c = ±0.731013+2.280174*i*), the Julia sets on both sides, although geometrically distinct, appear to be homeomorphic to one another and each is hence automorphic to itself, by an inversion exchanging 0 and ∞, as indicated by a blow-up of the central regions of (9,10) in (9b,10b).

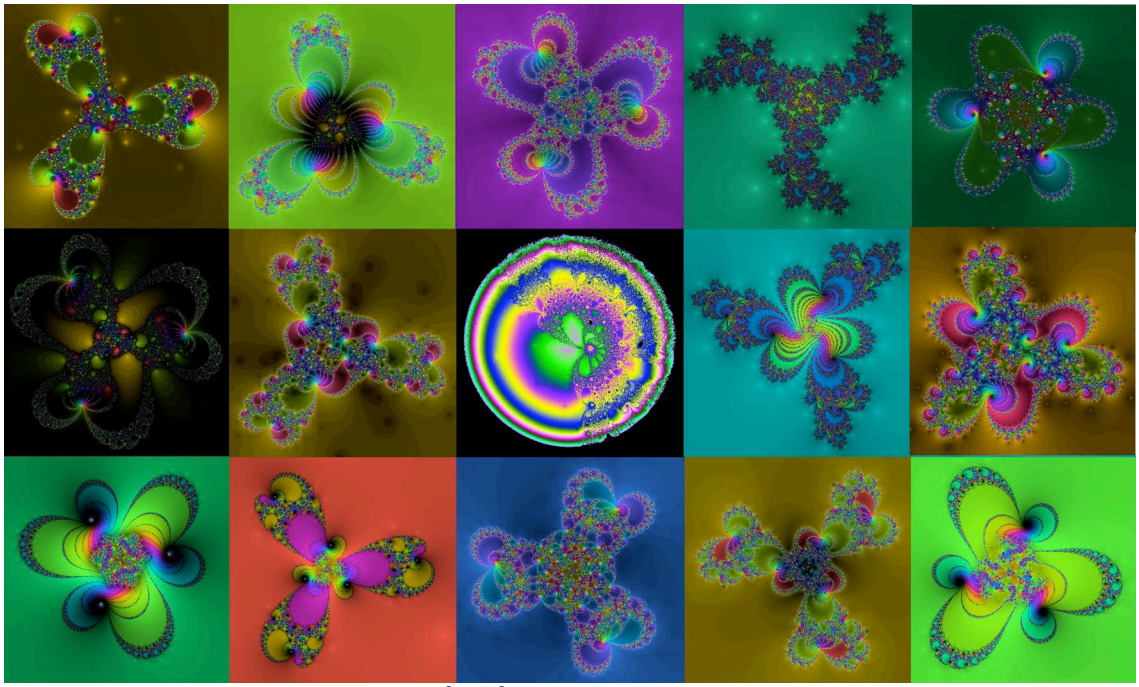

A Mandelbrot bulb portal in the function $f(z)=\frac{z^3-z-c^3}{z^3+c}$ generates an infinite variety of Julia sets. Portals frequently occur when the two parameter planes have coinciding internal bulbs, one of which has interference from the other critical point.

However, if a pre-periodic point is picked in a bulb on either side (if c is picked on the left $-c$ will have precisely the same effect and equivalent location on the right), the right-hand Julia sets will be fractal to 0 as in (11) and the left-hand Julia sets will become unbounded (fractal to ∞, as in (12). (13) & (14) show a value very close to the intersection of the Julia arcs lower-right in (5), giving a right-hand Julia with a double intersection very close to 0 and a left-hand Julia expanding toward infinity with a double 13 period array,

confirming the general picture. Other regions in the parameter plane either show non-inverting behavior (15,16) or complementary exchange e.g. of a 1,3 and a 3,1 mating, as in (17,18).

The function $f_c(z)=\frac{z^2-c^3}{z^2+c}$ can be generalized to the functions $f_c(z)=\frac{z^n-c^m}{z^n+c}$ and $f_d(z)=\frac{z^n-kz-c^m}{z^n+c}$.

These can still be solved in the same way viz: $f_c'(z)=2(c-c^m)z/(z^n+c)^2$, $f_c'(0)=0$, $f_c'((-c)^{1/n})=\infty\to 1$, and $f_d'(z)=2(c-c^m)(nz^{n-1}-k)/(z^n+c)^2$, $f_c'((k/n)^{1/(n-1)})=0$, $f_c'(k)=\infty\to 1$, where $k^n-k=-c$.

Hence we can still use 0 and 1 as the two critical points.

However the original case $f_c(z)=\frac{z^2-c^3}{z^2+c}$ is the only case where the parameter plane has the semi-reflection property $c^{m-1}/f_c(c^{m-1}/z)=-f_{-c}(z)$ because the only solutions of this equation, which reduces to the solutions of $n=\frac{m+1}{m-1}$ for integer powers *m* and *n*. These are (3,2), as above and (2,3), but the power of c also has to be odd so the signs of both c powers in the numerator and denominator flip, eliminating this last case. Figure 7d shows a variety of the parameter planes and Julia sets. These show the unique capacity to generate symmetry-broken higher-degree rational functions with perfect Mandelbrot and Julia sets.

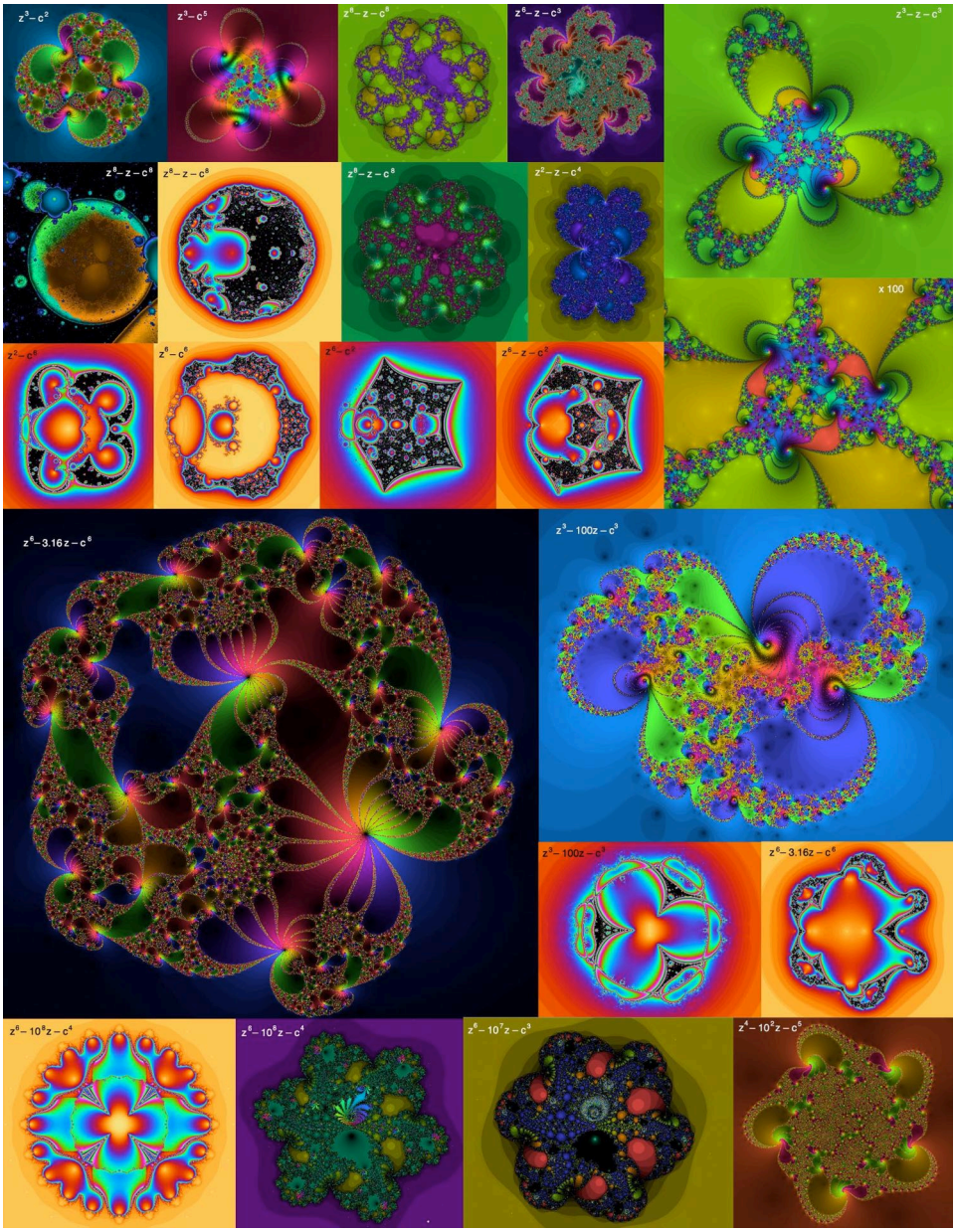

Fig 7d: Varieties of Mandelbrot and Julia set of $f_c(z)=\frac{z^n-c^m}{z^n+c}$ and $f_d(z)=\frac{z^n-kz-c^m}{z^n+c}$.

For $f_c(z)$ and $f_d(z)$, negative powers of *z* can also elicit bounded Julia sets, although many of the Julia sets are now of infinite extent due to the negative powers. Figure 7e shows four functions with sample Julia sets where, in the latter three, the *z* term dominates, so the intrinsic degree 2 and 3 symmetries appear to be completely lost.

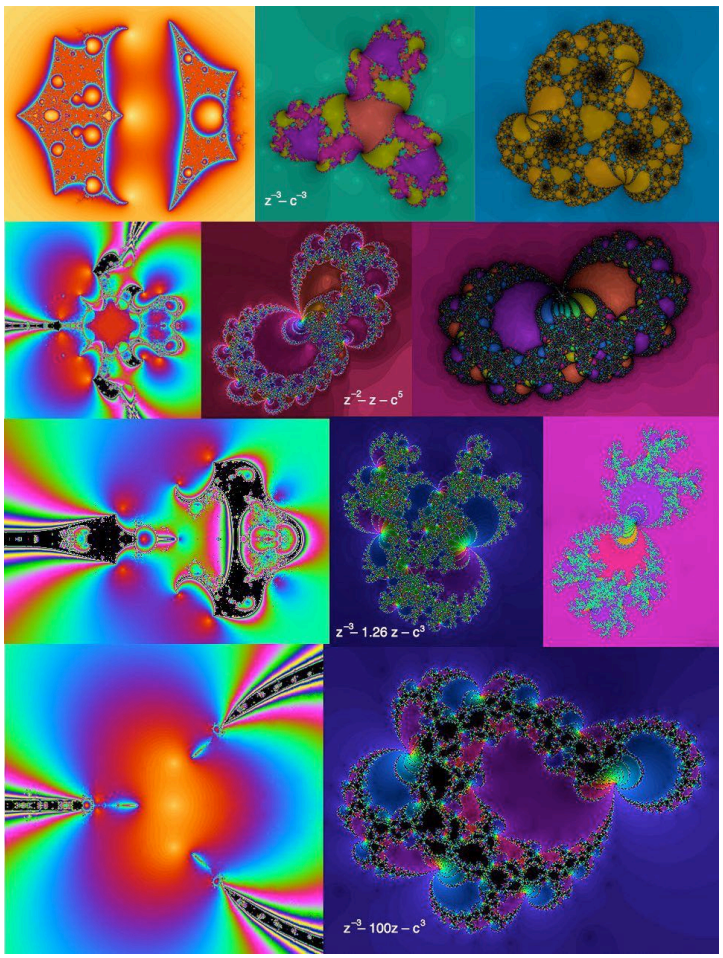

Fig 7e: Examples with negative powers of z. In the latter three, effective degree 1 symmetry-breaking occurs due to negative powers of z in the first term being dominated by the linear second term.

Functional Transcendence

Transcendental functions exp, cos and sin expand the repertoire to include a variety of new phenomena. In fig 8 top row are (A) the escaping fronds of $f(z) = e^z + c$ with increasing periods colour coded (B). The Mandelbrot set here is black. In (C) is the Julia set of e^z/e. The Fatou set here is in black. The Julia set, in colour, consists of an uncountable infinity of closely packed disjoint curves of fractal dimension 2, forming a Cantor bouquet. When the main basin has a higher period, the bouquet can become pinched causing the curves to intersect, as in the period 3 example (D). The exponential function, shown to have a plateau in fig 4 can be perturbed to include polynomial critical points. In (1) is the parameter plane of the critical point *z* = -1 of the function $f(z) = ze^z + c$, which has small clearly defined yellow period 3 bulbs giving rise to period 3 Julia sets (2). These also have green period 6 exponential bays resulting from the plateau critical at negative *x*, as indicated by the green fronds in the period 3 bulb (inset centre). When we change to the multiplicative version $f(z) = cze^z$ in (3) we find we have a local parameter plane very similar to that of the polynomial $f(z) = cz(1-z)$ illustrating the difference between additive parameter planes and multiplicative ones, which operate more simply by scaling rather than translation. A period 3 Julia set is shown in (4).

The trigonometric functions sin and cos are combinations of rotated complex exponentials, which are themselves periodic in the imaginary direction e.g. $\cos(z) = (e^{iz} + e^{-iz})/2$. By superimposing a positive and negative exponential we arrive at a transcendental function with a chain of quadratic maxima and minima along the *x*-axis and consequently the parameter plane of $f(z) = \cos(z) + c$ (5) looks almost exactly like a

chain of copies of the cubic function in fig 5 with corresponding two factor Julia set kernels as shown in (6). Rather than isolated Julia sets as we see in polynomials we now have networks of kernels connected by dendrites, or in a Cantor set arrangement. In (7) we see the multiplicative Mandelbrot set and a Julia set of $f(z) = c\cos^2(z)$, which displays combined quadratic and quartic dynamics and (8) superimposed Mandelbrot and a Julia set of $f(z) = c(\cos(z) + \cos(2z))$, at c = 1.5 + 0.15*i*, showing 3 kernel types.

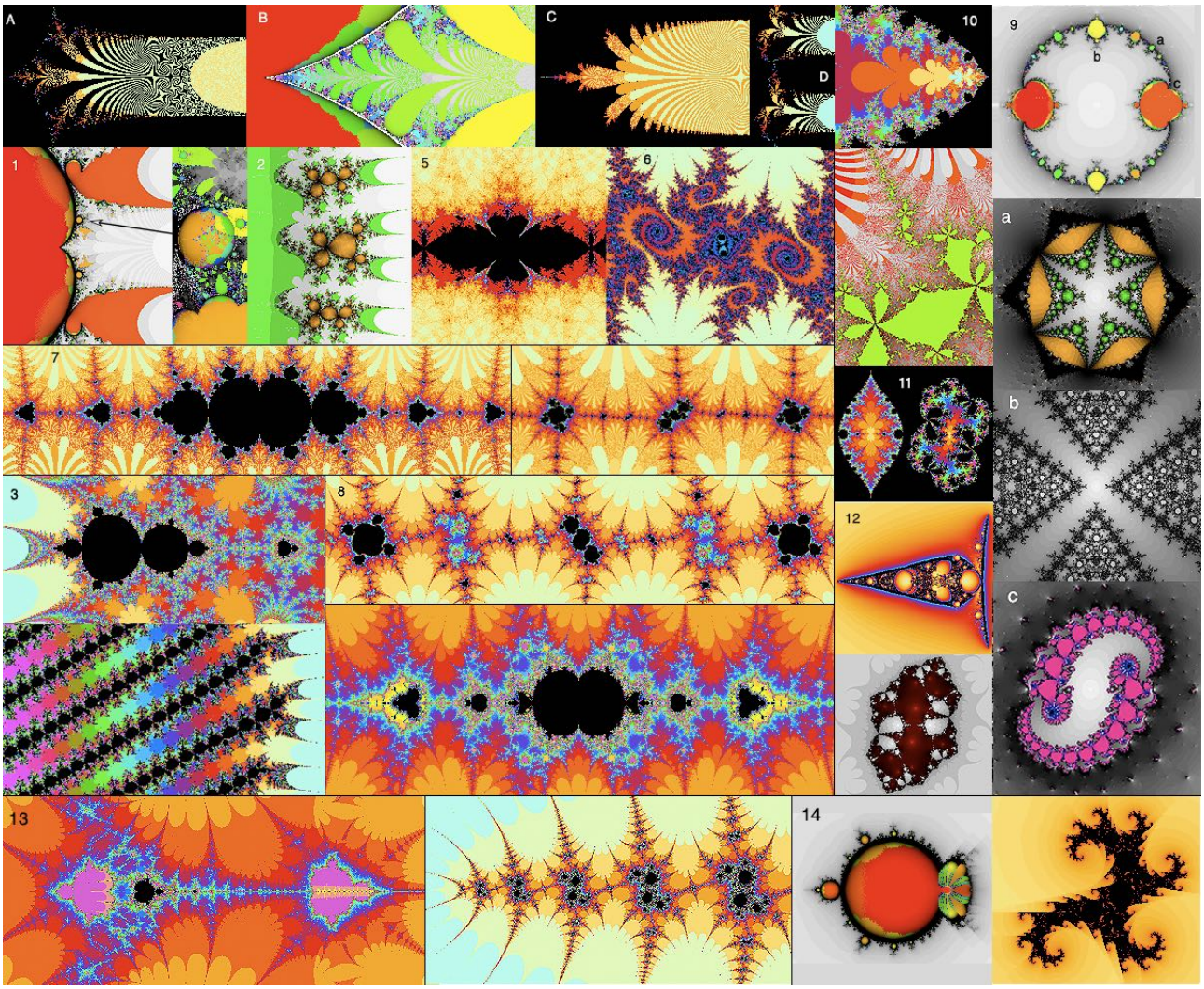

Fig 8: Transcendental parameter planes and Julia sets.

To explore transcendentals with both zeros and infinities, we now look for tractable functions involving the tangent. (9) shows the function $f(z) = c(\tan(z) - z)$, which has derivative $f'(z) = \tan^2(z)$ and thus has alternating zeros and infinities of the derivative. Applying the zero criticals, we arrive at (9) which like the Herman ring example of fig 7, has inward and outward pointing bulbs due to the singularities. Examples of Julia sets (a-c) show the dynamics. Note that the actual periodicities of the bulbs to the left and right differ although the parameter plane is symmetric because the winding involves real sing inversions in one half but not the other, resulting in different 'spirograph' periodicities in the ascending periods.

Journey through the top bulb of $f(z) = c(\tan(z) - z)$: https://www.youtube.com/watch?v=LOxr2B-VfF8

(10-12) illustrate the parameter planes and a Julia set of $f(z) = cz^{-1}e^{1/z}$, $f(z) = \cos^{-2}(z^{-1}) + c$, $f(z) = c\cos^{-1}(z^{-1})$, showing **rational transcendental** functions. (13) shows the parameter plane and Julia sets of $f(z)=c\cos(z^{1/2})$. Half-integer powers work seamlessly for the cosine function because it has only even powers of *z*, $f(z) = c\cos(z^{3/2})$ is also shown in fig 10. (14) shows the logarithm $f(z)=c\log(z)$ which fractally splits the complex plane, as do non-integer powers of *z*.

Dark Heart contains a series of further examples to explore various issues with transcendental functions. For example attempts to produce other kinds of critical points than those of fig 4 appear to fail because Fourier transforms, such as those producing square or triangular waves in the limit converge to a real function on the *x*-axis. Also included are log function examples, which are not defined on the complex plane, but on a Riemann surface, requiring the plane to be cut in a way which results in fractal splits in the Mandelbrot and Julia sets. A complex function implementation of the Collatz 3*n*+1 problem is included.

The Ultimate Challenge: Zeta and L-functions

We now turn to the most challenging functions of all, those defined by Dirichlet series, requiring analytic continuation using gamma functions and Mellin integral transforms to put together a complete picture. I have designed Riemann Zeta viewer to specialize in these functions, including Rieman zeta, and the related eta, xi and Dirichlet and other L-functions, running right to the limits of current analytical number theoury research. This runs in the same way as Dark Heart but with some additionally focused controls.

The archetypal and most famous example is the Riemann zeta function shown in fig 9 - 1(a). This has a single infinity at $x = 1$ due to the harmonic series $\sum_{n=1}^{\infty} 1/n$, multiple (trivial) zeros along the negative *x*-axis due to the analytic continuation, and a string of irregularly placed (non-trivial) zeros forming a kind of Fourier transform of the primes along the critical line $x=1/2$. In fig 9, 1(a) is the Riemann zeta function showing trivial *x*-axis zeros, non-trivial on $x = 1/2$ zeros and the red infinity at $z = 1$. In (b) is the derivative of zeta showing the critical points. (c) shows the additive parameter plane $f(z) = \zeta(z) + c$ for the critical plateau $z \sim 1000$ showing sample Julia sets with the periods illustrated filling the right half plane. In (d) the multiplicative parameter plane is portrayed.

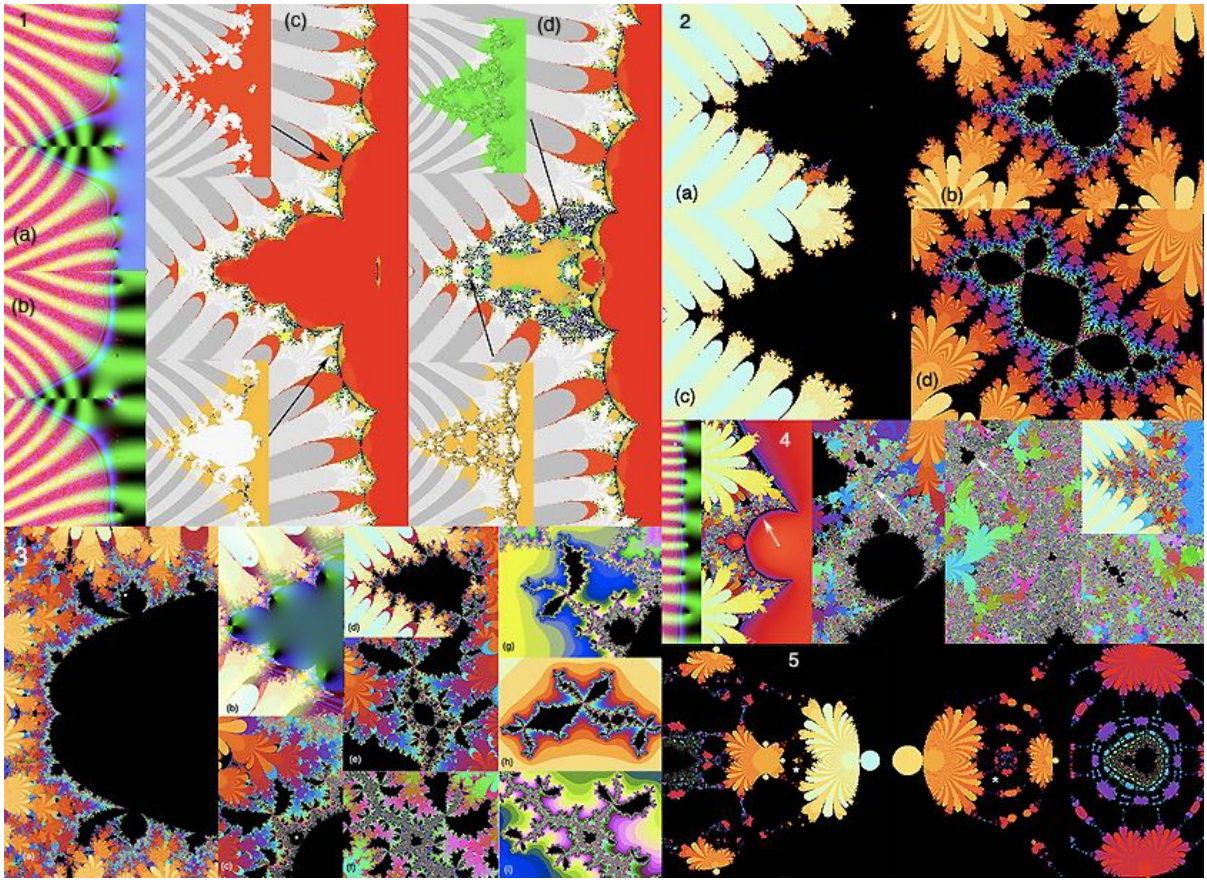

Fig 9: Sample illustrations of parameter planes and Julia sets of the Riemann zeta function.

The four illustrations in (2) show the dark heart at the end of the central valley for the critical point $z = -17.3$ along with a sample period 3 Julia set, (3) the central basin with quadratic bulbs of critical $z = -15.33$ and obvious cubic interference similar to fig 5. (4) Details of the basin of the non-trivial critical point around $z = 1/2 + 95i$ exploring a satellite dark heart and an associated period 3 Julia set, and (5) a dark heart in the singularity island for the critical point $z = -13.29$. These provide an introductory view of the immense

complexity of the fractal geography of Riemann zeta, whose parameter planes and Julia sets involve an infinite number of trivial and non-trivial critical points whose critical values lie all over the spectrum and whose localities are as varied as we can possibly find. The Julia sets are dynamically responding to the dynamics of all the critical points, so are as complex in their dynamics as the infinite collection of parameter planes. The geography of the multiplicative zeta function is in many ways even more intriguing (see fig 9b).

The Riemann zeta function is formally defined as either a sum over negative powers of the integers or an Euler product over the primes $\zeta(z) = \sum_{n=1}^{\infty} n^{-z} = \prod_{p\ prime} \left(1 - p^{-z}\right)^{-1}, \mathrm{Re}(z) > 1$. But neither definition is convergent to the left of 1, but can be analytically continued to the entire complex plane, using the gamma function $\Gamma(z) = \int_0^{\infty} t^{z-1} e^{-t}\, dt$ - a generalization of *n*! =n(n-1)…3.2.1 - to derive the functional equation $\Gamma\left(\frac{z}{2}\right) \pi^{-\frac{z}{2}} \zeta(z) = \Gamma\left(1 - \frac{z}{2}\right) \pi^{-\frac{1-z}{2}} \zeta(1-z)$ expressing values for $z < 0$ in terms of those for $z > 1$.

The functional equation would enable us to produce a portrait were it not for the fact that in the critical strip $0 < z < 1$ the function is still divergent, so we have to resort to a trick, which is to use the fact that the Euler eta function converges for $z > 0$ because it is an alternating series $\eta(s) = \left(1 - 2^{1-s}\right)\zeta(s) = \sum_{n=1}^{\infty} (-1)^{n+1} n^{-s}$ and can be used to represent zeta. So we use eta to get zeta for $z > 1/2$ and the functional equation to get $1 - z$.

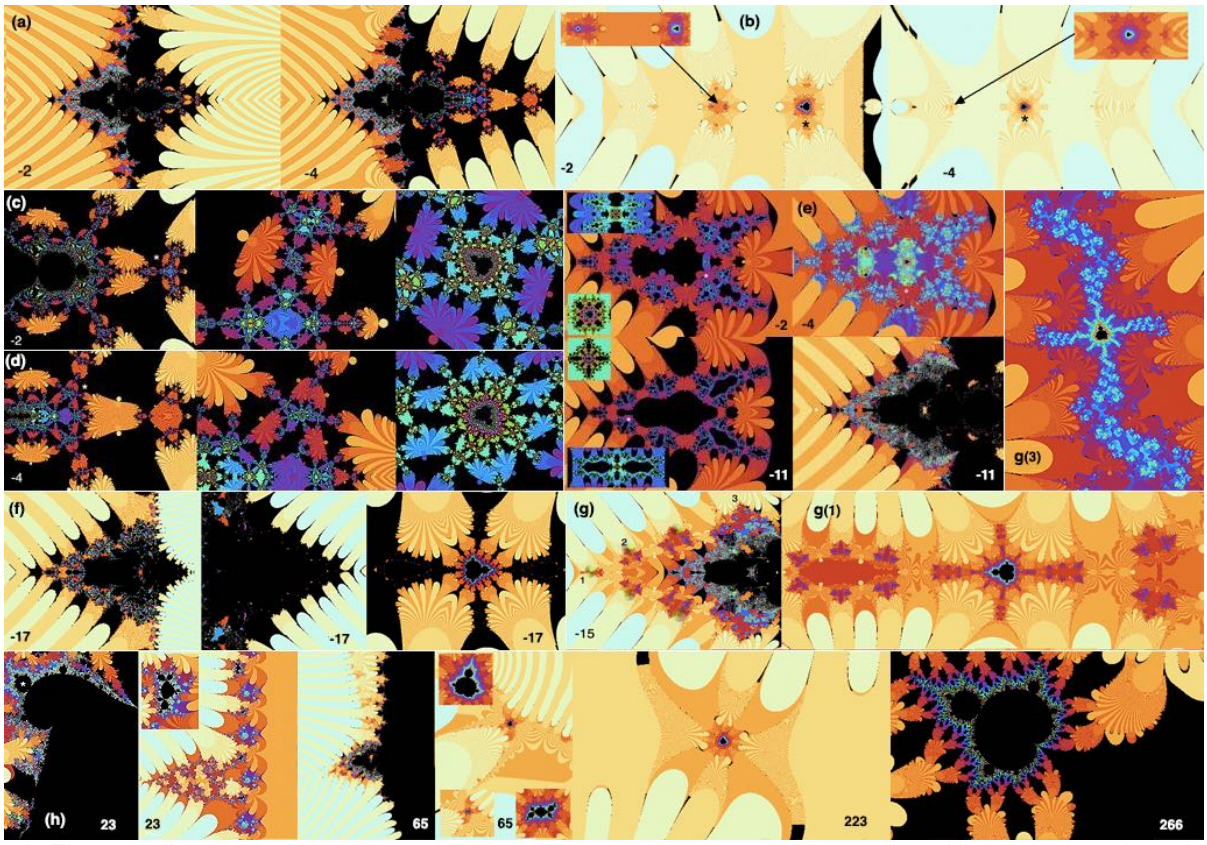

Fig 9b: The multiplicative parameter planes of the zeta function have many more surprises: (a) As we move through the negative real criticals, the global parameter plane goes through tectonic shifts in which the ocean in the right half plane becomes drained with new landscapes emerging. (b) The first negative real criticals near -2 to -13 have miniscule critical values, resulting in huge Mandelbrot sets from the large *c* values involved. (c, d) They also generate fractal Mandelbrots in the island generated by the singularity at $z = 1$, and in (e) we find more in the central basin. (f) The succeeding negative criticals from -17 on have vast critical values giving Mandelbrot satellites pinched in the vast coastline. (g) The boundary case -15 has a string of 'jewels' in the crown of the central basin (1, 3). Finally the unreal criticals neighbouring the critical line zeros, each have their own well-defined Mandelbrot satellites.

Explosions of additive Riemann zeta Julia sets: https://www.youtube.com/watch?v=spXaRTJPtvk

The situation is even more complicated for other zeta and *L*-functions $\zeta(z) = \sum_{n=1}^{\infty} a_n n^{-z}$, which may have higher degree Euler products and multiple gamma factors and no eta function to smooth the critical strip, but here a Mellin integral transform can be used in the central region.

Here for illustration is the Mellin transform version of the Riemann zeta function analytic continuation.

$$\zeta(s) = \pi^{s/2} / \Gamma\left(\frac{s}{2}\right) \int_0^{\infty} y^{s/2} \left(\theta(iy) - 1\right) \frac{dy}{2y}, \phi(t) = e^{-\pi t^2}, \theta(iy) = \sum_{n \in \mathbb{Z}} \phi(ny) = \sum_{n \in \mathbb{Z}} e^{-\pi n^2 y}, \theta(iy) = \frac{1}{\sqrt{y}} \theta\left(\frac{i}{y}\right)$$

$$\pi^{-s/2} \Gamma\left(\frac{s}{2}\right) \zeta(s) = \int_1^{\infty} \left(y^{s/2} - y^{(1-s)/2}\right) \left(\theta(iy) - 1\right) \frac{dy}{2y} + \frac{1}{2}\left(\frac{1}{s-1} - \frac{1}{s}\right) = \pi^{-(1-s)/2} \Gamma\left(\frac{1-s}{2}\right) \zeta(1-s)$$

A full set for more diverse functional equations used is included with the RZ flight manual.

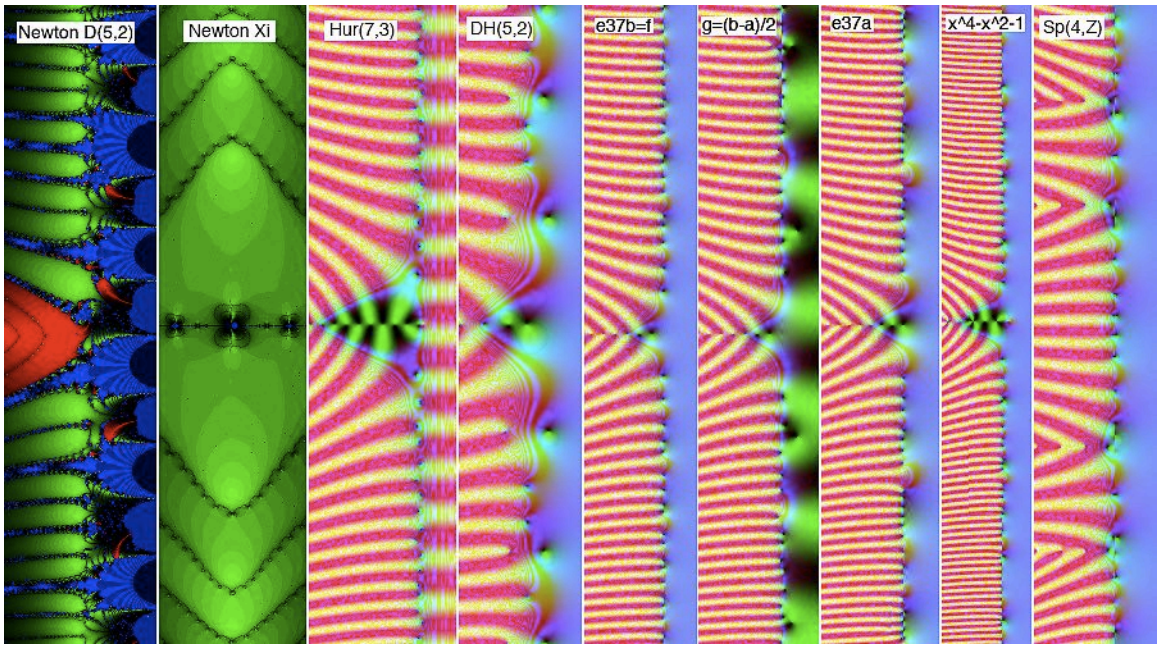

Fig 9c: Left to Right: Julia sets of Newton's method on the Dirichlet L-function (5,2) and Riemann xi function, a Hurwitz zeta function and a Davenport Heilbron function both with off-critical zeros, two Elliptic curve L-functions merged using an RZV C-script to produce the echelon modular forms, the Dedekind zeta function of the rational extension field of x^4-x^2-1 with central region overlayed using Computel, and a fourth degree symplectic L-function.

Riemann Zeta viewer can portray virtually any zeta or *L*-function which can be represented by analytic continuation via gamma factors and Mellin transforms, including those of number fields, elliptic curves, and modular and Maas wave froms on hyperbolic spaces. Parameter files for all the known examples are included with the package. The RZ flight manual illustrates the use of a third degree Maass *L*-function to generate Mandelbrot and Julia sets.

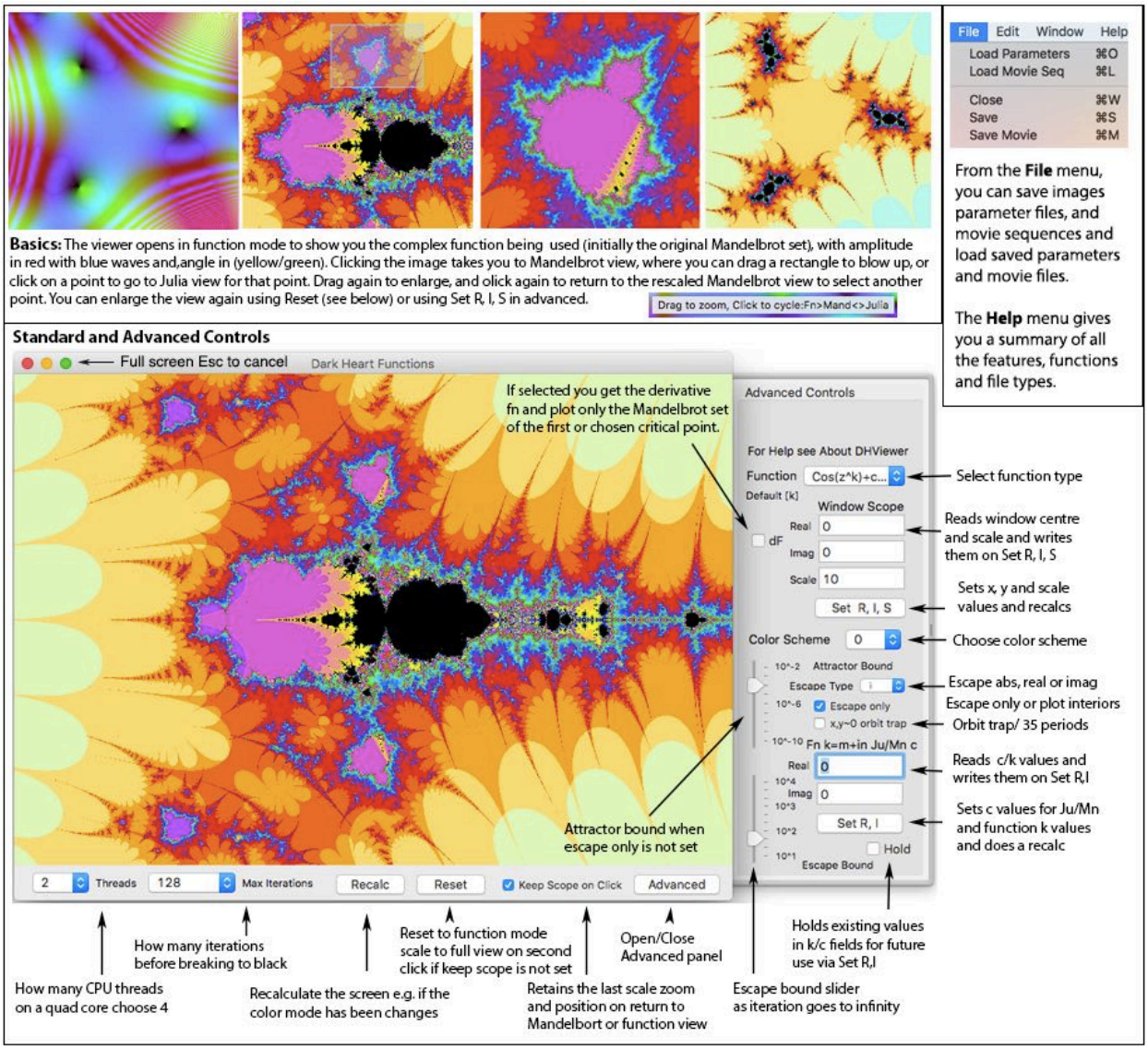

Fig 10: Dark Heart controls portraying $f(z) = c\cos(z^{3/2})$

Dark Heart Complex Function Viewer Flight Manual

Dark Heart allows you to interactively explore the fractal dynamics of a wide variety of complex polynomial, rational and transcendental functions.

See http://dhushara.com/DarkHeart/ for research, updates and source code.

DHViewer is a matched pair application with the Riemann Zeta Function Viewer, RZViewer, which explores the corresponding L-functions based on Dirichlet series rather than power series.

Basics:

Drag a rectangle to enlarge a portion of the current image.

Click a point to cycle:
Function > Mandelbrot > Julia(*c*)*
**c* at the clicked point on the Mandelbrot set.

With ***keep scope*** on Julia view will take you back to the previous Mandelbrot screen to save computation time and enable you to explore several related Julia sets in the region. It will also retain scope on a reset to function mode. To return to full screen unclick keep scope and reset twice.

By clicking, you can investigate the discrete dynamical parameter plane (Mandelbrot set) of the critical values and the Julia sets of $z=f(z,k,c)$ for $(x,y)=c$, with k an additional parameter associated with the power.

The additional parameter *k* can be set to a value other than *k*=2 by using **Set R, I** in advanced mode. It generally sets the exponent but for Sin(z)/z it sets the number of critical points. For *c*Cos(*z*^*k*), Cos(*z*^*k*)+*c*, one can set half-integer values such as *k*=0.5 to get inverse quadratic cosines.

The controls all have ***floating help panes*** to guide you.

The window can be resized to suit in real time, resulting in a refresh and recalculation, or set to full screen using the green button. Esc to return to windowed mode.

Standard settings:

Threads enables a multi-core machine to work faster using as many threads as coprocessors. ***Max Iterations*** gives how many iteration steps of a point on the Julia or Mandelbrot set before maximum iteration cutoff. ***Recalc*** refreshes and recalculates the existing screen. ***Reset*** returns to the function and default scale but doesn't alter any other settings. ***Keep scope on click*** keeps the window centre and scale when clicking between Mandelbrot, Julia and function, so the other parameters can be changed without changing the point of view.

Menus:

About gives a complete instruction summary. ***Save*** saves the current window's image as a tif file and all the settings for a given calculation in a text file (see format below), enabling you to save all the parameters for future investigation and redrawing. It will overwrite any files of the same name. ***Load Parameters*** will load a previous calculation and redraw it. ***Load Movie Seq*** loads a sequence text file to generate a series of images to make a movie (see format below). ***Save Movie*** saves the sequence as a series of LZW compressed tifs, which can then easily be composited into a movie e.g. using open image sequence in Quicktime Player 7 (https://support.apple.com/kb/dl923?locale=en_US), or using the included app Mpeg Streamclip. ***Print*** enables an image to be printed or exported to pdf format. ***Page Setup*** needs to be landscape in 80% to fit the standard window on one A4 page. ***Help*** directs you to the about menu.

Advanced Settings:

Pop-up Menus: ***Color schemes*** can be changed in real time using the color pop up menu. All the other controls require window recalculation.

A Variety of Functions as discussed above can be explored using the function pop-up menu.

The ***escape bound*** can be set but resets on function change to the one most appropriate for the given function.

Buttons and Text Fields: Current window parameters and *c* values can be read out from and written into the text fields and set by pressing the appropriate button. Numbers in the text fields are double precision and may appear in floating format e.g. -7.000000186963007e-05 manifestly too large to see in their entirety in the text box without dragging or selecting all and copying. The Julia *c* values will be overwritten by the Mandelbrot critical point origin and current Julia click point each cycle but can be manually re-entered as desired. You can use ***dF*** as a computation of the derivative of the function to locate critical points as its zeros and then when you click twice and carry it to Julia with this *c* value, checking ***hold*** will keep it in the ***real*** and ***imag*** fields so you can click ***SET R,I*** to get the Mandelbrot set to have the correct critical point. While ***dF*** is on, you will only get the chosen Mandelbrot set of one critical point rather than all superimposed. This enables you to explore individual Mandelbrot sets of each critical point by inserting it in c.

Tick boxes: There is an imaginary axis ***orbit trap*** option. ***Escape only*** tests only for escaping points. When turned off the routine also checks for attractors up to period 18, coloring internal basins, but this can also flood surrounding regions if the attractor bound is set too high for the region being investigated. When color mode is 1 instead ***orbit trap*** doubles the period search to 35.

Sliders: ***Attractor bound*** adjusts the size of the epsilon neighbourhood testing for fixed point or periodic attractors. ***Escape bound*** sets the numerical bounds on points escaping to infinity. The **escape type** is usually **a** (absolute) for polynomials and rational functions and **r** (real) for exponential and **i** (imaginary) for trigonometric functions. Setting **r+** for real positive enables fine depiction of exponential Cantor bouquets, as is **i+** for cos and sin.

Color Schemes: There are several **colour schemes** for function, Mandelbrot and Julia, which are useful at highlighting different features:

Function: (0,4) rgb = logarithmic abs(z), blue cosine abs(z), green ang(z). (1) rgb = real, imaginary and angle, (2) bg = abs(z) and angle (3) rgb = real, imaginary and cos(angle).

Mandelbrot: (0) Non-repeating sine wave colours (1) **Period-coded** colours that show the periodicities inside the

dark hearts when ***Escape only*** is off. (2) **RGB ranked colours** which can also show which attracting fixed point is involved in Newton's method for *k*=3 and the Herman ring (3) **Attractor-coded** rainbow which highlights individual attractors in rational mappings, including Newton's method, which also shows the mapping on individual sub-regions of Julia sets. (4) Same as 0 but with square root behavior. Very good for highlighting boundaries and complex dynamics. (5) KBCGYRM colour rotation with W. Modes 1 and 5 also portray the velocity coded cosine in b&w for non-periodic rotations with **Escape only** off and ***orbit trap*** is set. You can adjust the effect for different rotation rates using the escape radius slider.

Period coding in mode 1 gives escaping points tending to real infinity shades of grey from white to black in waves by iteration number in the same way as mode 4, giving clean exteriors, with periodicities coloured approximately by the following **1 2 3 4 5 6 7 8 9 10 11 12 13 14 15 16 17** 18 mildly shaded by iteration number. You need to **turn off escape only** and set the **attractor bound** e.g to **10^-2** (default). When ***orbit trap*** is set in Mandelbrot mode, it doubles the period search to 35 colouring the higher values in lighter shades mod 18, but this will also slow the computation. In Julia mode periods always go up to 35. With ***orbit trap*** off you can adjust the **escape bound** slider to get the right degree of color-coded shading. For periods up to 18, this shades to black but for higher periods with lighter shades, the base colour varies. With ***orbit trap*** on both views portray the velocity coded cosine in b&w for non-periodic neutral rotations, as in mode 5 and gives an average colour coded view for periodic sets.

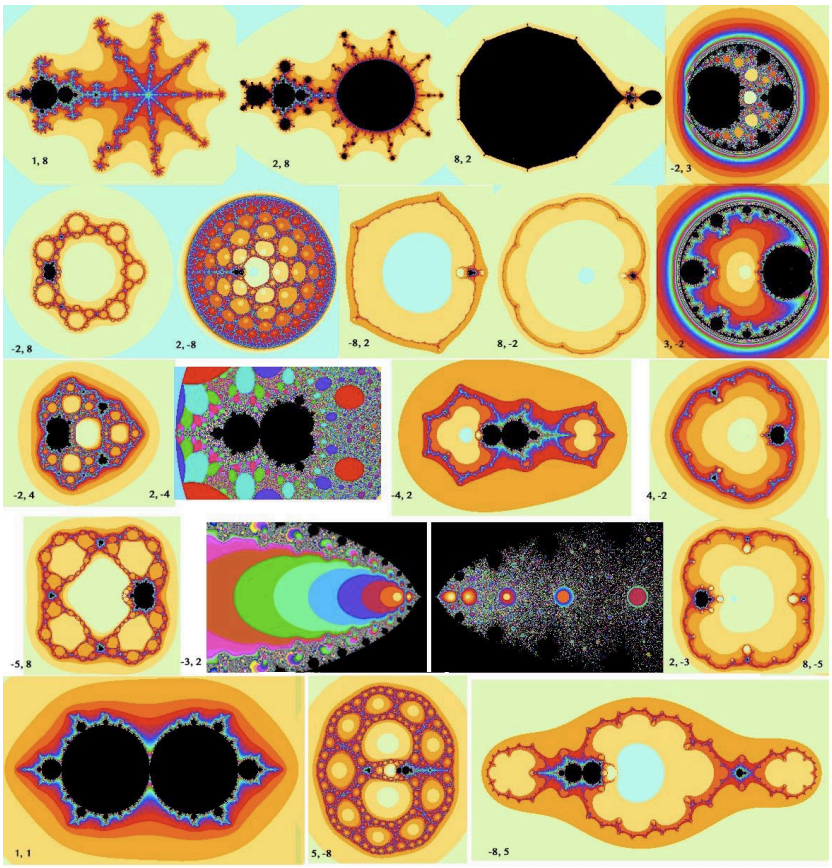

Fig 10b:Variety of parameter planes using the second menu function: *cz^m(1-z)^n*

Attractor coded colours in modes 2 and particularly 3 can distinguish each basin by color in periodic Julia sets and when there are several attractors, such as in the **Newton's method** iteration. Occasionally, e.g. when you set the c values of a Newton Julia set to 0, this may give a Moire pattern anomaly due to underflow in the angle, which you can suppress by choosing a neighbouring non-0 point e.g. 0.01.

Julia: (0) Sine wave colours, (1) periodicity coded colours, as above, (2) RGB ranked colours, (3) attractor coded colours by argument. (4) As 0 but with square root behavior. Very good for highlighting boundaries and complex dynamics. For example the classic quadratic Seahorse Valley Julia c = -.74543 + .11301i. (5) KBCGYRM colour rotation with W, as above.

Functions:

You can investigate a variety of functions, [1] *z^k+c,* [2] *cz^m(1-z)^n,* [3] *z^m-nz+c,* [4] *(z^m-n)(z+c),* [5] Int*(z^m-n)(z+c),* [6] *z^k+(c-1)z-c,* [7] Newton's method on the previous function i.e. *((k-1)z^k+c)/(kz^(k-1)+c-1),* [8] *cSin(1/z),* [9] *cCos(z^m)^n,* [10] *Cos(z^k)+c,* [11] *c(Sin(z)+Sin(2z)/2),* [12] *c(Cos(z)+Cos(2z),* [13] *cSin(z)/z,* [14] *c(z^m)e^(z^n),* [15] *(z^n)e^z+c* [16] Transcendental (see list below), [17] Rational (see list below), [18] *z^m-10qz^-p n=p.q* [19] *cz^(z+k),* [20] *c(z^3+(k-1)z^2-kz),* [21] *e^(-z^k)+c,* [22] Quintic, [23, 24] Herman ring function, [25] generalized Collatz iteration, [26] *z^m+cz^-n k=m+in* [27] *cCos(z^m+z^-n),* [28] Milnor rational examples, [29] *z^m-10qz^-p n=p.q.* [30] *z^3-(m+in)z* [31] Mating (see below).

Here is a function number list mapping to the app menu.

function	menu
1-3	1-3
18	4
20	5
4-15	6-17

19	18
21	19
22	20
16	21
17	22
23 on	23 on

Some of the transcendental functions are comparable with the gamma and zeta functions in Riemann Zeta Viewer. All but a few of the functions are unique valued on the complex plane. Although cCos(*z*^(1/2)) has no branch cuts, all those implicitly involving log(*z*), including *cz*Log(*z*), and *cz*^(*z*+*k*), do.

The function *z^m-nz+c,* can be used to explore variations of the parameter planes as we move from *z^m+c* by increasingly separating the critical points. *n* can be either positive or negative, giving real or imaginary critical points in the cases of *z^3 ± z*.

The functions *z^m-10qz^-p n=p.q* and *z^m-10qz^-p n=p.q* (listed at the end) are accessed by inputting k=[m,p.q] e.g. for *z^3-2z^-1* we input *k* = [3, 1.2]. You can also input negative values for *p* e.g. to get *z^3-z^4* we input *k* = [3, -4.1]. Some functions might look more interesting with small values of *q* which bring the parameter planes into intersection.

You can input positive or negative values for n in *(z^n)e^z+c*. The value n=0 has only the exponential plateau at x=-1000 as critical and n=1 has this and the other critical at x=-1 as criticals so you can see the effect of both together in mode 1. To turn off and see the Mandebrot bulbs select dF to get only x=-1 critical.

Transcendental (k = (m,n))

1 c(e^z-1) *2* *z*Log(*z*)+*c,* *3* *cz*Log(*z*), *4* *z^z+c,* *5* *cze(-e^z),*
*6 z=z*e^(-e^z)+c,* *7* *z=(z^2-2z+2)*e^z*c,* *8* *z=(z^3-3z^2+6z-6)e^z*c*
*9 n=1..4 step triangle wave sum[j=0..n] cos((2j+1)z)/(2j+1)^2 *c*
*10 n=1..4 step square wave sum[j=0..n] (-1)^n cos((2j+1)z)/(2j+1) *c*
*11 -log(cos(z)*c* whose derivative *tan(z)* has both zero and infinite criticals.
*12 (tan(z)-z)*c* whose derivative *(tan(z))^2* has both zero and infinite criticals
*13 (z-tan(z)+((tan(z))^3)/3)*c* whose derivative *(tan(z))^4* has both zero and infinite criticals.
14 z-atan(z)+c
15 ce^c(z-(1-c))e^z input real c>1 in Julia mode
16 cze^(..n times..(e^z)) n-fold tetration (you will need to choose a critical point using dF in function mode and then homing in on a critical point, click to julia and select hold to insert the c into mandel mode with Set RI)
17 ce^(..n times..(e^z)) n-fold tetration

Rational (k = (m,n))

*1 z^2-1/nz*c,* *2* *((z^3-1)/(z^2-1))^2+c,* *3* *(z^6-1)/(z^4-1)+c,* *4* Int(z^3(z+1)(z^2-1))+c,
*5 ((z^3-1)/(z^2-1)) ^2*c,* *6* *(z^n-z)*c,* *7-8* Peterson graph zeta function and reciprocal (*+c* **c* 0/1)
9 1/(z^2-c2)+c (Milnor) *10 2z^3/(27(2-z))+c* (Milnor)
Rational PrePer(2,1) Needs scale=200 Esc only off Esc Bd =10^4
11 0 1-8(c+8)/(c-8)*(1/z-1/z^2)*
Rational Period 1 mating *11 1* Per1(0) *z=z^2+c*
Rational Period 2 matings *11 2, 2.5* Per2(0) *z=c/z/(z+2), z=(z^2+c)/(z^2-1)*
Equivalent symmetric Julia representations
Rational Period 3 matings. *11 3, 3.5* Per3(0) *z=(z-1)(z-c/(2-c))/z/z, z=(z^2+c^3-c-1)/(z^2-c^2)*
Asymmetric and symmetric Julia reps.
Rational Period 4 matings.
11 4, Per4(0) *z=(z-c)(z-(2c-1)/(c-1))/z/z,* Asymmetric.
*11 4.5, 4.75 z=(z*z+((c-1)±sqrt(5*c*c-6*c+5))/2)*(1-c*c)-1)/(z*z-c*c)* Double plane symmetric Julia reps.
*12 z^2+exp(2*pi*i*c)z* Explores boundary of quadratic central domain c=n e.g. n=0.618034
*13 z^3-3cz+sqrt(4*c*(c+0.5)^2)* Cubic Per1(0)
*14 2z^3/(3c-2)-3cz^2/(3*c-2)+1* Cubic Per2(0)
*15 z^3+cz^2+z*cexp(2*pi*i*n)* Cubic exp(2*pi*i*n) e.g. n=0.618034 (Reset on 15)
16 (c^3-c+1)/(c^2(c-1))z^3-(c^4-c+1)/(c^2(c-1))z^2+c Cubic Per3(0)
17 (c^2-1)/(c^2)z^3-(c^3-1)/(c^2)z^2+c Cubic PrePer(2,1) 0>c>1>1
18 1/c/(c-1)(z^3-z^2)+c Cubic PrePer(1,2) 0>c>1>c
19 0,1,2,3 Cubic PrePer(2,2) 0>c>1>d>1 *4* same as 17 *5* equivalent to 18
20 0,1,2,3 Cubic Per4(0) Four split parameter planes
When **dF** is **on** the particular split plane is chosen. with its Julias.
When **dF** is **off** a superimposed plane is generated. If you start with n=0 you can then click through the four Julia sets by turning on **hold** after the

first and pressing **Set R,I** after each click to retain the original location.
21 0,1 Cubic PrePer(1,3) Two parameter planes.
Per1(0) is *cz^2(z-1)* (Fn 6 with k=0. Equivalent to Fn 2 with *z* > -*z*)
PrePer(1,1) 0>1>1 is *cz^2(z-1) +1* (Equivalent to *c(z^3-2z^2+z)= cz(z-1)^2* 1>0>0, fn 6 with k=-1, since the two iterations commute under [c,z]->[c,1-z])
Parameter files for Per1(0), PrePer(1,1) are included in the quintics folder.
22 c^2(2c-3)/(3-3c)(z*z*z-z*z)+1/c* Critical 0 -> 1/c -> crit 2/3.
The quintic folder also contains cz^2[z-1]+2l3 where crit 0 -> crit 2/3.
23 c(z+0.5/z^2) Similar to Newton's example with rotational symmetry.
There is a similar example Mandel1 in Milnor. Both use mode 3 to effect.
24 (z^2+10qc^p)/(z^2+c) n=p.q>=0, (z^2-10qc^abs(p))/(z^2+c) n=p.q<0
E.g. (24,-3.2) is *(z^2-2c^3)/(z^2+c)*
25 (z^3 -10.qz ± c^p)/(z^3-10.qz+c) n=p.q as above for ±
26 (z^3 ±10.qc^p)/(z^3+c^2) n=p.q as above for ± E.g. (26,-4.1)
27 (z^q+c^p)/(z^q+c) n=p.q n<0 ->q<0 E.g. (27, 3.2) is *(z^2-c^3)/(z^2+c)*
28 (z^q-z+c^p)/(z^q-z+c) n=p.q n<0 ->q<0

Matings are rational function Julia sets which have complementary components consisting of two types of quadratic Julia set fractally intertwined. The above rational examples Per*k*(0) define parameter planes of quadratic rational functions with the critical point having a fixed period but the other one free. The Julia sets of these exemplify matings of the root Julia set of periodicity *k* with the spectrum of Julia sets defined by the other critical point's *c* values in the parameter plane. A broad palette of precompiled Medusa mating parameter files are included in the matings folder which upload to the **Mating** function *f(z)=(az^2+1-a)/ (bz^2+1-b)* where *a* and *b* are input as coefficients in the file. These allow one to use the Medusa algorithm to define the rational function mating the Julia sets having two fractional external angles p/q and r/s. **Medusa** is included with Dark Heart, with source code, as a command line tool which can be run from Mac Terminal by typing "./Medusa". The final complex coefficients of this once convergence is reached can be portrayed in Dark Heart by entering them into the *c*-script mating.c. Medusa is consistent with the **symmetric** representations of Per*k*(0).

By saving and adjusting the coefficients and powers of c in the text file, and reloading, you can portray parameter planes and Julia sets of **any polynomial up to degree 5**. The application will automatically find the critical points up to degree five. The application comes preprogrammed with a sample quintic *f(x)=x^5-3.25cx^3+2.25x+c* to illustrate how to program different parameter planes. This will be overwritten on loading a saved parameter file. You can use this to replicate several parametrizations e.g. *z^4+(c-1)z-c* can be cloned as *z^4-sz-1+s*, *s*=1-*c*. See parameter file contents below for details.

Newton's method on the *k*-th roots of unity shows how seeking for the roots of a function by iteration can leave behind a chaotic boundary set where the iteration can't reach the attracting roots. To see the standard Julia set of the roots of unity, insert the value (0,1) into Julia mode, since *c* = 1 gives *z*^*k*+(*c*-1)*z*-*c* = z^*k*-1. *If* this is run in attractor coded modes 3 (or 2) the basins are individually colour coded. For *k* = 3 in RZ 2.0.6 you can set the imaginary part to -1 to get the repelling version. Higher powers don't work here because the forward Newton's method has critical points determined by *z*=0 and the *c*-displaced roots of unity, since the derivative of *g*(*z*)=*z*-*f*(*z*)/*f* '(*z*) is *g*'(*z*)=*f*(*z*)*f* ''(z)/(*f* '(*z*))^2, and the super-attracting displaced roots have infinite parameter planes and can be ignored, but the inverse repelling process gives *g*'(*z*)=2- *f*(*z*)*f* ''(z)/(*f* '(*z*))^2, whose 2*k*-2 degree equation can be solved only for k ≤ 3. This dynamic is almost entirely repelling except for Julia kernels determined by the small isolated Mandelbrot islands.

The **Herman ring** in *cz^2(z-4)/(4z-1)* is a famous special rational function case with an irrational annular flow for Julia sets for which c= exp(i*g*pi/2) = 0.564635 + 0.825341i, or c= exp(i*g*pi)= -0.3624 + 0.9320i where g = (5^(1/2)-1)/2 the Golden Mean. Choose **colour mode 5** and have **escape only** turned off and input the precise numbers into Set R/I and you can see the rotation pictured in cosine of the velocity. You can adjust the effect for different rotation rates using the **escape bound** slider.

You can view the Herman ring system in two configurations, making Mandelbrot sets for each of the two parametrizations *cz^2(z-k)/(1-kz)* and *kz^2(z-c)/(1-cz)*. If you switch from the second function to the first just before clicking a point in Mandelbrot mode it will retain Mandelbrot mode, save c as k, and allow you to input the second parameter c by clicking. You can see the k=m,n values in Set R, I in function view. A further click takes you to the *k*, *c* Julia set.

Similarly to the Herman ring, the standard quadratic function *z^2+c* has Julia sets with irrational flows on Siegel discs between all the fractal bulbs on its boundary for example at c = -0.390541-0.586788i , which is a solution of the cardioid c=exp(ig2pi)/2-exp(ig4pi)/4 for g = (5^(1/2)-1)/2. You can contrast this with the period 3 parabolic petals on the boundary of the cardioid c=-0.125000-0.649519i, which clearly shows it is in transition between period 1 and 3 at 1024 in mode 1. The 20 leaf parabolic Julia set c = .27334 + .00742i shows its leaves on mode 5 with escape bound 10^3 at 4096 iterations.

A series of C-script examples of rational parameter planes are also provided under the **Milnor** function option which explores the rational iterations $z \to (z+r.c+s+1/z)/c$ and its dual $z \to r\,(z+c+s+1/z)/(c-s)$.

One can use *z^m-nz+c,* and *(z^m-n)(z+c)* in mode 3 with orbit trap selected to explore **moduli spaces** of these Mandelbrot sets, as they have dihedral symmetries. Two c-values c1 and c2 of such functions are conjugate under a Mobius transformation f(z)=(*az+b*)/(*cz+d*) if and only if *c*2=*w***c*1 with *w* an *p*-th root of 1 (*p*=*m*-1 in the former case) where the symmetry is by an *p*-th of a revolution. Hence we can take equivalence classes of such *c* to form a new complex plane *C*=*c*^(1/*p*), displaying each equivalence class and its conjugate, which fully classifies the resulting Julia sets up to rotations by 2*pi/*p*.

One can also use *z^m-nz+c* to explore the **Mandelbar** equivalents conj(*z*)^*k-nz+c* , by inputting *k*=(*m+100*,*n*) for *m* a positive integer ≥ 2. The classic **Mandelbar** is conj(*z*)^*2+c* , which you will get by setting *k*=(102,0).
However here the **moduli spaces** option gives *C*=*c*^(1/(*m*+1)) for *n*=0 but for *n*≠0 the Mandelbrot set now only has symmetry by *x* and *y* reflection, so we have to assert a reduced symmetry equivalence class.

The complex **Collatz** system gives one the complex generalization of the 3*n*+1 problem *n* -> *n*/2 if *n* is even or n -> 3*n*+1 if *n* is odd (or (3*n*+1)/2 for k=2, since this saves one step. This is generalized to (*cz*+1) (k=1 for c=5,7,9) (*z*/2)Cos^2(piz/2)+((*cz*+1)/*2*)Sin^2(piz/2)
and shows why although all positive integers in the 3*n*+1 problem eventually end up in the 3-cycle 4>2>1 for complex values we have fractal chaos.

Set **k** using **function view** and then **c** using **Julia view**. (k,c) = (1,3) and (2,3) give the standard and reduced Collatz sequences as above. You can also set 5*n*+1 and 7*n*+1, which give both periodic and chaotic escape to infinity for given values.

You can use color mode 1 to check the periods of the **Collatz (3*n*+1 *n* odd *n*/2 *n* even)** iteration. Set up the Julia iteration as above, and set color **1** with **escape only off** and **attractor bound 10^-2 (**default**)** with **Max iterations set to 1024**. Then set RIS for (*x*=*n*,*y*=0) and use scale to zoom in. For positive integers you get period (3), for -1 (2), -5 (5) and -17 (18). You can also check **5*n*+1** e.g. 4, 6 give period **(7),** 5 gives **(10)**, 7, 9 give (chaos) and -4 gives (3). **7*n*+1** gives either period (4) or (chaos).

The function *z^m+cz^-n* gives symmetrical Mandelbrot sets with unique Julia sets of thre e types, Cantor set (Fatou dust) of points, Cantor rings (simple closed curves) and Sierpinski curves (fractal Swiss cheese). The function and Julia sets have *m*+*n*-fold rotational symmetry while the Mandelbrot set has (*n*-1)-fold symmetry, despite there being *n*+*m* free critical points.

The final function is the inverse of the zeta function of the Petersen graph, a degree-24 polynomial with multiple critical values, giving high order Julia sets. The parametrizations of both *cPetersen* and *Petersen+c* are given for comparison (k=0 inverse *+c* k=1 inverse **c* k=2 original *+c* k=3 original **c*). You need to have escape only turned off for the last two.

You can investigate the Riemann Zeta function and a variety of other zeta and *L*-functions using Riemann Zeta Viewer which is designed to deal with these advanced functions.

Parameters Text file format: [0] mandel (2=function, 1= Mandelbrot, 0=Julia), [1-5] Scale, X, Y, (Fn k J/M c) R, I, [6] the current function, [7] escape type (abs real or imag), [8] orbit trap (0/1) +2*dF (0/1) + 4*mval (0=use std crit / 1=use input crit), [9] escape only (0 or 1), [10] color scheme (0 to 3), [11] escape bound (exponent 10^n), [12] attractor radius epsilon bound (negative exponent 10^n), [13] maximum iterations, [14-15] real and imaginary values of k, [16] previous function [17] dummy 987.654321 so you can find >> [18-29] complex coefficients *a* + *b*i of a polynomial up to degree 5 (6 pairs of reals), [30-35] powers of *c* (usually 0 or 1) multiplied into each coefficient of the polynomial for the Mandelbrot plane. [36] Additive *c*.

Two C-scripts are provided to explore polynomials. The C-script crits.c will generate any polynomial up to degree 5 from its critical points, scaling and rotating these together as required, enabling one to generate examples with arbitrary criticals in a given position. The script coefs.c provides an easy way of setting up an arbitrary polynomial up to degree 5 from its coefficients and parameter plane c values. See additional software for scripts below. A series of rational function parameter plane examples are also provided which use an amended polynomial coefficient format to explore the **Milnor** function option.

Movie Sequence Formats: The text file consists of series of floating point numbers. (1) File format 1-3 (2) N<=1000 number of frames (3) 1/0 Mandelbrot/Julia followed by a sequence of frame parameters [X, Y, Scale CX, CY].
Format 1: only the start and end parameters are specified and DHViewer will generate N frames in a linear sequence between these values. **Format 2:** the file supplies a series of N parameters on any trajectory, for instance computed values running around the cardioid of a Mandelbrot set. Format 1 and 2 files can either generate blowups of Mandelbrot sets or movies of Julia sets as CX and CY vary. The sequence file has no parameters except mandel, so you can set all the other settings manually before saving the movie. If you want to determine in advance the complete parameters for a movie run, save your parameters and load them before loading the movie sequence file.

Format 3: The format file contains only parameters 1 & 2 and is accompanied by a series of full parameter files, generated by another application such as the C-scripts attached which can be run from Terminal. If the format file is myfile.txt, the parameter files need to be numbered myfile0.txt - myfileN,txt. This format enables batch programming of any sequence of images automatically.

The file moduli8.c illustrates an extreme geometric scaling blowup using scientific notation fprintf("**%e**") rather than the 6 decimal point precision of fprintf("%f"), which can be used in any of the other c-scripts as well.
You can also use geometric, or linear scaling:

```
apos=xstt*pow((xend/xstt),((double)k/((double)frames-1))); (geom)
apos=xstt+(xend-xstt)*k/(frames-1);   (linear).
```

Ultra-large images: The file 'large.c' in the rational folder enables the generation of very large Julia and Mandelbrot images suitable for poster size displays. The script can be adjusted to generate a set of tiles in the standard window size of 750x513 using a set of image parameters you have saved as a parameter file. A file 'page.png' is also included in the folder, which forms a white background 7500x5130, which can be opened in Preview. You can then paste each of the tiles into the large page to get an expanded size image, by choosing actual size and pasting and lining them up carefully. An app to do this automatically is in development.

A series of movie scripts to generate the movies of the cubic separations is included with a manual of how it was created to give an example of using Dark Heart to generate trajectory variations in the field of view as satellite Mandelbrots or Julia parameters change in non-linear ways.

Associated Files
Along with DHViewer are a large array of parameter files and C-scripts, including some tutorial sample projects to show file handling:
1. Load Parameters for z^5-z^4+z^3-cz^2+z-c to see an example of a Mandelbrot plane of a 5^{th} degree polynomial.
2. To generate a movie sequence sample:
   (a) Load Parameters for z^3-z+c.tx (b) Load Movie Seq cubic.txt
   (c) Save Movie to an empty folder get a 500 frame Julia movie sequence.
3. To generate an 8 frame sample movie using Format 3:
   (a) load test.txt
   (b) Save Movie to an empty folder to get an 8 frame evolution of cz^(z+k) defined by parameter files test0.txt-test8.txt
4. Four template movie sequence files are included in movie C-scripts. You can run the sample files from Terminal as shown in each file header. This is a fully programmable interface, providing a template for more powerful movie making.

Additional Software for Scripts and Movies Movie frames are in tiff images, which can be turned into Quicktime movies with Quicktime Player 7 pro's open image sequence option, or using Mpeg Stream clip, which is included with the package. If terminal doesn't recognize the gcc command, open an Apple Developer account (free) and install Mac OSX Command Line Tools for your system from https://developer.apple.com/download/more/

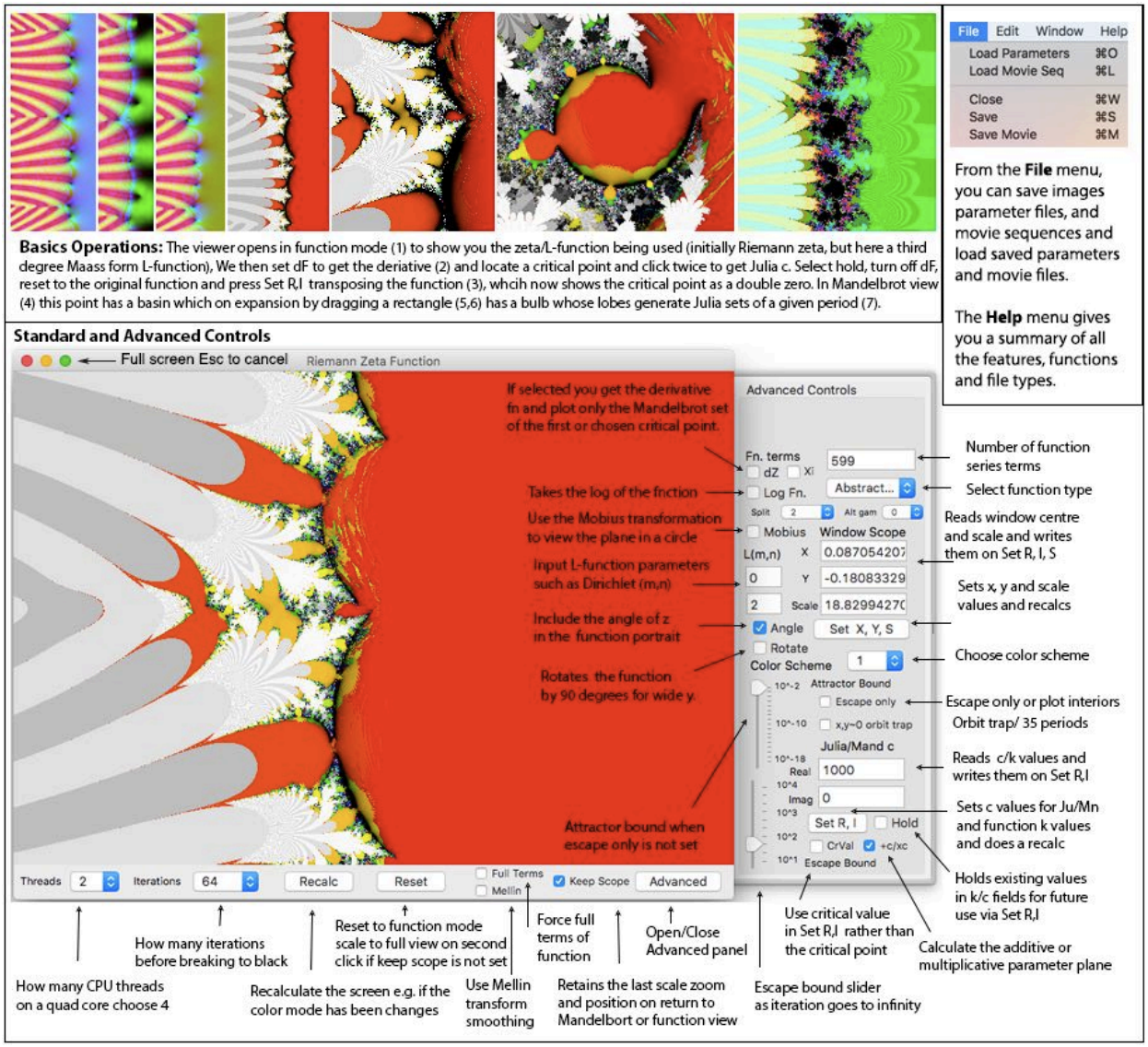

Fig 11: Rieman Zeta Viewer controls portraying a degree-3 Maass form *L*-function.

Riemann Zeta and L-function Viewer Flight Manual

Riemann Zeta allows you to interactively explore the complex **Riemann zeta function**:

$$Zt(z)=\text{Sum}[1,\infty](1/n^z)=\text{Xct}[p\text{ prime}](1/(1-p^{-z}))$$

a host of its **Dirichlet *L*-function** variants and their transformations and those of a diverse spectrum of abstract zeta and *L*-functions as well, right to the cutting edge of mathematical science.

RZ operates in the same way as Dark Heart viewer, but has some additional controls, so we will go through the manual from scratch for completeness.

By clicking, you can investigate the Mandelbrot set of these functions for a variety of critical values, and the Julia sets of $z=f(z)+c$ (or $z=cf(z)$) for $(x,y)=c$.

You can also investigate related functions eta, xi, the derivatives of each function and Newton's method (see below).

By uploading the provided parameter files you can also investigate abstract ***L*-functions of elliptic curves**, **extension fields** and **modular forms** and/or generate **movies** of the dynamics.

Basics:

Drag a rectangle to enlarge a portion of the current image.

Click a point to cycle:

Function > Mandelbrot > Julia(c)

at the clicked point *c* on the Mandelbrot set.

Clicking the Julia with ***keep scope*** on will take you back to the previous Mandelbrot screen to save computation time and enable you to explore several related Julia sets.

The controls all have ***floating help panes*** to guide you.

The window can be resized to suit in real time, resulting in a refresh and recalculation, or set to full screen using the green button. Esc to return to windowed mode.

Standard settings:

Threads enables a ual, or multi-core machine to work faster using as many threads as coprocessors. ***Max Iterations*** gives how many iteration steps of a point on the Julia or Mandelbrot set before maximum iteration cutoff. ***Recalc*** refreshes and recalculates the existing screen. ***Reset*** returns to function view. ***Keep scope*** keeps the window centre and scale when clicking between Mandelbrot, Julia and function, so the other parameters can be changed without changing the point of view. A double ***Reset*** with ***keep scope*** off returns to the default scale on the second click. To ***Reset*** to other functions after loading an abstract L-function, you will first need to renter a suitable L(m,n) such as (1,1) for zeta, as the value of m has been set to 0 to override these settings with the loaded coefficients.

To facilitate locating critical points for calculating Mandelbrot sets, tick ***dZ*** and explore the derivative function for a critical point (a zero of the derivative looking like a dimple). Use dragging to blow up to high resolution. Tick ***Keep scope*** and slowly click twice right on the zero without moving the mouse. The *c*-values will now appear in the Julia portrait. Then tick ***Hold***, untick ***dZ*** and click twice through the original function to the Mandelbrot set. The *c*-values are retained in the text field by Hold. Now untick ***Hold*** and click the ***Set R,I*** button and you will get the Mandelbrot sets of the given c-value.

To facilitate fast fractal iteration, the default is 100 function series terms and a cutoff of 64 iterations for each point of the Mandelbrot and Julia sets, but these can be adjusted for greater accuracy.

Menus:

About gives a complete instruction summary. ***Save*** saves the current window's image as a tif file and all the settings for a given calculation in a text file (see format below), enabling you to save all the parameters for future investigation and redrawing. It will overwrite any files of the same name. ***Load Parameters*** will load a previous calculation and redraw it. ***Load Movie Seq*** loads a sequence text file to generate a series of images to make a movie (see format below). ***Load Bitmap*** loads a bitmap of values of a function generated by another application. Computel and Sage scripts are included (see below). ***Save Movie*** saves the sequence as a series of LZW compressed tifs, which can then easily be composited into a movie e.g. using open image sequence in Quicktime Player 7 (Download: https://support.apple.com/kb/dl923?locale=en_US), or using the included app Mpeg Streamclip. ***Save Bitmap*** saves a bitmap of complex function values for subsequent math processing if the image has previously been refreshed in colour scheme 5, which also produces a useable bitmap in its tif files. This is to keep the other colour modes as fast as possible. The bitmap saves the values of the function, so doesn't care about the colour scheme. ***Print*** enables an image to be printed or exported to pdf format. ***Page Setup*** needs to be landscape in 80% to fit the standard window on one A4 page. ***Help*** directs you to the about menu.

Advanced settings:

Pop-up Menus: ***Color schemes*** can be changed in real time using the color pop up menu. All the other controls require window recalculation.

Functions related to zeta, including eta, xi, gamma, psi and others discussed below can also be explored using the function pop-up menu. For completeness, an *alternative Gamma* product formula, can be used instead of the default Lancos approximation, by pulling down the pop-up menu to choose a power of 10 terms in the product, but is slower and less accurate unless 10,000 iterations are used.

Buttons and Text Fields: A ***function terms*** text field is provided to set how many terms are calculated in the chosen sum or product function, with a default of 100 for speed of initial exploration. This can be adjusted to exact large values which have anomalous behavior (see end). Current ***window parameters*** and ***c values*** can be read out from and written into the text fields and set by pressing the appropriate button. ***L(m,n)*** text fields enable examining a wide variety of Dirichlet L-functions as well as Zeta and Eta. Numbers in the real text fields are double precision and may appear in floating format e.g. -7.000000186963007e-05 manifestly too large to see in their entirety in the text box without dragging or selecting all and copying. The Julia *c* values will be overwritten by the Mandelbrot critical point origin and current Julia click point each cycle but can be manually re-entered as desired.

Tick boxes: ***dZ*** finds the approximate formal derivative of any function being displayed. Good for finding critical

points since these are the zeros of the derivative. It works only in function mode. For fractals use dZeta or dXi. You cand get the second derivative approximation by combining the two. ***Full Terms*** is located on the pain page as a control and as an attribute. It forces the current function to use all the specified series terms. Otherwise it breaks off if the terms get smaller than 0.001 the size of the sum. Occasionally not having *Full* causes strip dislocations in a few regions. The control has immediate effect during drawing and is useful if a slow blow up of a Julia set needs to have full iterations just for the complex boundaries of the kernel. ***Mellin*** uses a Mellin transform in the central region if the function admits an analytic continuation. Like Full Terms, it is active during drawing. The ***logFn.*** tick box examines the log of the selected function. ***Split*** sets the functional equation split (-1 > -100, 0>0, 1>0.25, 2>0.5). ***Xi*** calculates the xi function instead of zeta/L. ***R- escape*** makes the escape path negative only highlighting the Cantor bouquet structure. ***Mobius*** transforms the complex plane, mapping the line x=1/2 onto the unit circle, so you can see the whole extent of the Dirichlet functions. For the exact mapping see below. ***Escape only*** tests only for escaping points, to avoid spurious periodic solutions from overwriting escaping orbits, but is slower because attracting orbits have to run to the Max interations for each point. The application defaults to this being off and colours most modes so escape to the right is colored the same as non-escape speeding the calculations, but to get high resolution images of small Mandelbrot and Julia kernels you may need to turn it on. ***crVal*** uses critical value instead of critical point for Mandelbrots. This is useful for generating parametric movies running between critical values. See blue skies method below for finding critical values. The tick box ***+c/xc*** changes the parametrization from $f(z)+c$ to $cf(z)$ giving a second parameter plane and collection of Julia sets for each function. ***Angle*** turns on and off the green/yellow display of the angle (argument) of $f(z)$ in function view for each mode. ***Rotate*** rotates the image by pi/2 to assist viewing the critical line.

Sliders: ***Attractor bound*** adjusts the size of the epsilon neighbourhood testing for fixed point or periodic attractors. ***Escape bound*** sets the real absolute bounds on points escaping to infinity.

Colour Schemes: There are several **colour schemes** for function, Mandelbrot and Julia:

Function: (0) ***Absolute-Angle mode*** rgb = red logarithmic abs(z), blue cosine abs(z), green angle(z). This is the most informative although not the most appealing (1) ***Real-Imaginary mode*** rgb = real, imaginary and angle, (2) ***X-ray mode*** with red, cyan real~0 and imag~0, by exp(-x^2), adjustable by the attractor bound, overlaying bg = abs(z) and angle(z) Highlights gram points with real=0 on x=1/2 and zeros at the intersections of real~0 and imag~0. (3) ***Positive-Negative mode***. Highlights the positive and negative real (r~c), imaginary (g~m) and angle by 1-cos (b~y). (4) ***Log-angle mode*** This method uses ***abs(log(1/(1-Z(z)))*** for the absolute value, adjustable using the escape bound slider, retaining the angle of ***Z(z)***. This still highlights the zeros since log(1/(1-0))=log(1)=0 but highlights variations in the function to the right of the critical line. It is good at highlighting the function in the right half-plane and in the critical strip in a way which evenly compares asymptotical large and near-unitary values. (5) Soft mode rgb = cos(angle) sin(angle), abs(z). Good for retrieving function data from the tif file.

Mandelbrot: (0,5) Sine wave colours, (1) Attractor coded colours, giving escaping points tending to real infinity shades of grey from white to black in waves by iteration number with periodicities coloured approximately by the following **1 2 3 4 5 6 7 8 9 10 11 12 13 14 15 16 17 18** mildly shaded by iteration number. You need to **turn off escape only** and set the **attractor bound to 10^-2** (default). (2) RGB ranked colours (3) Potential function rainbow. (4) attractor coded inverse quadratic. (Highlights geometrical details lost in high iteration numbers). (5) Attractor coding giving escaping points tending to real infinity green through orange and points remaining finite coloured by decreasing blue by iteration, combined with redness corresponding to the attractor period. When ***R- escape*** is set in mode 1 it doubles the period search to 35 colouring the higher values in lighter shades mod 18, but this will also slow the computation.

The 'critical' point for the Mandelbrot set is chosen to represent a prominent critical landmark. For zeta, eta, mu, and sigma it is chosen to be 1000 corresponding to the limit $f(z)>1$ as real(z)>+∞. For gamma it is 1.465. For Xi it is 0+ki, k=0.00000001~0. Other critical points can be chosen using the advanced settings and inputing CX CY values under Mandelbrot mode, just as c values can be inserted for any Julia set. A list of critical points for zeta eta and xi is provided below, or can be approximated using the values of observed zeros of dzeta etc. You can also input CX and CY in function mode to generate a transform of the function, whose zeros are at the fixed points of the critical values [f(cv)-v=0 or f(c+v)-v=0] and hence candidates for being in Mandelbrot kernels of the critical points.

You can flip easily between Mandelbrot mode and transformed function mode using 'keep scope on click'. To exit reset. This can potentially find a finite number, out of the infinite collection of kernels, but sometimes the one located is vanishingly small, leading to blowing the mantissa of the floationg point doubles before we reach it.

Not all the functions have meaningful Mandelbrot sets. The zeta attracting fixed point is at -0.2959050055752.

Julia: (0) Sine wave colours, (1) Attractor coded colours, (2) RGB ranked colours, (3) Rainbow with potential function on escaping points. Colour coded Julia attractors have blue shaded to escaping real, red shaded to periodic attractor, green non-negative periodic attractor, with grey indeterminate. The red and green are tinged with blue to indicate the period. (4) Attractor coded inverse quadratic. (5) Attractor coded with RGB mapping.

For exploring the higher zeros of zeta, a high number of series terms can be set using the slider. Values of the RZ

function outside the critical strip [0,1] are set to 0 after y=±450i because the sin/cos component of the analytic continuation overflows to Inf. This leaves the zeros in the critical strip still well rendered up to values in the millions with the highest number of zeta iterations set in the slider.

The Functions:
The package is designed to facilitate research into the **widest spectrum of zeta-related and *L*-functions possible**. Each of zeta, eta and all the L-function variants $L(m,n)$ for m up to 63 are encoded as a generalized zeta function which can then be differentiated, or have any of the functions from xi, through those like lambda and mu whose coefficients are important arithmetic functions, to the Newtons method's and differentiation applied to them. This creates a widest a diversity of exploratory functions as possible.

Zeta
$Zt(z)=Sum[1,\infty](1/n^z)=Xct[p\ prime](1/(1-p^{-z}))$
Zeta is represented here in terms of Eta as:
$Zt(z)=E(z)\ /(1-2^{1-z})$ for real(z)≥0
and by analytic continuation using:
$Zt(z)=2((2pi)^{z-1})cos(pi(1-z)/2)G(1-z)Zt(1-z)$ for real(z)<0.
http://en.wikipedia.org/wiki/Riemann_zeta_function

Eta $E(z)=Sum[1,\infty]((-1)^n/n^z)$
$E(z)=(1-2^{1-z})Zt(z)$
Used to extend Zeta from real(z)>=1 down to real(z)>=0.
To access it set L(m,n)=(1,-1).
http://en.wikipedia.org/wiki/Dirichlet_eta_function

Dirichlet L-functions
$DL(z)=Sum[1,\infty](X(p,q)/n^z)$
where X(p,q) is the qth set of Dirichlet characters of period p.
Enter p=Xm and q=Xn into the L(p,q) text field. Each of the other variant zeta functions can be applied to any of the L-functions as well as zeta and eta. The viewer calculates the finite residue groups *Z*/*Zn* generating the characters, factors both for sub-periodicities and for conductors, and then applies the correct functional equation and prime multiplicative factors to give the full representation on the complex plane. A Mellin transfor is performed in the central basin to improve fidelity.

A Terminal C-script is included with the application files which shows how a given character cast X(m,n) is generated and reduced to its primitive form.

Abstract zeta and *L*-functions
Examples such as those of elliptic curves, number fields and modular forms can be uploaded by including their coefficients and functional equation parameters in the appropriate file format and viewing as raw/abstract.

A suite of preloadble cases is provided in the files along with the Terminal C-scripts which generated them and Computel PARI-GP and Sage scripts which generated the Dirichlet series coefficients. Some of the examples (particularly the field extensions) display convergence problems in their critical strip similar to naked Riemann zeta, requiring a Mellin transform treatment as is done for Dedekind/Hecke functions, but many of the elliptic curve and the modular form examples give quite accurate portraits. A working copy of PARI-Computel is included with RZViewer, so all the examples, except for the modular form coefficients, can be generated without use of Sage.

Gamma G(z) the compex number extension of integer factorial $n!$
By default, the Lanczos approximation is used:
http://en.wikipedia.org/wiki/Lanczos_approximation
or alternatively the product formula
$G(z)=Xct[(1+1/n)^z\ /(1+z/n)]$
with n=10^k terms if **alt gamma** is set to a non zero value.
http://en.wikipedia.org/wiki/Gamma_function

Xi/xi $X(z)=(z-1)G(z/2+1)pi^{-z/2}Zt(z)$
This is now included for every function possessing a functional equation, including abstract *L*-functions, by selecting in the Xi tickbox.
The unction provides a symmetrical presentation of the zeros on x=1/2.
http://en.wikipedia.org/wiki/Xi_function
The xi functions of Dirichlet L-functions are also included, as well as the equivalent singularity bearing Xi function of zeta for Xm=1 Xn=0.

Note: Xi is rotated so the zeros are on the critical line, rather than the real axis.

The following set of derived zeta functions all work also for any L-function.

Mu $M(z)=\text{Sum}[1,\infty](\text{mu}(n)/n^z)$
$M(z)=(1/Zt(z))$
The ***Möbius*** function mu(n) = (-1)^k when n has k distinct prime factors of multiplicity 1, and 0 otherwise.
http://en.wikipedia.org/wiki/Möbius_function

Sigma $S(z)=\text{Sum}[1,\infty](\text{dvs}(n)/n^z)$
$S(z)=Zt(z\text{-}1)Zt(z)$

The ***divisor*** function dvs(n)= Sum(d : d | n).
$S[k](z)=Zt(z\text{-}k)Zt(z)$
gives dvs{k}(n)=Sum(d^k : d|n).
http://en.wikipedia.org/wiki/Divisor_function

Lambda $L(z)=\text{Sum}[1,\infty](\text{Lam}(n)/n^z)$
$L(z)=(-Zt\ '(z)/Zt(z))$

The ***Mangoldt*** function Lam(n) = log(p), n=p^k and 0 otherwise.
http://en.wikipedia.org/wiki/Mangoldt_function

lambda $l(z)=\text{Sum}[1,\infty](\text{Lio}(n)/n^z) = \text{Xct}[p\text{ prime}](1/(1+p^{-z}))$
$l(z)=Zt(2z)/Zt(z)$

The ***Liouville*** function lam(n) = (-1)^om(n), om(n)=no. of prime factors of n counted with multiplicity.
http://en.wikipedia.org/wiki/Liouville_function

Phi $H(z)=\text{Sum}[1,\infty](\text{tot}(n)/n^z)$
$H(z)=(Zt(z\text{-}1)/Zt(z))$
The ***totient*** function tot(n) = no.of positive integers $k \le n$ coprime to n.
http://en.wikipedia.org/wiki/Totient_function

dGamma, **dXi** and **dZeta** are the derivatives $G'(z)$, $X'(z)$ and $Zt'(z)$ or any of the L-functions in zeta with xm and xn set. You can also perform an approximate formal derivative of any function at all using the ***dZ*** tick box to loo for critical points to source Mandelbrot sets, but this is active only in function mode. To see fractals of the derivative function use **dZeta.** You can also view the second derivative of a function, but not its fractals by combinining both.

NewtonZ, **RepellngNZ** and **NewtonX** are the Newton's method functions for zeta, and xi.

$NZ(z)=z\text{-}Zt(z)/Zt\ '(z)$, $NZ(z)=z+Zt(z)/Zt\ '(z)$

They are provided because they naturally relate to the zeros.

zZeta is included to demonstrate the periodicities in the multiplicative parameter plane

zetaprod is the product version of zeta or any L-function
$\text{Xct}[p\text{ prime}](1/(1\text{-X(m,n)}p^{-z}))$, which is technically defined only for real(z)>1, included for comparison with zeta the analytic continuation version above. Zetaterms adjusts the product terms in the same way as with zeta.

primeZeta is the function
$Zp(z)=\text{Sum}[p\text{ prime}](1/p^z)=\text{Sum}[1,\infty]\ (\text{mu}(k)/k)\log(Z(kz))$
where mu is the Möbius function (see above). It is included for completeness. It is defined only for real(z)>0.

Dedekind/Hekke L(m) Explores the Dedekind zeta and Hekke L-functions of the field extnsion of Q to include the Gaussian integers $Z[i]$ = {a+ib) a,b, in Z}
$L(z,l)=\text{Sum}[(m,n)\ne(0,0)\ \infty]X(m+in)/(4(m^2+n^2))=\text{Xct}(1/(1\text{-X(p)}/(4(m^2+n^2)))$
X(a)=(a/conj(a))^l
Enter l into Xm. Xn has no effect. These functions have a Mellin integral transform in the critical strip $0 < x < 1$, for small y for |Xm| <10.

abstract/raw zeta/L is a direct computation of $\text{Sum}[1,\infty](\text{X(m,n)}/n^z)$.
Used from saved parameter files it can also be used to generate abstract
zeta and L-functions, including those of elliptic curves and modular forms with varying functional equations and gamma factors. See the section on uploading parameter files and the installation file set for examples of each.

Davenport consists of a finite collection of zeta functions which have a similar functional equation, but (5,1), (5,2) and (7,1) have no Euler product. (5,1) is the Davenport-Heilbronn zeta function which has occasional zeros off the critical line, e.g. at .808517 + 85.699348i, .650830 + 114.163343i, .574356 + 166.479306i, .724258 + 176.702461i.

(5,2) and (7,1) also have interesting off line zeros. The remainder: (2,1), (2,2), (3,1), (3,2), (3,3), (4,1), (4,2), (6,1), (6,2) and (8,1) are derived functions of Riemann zeta and Dirichlet *L*-functions. In addition (1,*n*) gives (5,4)*n/1000+(5,5)*(1-n/1000) a linear combination of two zeta/L-functions with the same functional equation with zeros off-critical. (9,*th*) gives a functional combination
{0,1,tan(*th*),-tan(*th*),-1}=(sec(*th*))/2[DL(5,4)*e*^(-*i th*)+DL(5,2)*e*^(*i th*)]
which equals (5,1) at *th*=100 and (5,2) at *th*= -468. [-*pi pi*] = [-567 567].
As this function writes and reads DL information from memory, threads are set to 1. A gif file of the definitions of these functions is in the attached files.

theta is the Riemann-Siegal theta function
Th(*z*)=log(G((1+2*zi*)/4)-log(G((1-2*zi*)/4)-*z*log(pi)/2

RSZ is the Riemann-Siegal Z function
Z(*z*)=exp(*i* theta(*z*))Zt(1/2+i*z*)

Hurwitz zeta functions $H(z,a)=\sum_{1}^{\infty}(1/((n+a)^z)$ generalize Riemann zeta.
Xm, Xn provide *a*=*Xn*/*Xm*, (*Xm*,*Xn*)=1 *Xn*<*Xm*. These also have unreal zeros off the critical line. *H*(*z,1*)=Zt(*z*),
H(*z,1/2*)=(2^z-1)Zt(*z*),
H(*z*,*p*/*q*)= (*q*^*z*)Sum[1,*q*](conj(*X*(*p*))*DL*(*q*,*p*))
As this writes and reads DL information from memory, threads are set to 1.

zeta-z enables one to explore the behavior of the atrtracting fixed point of zeta

pi^(-z/2)*zeta gives a function demonstrating all zeros are simple of first order as Z(z)=pi^(z/2)Prod[1-z/r]/(2(z-1)Gamma(1+z/2)), r non triv 0

Psi (Digamma) *P*(*z*)=G'(z)/G(z) the logarithmic derivative of gamma
http://en.wikipedia.org/wiki/Digamma_function

Bitmap imported bitmap to display (see below)

Power Series gives the power series *P*(*z*)=Sum[1,∞](*a*(*n*)*z*^*n*) corresponding to the Dirichlet series *L*(*z*)=Sum[1,∞](*a*(*n*)/*n*^*z*) either of character *Xm*, *Xn* or uploaded as a coefficient set (see below).

Fourier does the Fourier series viz *F*(*z*)=Sum[1,∞](*a*(*n*)exp(2pi*nz*)) either of character *Xm*, *Xn* or uploaded as a coefficient set (see below).

Both the two above functions are useful when examining modular forms which are expressed as Fourier series in the upper half-plane or as power series in the unit circle. By selectng ***Escape Only***, you can set the areas where the functions are formally undefined to black. By also selecting ***R- escape*** you add 1 to the result which enables loading an Eisenstein series leaving out its leading 1 in the same way as an L-function so that one can do a Fourier or Taylor portrait of all the components of a modular form space.

1/(k^z) and 1/(1-k^-z) etc. give sum and product component functions input by k=function terms.

Weierstrass plots a Weierstrass modular function using the first two complex coefficients of any Dirichlet or loaded abstract L-function as periodic vectors w1 and w2 on a parallelogrammatic grid extending for 2*sqrt(fnterms) to illustrate what modular functions associated with elliptic curves look like.

zetaFact
If *Ln* = 1 $F(z)=\sum_{1}^{\infty}(Facts(n)/n^z) = Xct[2,\infty]\ (1/(1-n^{-z}))$
Facts(*n*)= number of unordered factorizations of *n*.
If *Ln* = -1 $F(z)=\sum_{1}^{\infty}((-1)^{Facts(n)}*Facts(n)/n^z)$
otherwise $F(z)=\sum_{1}^{\infty}((-1)^n*Facts(n)/n^z)$
This gives an example of a function with a product that doesn't involve primes. It is included as a script file example with the application files.

Theta and RSZ have been rotated so that the zeros are on the critical line rather than the real axis. The chequerboard effect is an artifact of the log when the gamma function rotates through the principle value as the imaginary part of *z* increases. A clearer view of RSZ is gained by turning off angle.

Mobius transformation: M(*z*)=(a*z+b)/(c*z+d) k=40.0, a=k+1/2, b=1-a c=d=1; with inverse M'(z)=(d*z-b)/(-c*z+a). This takes -1 to infinity, 1 to 1/2 and i to 1/2+40i, thus wrapping the critical line around the unit circle. In our case the inverse transformation is M'(z)=(x+39.5)/(z+40.5), so 0.9753 = 39.5/40.5 maps correctly to 0 to give the Julia set of zeta.

Parameters Text file format: [0] Mandel (=2 function =1 Mandelbrot =0 Julia), [1-5] Scale, X, Y, cr, ci, [6]

altgamma (0 or 2-4), [7] the current function, [8] theoretical dzeta (0, 1, -1 2), [9] R- escape [10] addtive or multiplicative c [11] escape only (0 or 1), [12] color scheme (0 to 3), [13] escape bound (10-100), [14] number of zeta terms, [15] attractor radius epsilon bound, [16] maximum iterations, [17] do log of fn [18] angle included in colour scheme [19] Mobius [20] cval (holds entered critical point), [21] old fn. [22] real k [23] imag k [24] crval+2*Xi [25] full terms+2*dZ+4*Mellin [26] xm [27] xn [28] flip.

Arbitary Dirichlet series: You can also add additional parameters to a saved text file or scripted movie file to define an arbitrary generalized Dirichlet series Sum[*an*]*[*n*+*bn*]^-*z* of up to 1024 terms. These are not saved, as they cannot be adjusted in the advanced settings. x*m* needs to be set to 0 and *xn* to 2 to cause the system not to override *k* and *h*. [29] character period length k, [30] chr. type h (2 or -999 or -998). Type 2 has *k* real and imaginary coefficients which can be varied in a movie script. Type -999 has both *k* coefficients *a*(*n*) and an additional *k* adjustments *n*+*b*(*n*) to the integers *n* forming the powers *n*^-*z*. In this way we can generate continuous movies which pass between L-functions, using non integer exponent bases. Type -998 is used to instead multiply the resulting function with integer coefficients by (1-2^(1-*z*))^-1 to convert an eta type series into its zeta form.

Abstract L-functions: you can upload an abstract zeta/L function using the character period length k [29] with Dirichlet series coefficients as above with chr. type *h* = -997, appended after the *k* complex coefficients by adding the following values also as complex coefficients: *d*=number of gamma factors *g*((*z*+*k*1)/2), *g*((*z*+*kd*)/2), k followed by *k*1, ... *kd*, *N* the conductor, *e* the sign of the functional equation, and finally *w* the weight. *h* = -995 has the same parameters entered as complex numbers to allow for Dirichlet and Mass *L*-series with complex gamma factors and *e* terms. For *L*-functions with very rapidly growing coefficients which would cause numerical overflow (large weights) enter chr. no -996, scale down the coefficients of n by a factor n^(-sh) and enter sh as a shift factor after the weight. If you set an *e* with absolute value *d* other than 1 you will get *d* ^(-*z*)**L*(*z*) which is useful for generating the full set of modular old forms (see my research article at the web site). If the imaginary part of the weight is set to 1 rather than 0 the powers of pi in the functional equation will be translated by the gamma factors or their conjugates.

You can explore abstract *L*-function fractal sets, save an image and parameter file. You can then load the parameters for the image later after making sure you have first loaded the correct *L*-function and the existing abstract function will continue to operate.

If the abstract L-function has 2 gamma factors of 0 and 1 respectively and Mellin is set, RZViewer will also use the Mellin transform for a modular form (or elliptic curve) in the region 0≤x≤w, -8≤y≤8 to improve fidelity in the central basin. This is useful for considering the Birch and Swinnerton-Dyer conjecture. Finally with version 1.7.3 a general Dokchitser type gamma function inverse Mellin transform routine has been instituted for arbitrary *L*-functions which is currently experimental, but works successfully on the genus 2 and 3 examples. To activate this full terms needs to be set to 4 in the parameter file. In both the modular and general cases, if the number of gamma factors is given a negative sign, the three terms after weight (or the shift factor with -996) will be the height and width of a Mellin transform window and the residue of any pole singularity at z=1.

The easiest way to generate parameter files is by using a C-script, which will generate all the parameters from the *L*-function coefficients and gamma factors. Example C-scripts ready to run including elliptic curve, modular form and Maass form L-functions are provided in the attached files.

A working copy of **Computel** with PARI-GP is included with RZViewer files, to facilitate high resolution plotting of small regions close to the critical line and central basins for some difficult examples such as the Dedekind zeta functions of number field extensions. Computel can handle the Mellin transforms of a wide class of Motivic functions. For the original examples in Computel see: http://www.dpmms.cam.ac.uk/~td278/computel/

The file “Installing&Running.txt” in the Computel folder gives working examples of generating a central region function portrait for the extension field of x^4-x^2-1 and the elliptic curve example 5077a. The Computel examples are designed to be able to be overlayed on the RZViewer image of the same function example using the coefficients and gamma functions generated by Computel in the example files and pasted into an appropriate C-script example in the fields folder. A C-script “overlay.c” is provided to facilitate merging the Computel bitmap over the RXViewer overview to give a high fidelity portrait. The Computel process is 14,500 times slower than RZViewer, so even a small central image will take 15 minutes or so to process.

PARI-GP and a compiled version of the Computel algorithm for elliptic curve *L*-functions is also incorporated into the open source cross-platform math package Sage http://www.sagemath.org/ from which the coefficients for several of the templates were generated. Example scripts enabling coefficient generation for elliptic curves and modular forms is included with RZViewer, but Computel can also generate all the elliptic curve and field extension examples without having to install Sage.

Bitmaps: You can both save and load bitmaps as well as parameter files and tiff images. You can save whole bitmaps as text files by using color option 5 and selecting the Save Bitmap menu item. These can then be merged, or overlayed and reloaded into RZViewer as bitmaps. The portrait will initially show in its exact size in pixels. Since it's a bitmap, blowing it up will reduce the resolution of individual pixels and you can’t use it to generate fractal sets. But this makes it possible to generate L-functions, which couldn't otherwise be accurately portrayed such as the

echelon basis functions of modular forms. Terminal C-scripts are included with several of the modular form examples to enable merging of saved bitmaps as shown in the illustrations in http://dhushara.com/DarkHeart/key/weights.htm. As noted above, one can also use Computel to generate bitmaps, which can be merged with RZ portraits and loaded into RZViewer.

The Sage file in the 57 folder shows the information to form the matrix expressing 57a, 57b, 57c, 19a and 19ax3 in terms of 57m0-4 and its inverse, thus enabling us to express the basis elements in terms of the elliptic curve eigenfunctions.

To regenerate the bitmaps:
1: In RZViewer, load one of the above parameter files for the elliptic curves in the parameter file folder in 57, turn on full terms and open the advanced drawer.
2: Slide the window to downsize it to the smallest possible to avoid overflowing bitmap memory on reload.
3: Set color mode to 5 and set scale e.g. to 25 and click Set X,Y,S.
4: When the window has refreshed with the L-function profile, save the bitmap under the same name as the parameter file - e.g. "57a.txt".
5: Do the same for each of the 5 files.
6: Put all the o files in a folder along with merge57e.c open terminal and cd to the folder, then execute "gcc -o rzo merge57e.c -lm && ./rzo". The merge script is already set to use the input filenames you have defined.
7: Rename the output file to something like 57m0.txt
8: Run the same c script again setting opt to 0 - 4 to generate 57m0.txt to 57m4.txt.
9: Upload each of these into RZViewer one at a time using Load Bitmap to view the results and save as required to get tiffs.

Movie Sequence Formats: The text file consists of series of floating point numbers. (1) File format 1-3 (2) *N*<=1000 number of frames (3) 1/0 Mandelbrot/Julia followed by a sequence of frame parameters [X, Y, Scale CX, CY]. **Format 1:** only the start and end parameters are specified and DHViewer will generate *N* frames in a linear sequence between these values. **Format 2:** the file supplies a series of *N* parameters on any trajectory, for instance computed values running around the cardioid of a Mandelbrot set. Format 1 and 2 files can either generate blowups of Mandelbrot sets or movies of Julia sets as CX and CY vary. The sequence file has no parameters except mandel, so you can set all the other settings manually before saving the movie. If you want to determine in advance the complete parameters for a movie run, save your parameters and load them before loading the movie sequence file. **Format 3:** The format file contains only parameters 1 & 2 and is accompanied by a series of full parameter files, generated by another application such as the C-scripts generated by Terminal in the files. If the format file is myfile.txt, the parameter files need to be numbered myfile0.txt - myfileN,txt. This format enables batch programming of any sequence of images automatically.

Blue-Skies Method for Finding Mandelbrot Kernels for Zeta Functions

This method enables exploration of a wide range of Mandelbrot sets of zeta functions intuitively taking advantage of the software algorithms without having to do complex arithmetic to look for the needle in the haystack.

Step 1: Explore the critical points of the function using the ***dz*** derivative option. Choose a critical point and scale the image by dragging rectangles to focus on a small region around the critical point. If the critical point has strip-like artifacts due to function term round-off, tick the ***full terms*** option while the process is drawing the immediate neighbourhood. If the imaginary value is large, you may need to increase the **function terms** to get an accurate critical point.

Step2: Tick the ***keep scope*** option and click the function twice right on the critical point to get Julia representation. This will insert the *c* value of the critical point into the ***Julia / Mand c*** text fields. Now tick ***Hold*** to lock these values in.

Step 3: You now need to decide whether you are exploring an additive or multiplicative Mandelbrot set. Untick +c/xc if you are using multiplicative.

Step 4: Untick ***dz*** so we are dealing with the original function (this didn't affect the Julia step because dz is active only in function mode) and do a ***Reset*** and then press ***Set R/I***. This causes the critical point values to modify the zeta function causing the fixed values and principal point of the critical point to be zeros of the modified zeta transfer function.

Step 5: Have a look initially at the principal point, which due to the maths is a double zero so has two yellow angular rays meeting in it. This is where one is most likely to easily find a principal Mandelbrot kernel. In the additive case the principal point will be quite close to the critical point because it only has an additive shift, but in the multiplicative case it may be rescaled and you will have to search for the double zero. You can insert a new Y value and click ***Set X,Y,S*** to move further up or down the imaginary axis.

Step 6: With ***keep scope*** ticked, click the point once to go into Mandelbrot mode. Click ***Set R/I*** again to make sure the

Mandelbrot is using the critical point you found. Drag a rectangle to zoom in on the neighbourhood of the point. This should give you a Mandelbrot kernel with reasonably well-formed bulbs, dendrites, and satellite black hearts if the number of function terms and iterations is high enough to be accurate at the values used.

Step 7: You can now explore the region of the Mandelbrot kernel or its islands and can check the corresponding Julia kernels by clicking once on a spot with ***Hold*** unticked to pick up the actual *c* value you are now investigating. The Julia set may have only very tiny connected periodic kernels representing the local dynamics near the Mandelbrot kernel and in the multiplicative case these may appear only in a region of the Julia set close to the principal point.

Step 8: You can also find a critical value to use with ***crVal*** by locating the critical point as a zero of dz scaling down to a microscopic domain around it and unchecking dz and refreshing to give the value of the function, which is stationary at the critical point. This can then be found by saving a bitmap and viewing it as a text file where the stationary value will be at the midpoint (see bitmaps below). Use the smallest size screen for a smaller bitmap. Selected critical values for zeta are included below.

Additional Software for Scripts and Movies

Movie frames are generated as tiff images, which can be turned into Quicktime movies with Quicktime Player pro 7's "open image sequence" option, or loading them collectively as files using Mpeg Stream clip, which is included with the package. If terminal doesn't recognize the gcc command, open an Apple Developer account (free) and install Mac OSX Command Line Tools for your system from https://developer.apple.com/download/more.

First Zeta Critical Points
x-axis

z = -2.7172 z(z) = 0.0092
z = -4.9368 z(z) = -0.0040
z = -7.0746 z(z) = 0.0042
z = -9.1705 z(z) = -0.0079
z = -11.2412 z(z) = 0.0227
z = -13.2956 z(z) = -0.0937
z = -15.3387 z(z) = 0.5206
z = -17.3739 z(z) = -3.7436
z = -19.4031 z(z) = 33.8083
z = -21.4279 z(z) = -374.4187
z = -23.4492 z(z) = 4988

Critical line (dzeta approximation plus Newton)
z = 2.463356 + 23.297678i, z(z) = 0.9289 + 0.0308i
z = 1.286578 + 31.708124i, z(z) = 0.7073 + 0.0110i
z = 2.306454 + 38.489796i, z(z) = 0.9919 - 0.0931i
z = 1.382872 + 42.2909775i, z(z) = 0.7930 + 0.1273i
z = 0.9646998675 + 48.8471714103i
z = 2.1016662620 + 52.4314144061i
z = 1.8960801201 + 57.1342532310i
z = 0.8487341239 + 60.1408464582i z(z) = 0.4881 + 0.1283i
z = 1.2073178358 + 65.9199666872i z(z) = 0.7776 - 0.2061i

z = 0.7806300097 + 95.2929688274i z(z) = 0.4295 + 0.0779i

Eta Critical Points
z = -3.0430 e(z) = -0.1252
z = -5.2330 e(z) = 0.2673
z = -7.3360 e(z) = -1.2390
z = -9.4020 e(z) = 9.8440

z = 2.758314+14.451968i, e(z) = 1.0548 - 0.0412i
z = 1.776063+20.348036i, e(z) = 0.9585 + 0.1994i
z = 1.386667+25.644800i, e(z) = 0.7875 - 0.2597i

Xi Critical Points
z = 0.5, x(z)= 0.5
z = 0.5 + 15.444i, x(z)= -0.0009
z = 0.5 + 21.918i, x(z)= 0

Zeta/Eta Critical Line Zeros

A short list of some zeta zeros mentioned in the dark heart research, which can be easily copied and pasted into the text fields, are as follows:

1-30: 14.13472514, 21.02203964, 25.01085758, 30.42487613, 32.93506159, 37.58617816, 40.91871901, 43.32707328, 48.00515088, 49.77383248, 52.97032148, 56.4462477, 59.347044003, 60.831778525, 65.112544048, 67.079810529, 69.546401711, 72.067157674, 75.704690699, 77.144840069, 79.337375020, 82.910380854, 84.735492981, 87.425274613, 88.809111208, 92.491899271, 94.651344041, 95.870634228, 98.831194218, 101.317851006

125-130: 278.2507435, 279.2292509, 282.4651148, 283.2111857, 284.835964, 286.6674454

287-293: 523.9605309, 525.0773857, 527.9036416, 528.4062139, 529.8062263, 530.8669179, 532.688183

171382-171390: 121412.139210209, 121412.990421458, 121414.488895067, 121414.739043607, 121415.047364581, 121415.640550747, 121416.302522095, 121416.823543637, 121417.618749154

NOTE: The 'trivial' zeros are at -2, -4, -6, etc: sin(piz/2)=0

Sinks

282.4651148, 391.4560836, 446.8606227, 527.9036416 H,
637.3971932, 653.6495716, 681.8949915, 762.7000333

For further zeros, see:
http://www.dtc.umn.edu/~odlyzko/zeta_tables/index.html

The number of function terms can also be adjusted to large exact values to show up anomalous behavior, for example the 84270 term zeta product up to the prime 1079999, has a value at the first zeta zero of 6.25, well above 0. That for the 1518898th prime 24199999 is a stunning 20067241.5306, anything but 0!

Functional Equations and Mellin Transforms:

RZViewer uses functional equations for analytic continuation to the left of the critical line, but also selectively applies Mellin transforms to the central basin of Dirichlet, Hecke, and modular *L*-functions and the Dedekind zeta. This gives a good compromise of rapid computation with central smoothing. Tim Dokchitser's Computel algorithm included in RZViewer as an adjunct package, using advanced generalized Mellin transforms, is accurate at depicting the zeros at the centre and in the critical strip for a wider collection of *L*-functions.

The following gives a summary of the analytic continuations and Mellin integral transforms for Riemann zeta, Dirichlet *L*-functions, Dedekind zeta, Hecke *L*-functions on Gaussian integers, and for the *L*-functions of elliptic curves and modular forms used in the package.

Riemann zeta

$$\zeta(s) = \pi^{s/2} / \Gamma\left(\frac{s}{2}\right)\int_0^\infty y^{s/2}\left(\theta(iy)-1\right)\frac{dy}{2y},\ \phi(t) = e^{-\pi t^2},\ \theta(iy) = \sum_{n\in\mathbb{Z}}\phi(ny) = \sum_{n\in\mathbb{Z}} e^{-\pi n^2 y},\ \theta(iy) = \frac{1}{\sqrt{y}}\theta\left(\frac{i}{y}\right)$$

$$\pi^{-s/2}\Gamma\left(\frac{s}{2}\right)\zeta(s) = \int_1^\infty \left(y^{s/2} - y^{(1-s)/2}\right)\left(\theta(iy)-1\right)\frac{dy}{2y} + \frac{1}{2}\left(\frac{1}{s-1} - \frac{1}{s}\right) = \pi^{-(1-s)/2}\Gamma\left(\frac{1-s}{2}\right)\zeta(1-s)$$

Dirichlet L-functions

$$L(s,\chi) = \pi^{(s+a)/2} / \Gamma\left(\frac{s+a}{2}\right)\int_0^\infty y^{s/2}\theta_\chi(iy)\frac{dy}{2y}$$

$$= \pi^{(s+a)/2} / \Gamma\left(\frac{s+a}{2}\right)\left(\int_{1/N}^\infty y^{s/2}\theta_\chi(iy)\frac{dy}{2y} + \frac{-i^a N^{1-s}}{\langle\bar{\chi},\varphi\rangle}\int_{1/N}^\infty y^{(1-s)/2}\theta_{\bar{\chi}}(iy)\frac{dy}{2y}\right),\ \langle\chi,\varphi\rangle = \sum_{n=1}^N \chi(n)e^{2\pi ni/N}$$

$$\text{where } \theta_\chi(iy) = \begin{cases} \displaystyle\sum_{n=1}^\infty \chi(n)e^{-\pi n^2 y}, & a = 0 \\ \displaystyle\sum_{n=1}^\infty \chi(n) n y^{1/2} e^{-\pi n^2 y}, & a = 1 \end{cases},\ \varepsilon(\chi) = \frac{\sqrt{N}}{\displaystyle\sum_{n=1}^N \bar{\chi}(n)e^{2\pi ni/N}},\ \theta_\chi(iy) = \frac{-i\langle\chi,\varphi\rangle}{N\sqrt{y}}\theta_{\bar{\chi}}\left(\frac{i}{N^2 y}\right)$$

$$N^{s/2}\pi^{-(s+a)/2}\Gamma\left(\frac{s+a}{2}\right)L(s,\chi) = \int_{1/N}^\infty (Ny)^{s/2}\,\theta_\chi(iy)\frac{dy}{2y} + \varepsilon(\chi)\int_{1/N}^\infty (Ny)^{(1-s)/2}\,\theta_{\bar{\chi}}(iy)\frac{dy}{2y}$$

$$= \varepsilon(\chi)\int_{1/N}^\infty \varepsilon(\bar{\chi})(Ny)^{s/2}\,\theta_\chi(iy)\frac{dy}{2y} + \int_{1/N}^\infty (Ny)^{(1-s)/2}\,\theta_{\bar{\chi}}(iy)\frac{dy}{2y} = N^{(1-s)/2}\pi^{-((1-s)+a)/2}\Gamma\left(\frac{(1-s)+a}{2}\right)L(1-s,\bar{\chi})$$

Dedekind zeta

$$\zeta_\circ(s) = \frac{1}{4}\sum_{m,n \text{ not both } 0}\frac{1}{(m^2+n^2)^s} = \pi^s / \Gamma(s)\int_0^\infty y^s\left(\theta(iy)-1\right)\frac{dy}{4y},\ \theta(iy) = \sum_{m,n\in\mathbb{Z}} e^{-\pi(m^2+n^2)y},\ \theta(iy) = \frac{1}{y}\theta\left(\frac{i}{y}\right)$$

$$\pi^{-s}\Gamma(s)\zeta(s) = \int_1^\infty \left(y^s + y^{1-s}\right)\left(\theta(iy)-1\right)\frac{dy}{4y} + \frac{1}{4}\left(\frac{1}{s-1} - \frac{1}{s}\right) = \pi^{-(1-s)}\Gamma(1-s)\zeta(1-s)$$

Hecke L-functions

$$L(s,k) = \pi^{(s+|k|)} / \Gamma(s+|k|)\int_1^\infty \left(y^s + y^{1-s}\right)\theta_\chi(iy)\frac{dy}{4y},\ \theta_\chi(iy) = \frac{(-1)^{|k|}}{y}\theta_\chi\left(\frac{i}{y}\right)$$

$$\theta_\chi(iy) = \sum_{m,n\in\mathbb{Z}}(m+ni)^{2k}\,y^{|k|}e^{-\pi(m^2+n^2)y} = y^{|k|}\sum_{m=0}^\infty\sum_{n=0}^\infty \mathrm{Re}((m+ni)^{2k})e^{-\pi(m^2+n^2)y}$$

$$\pi^{-(s+|k|)}\Gamma(s+|k|)L(s,k) = \int_1^\infty \left(y^s + y^{1-s}\right)\theta_\chi(iy)\frac{dy}{4y} = (-1)^{|k|}\pi^{-((1-s)+|k|)}\Gamma((1-s)+|k|)L(1-s,k)$$

Modular forms and elliptic curves

$$f(q)=\sum_{n=1}^{\infty}a_n q^n=\sum_{n=1}^{\infty}a_n e^{2\pi inz}\in S_k(\Gamma_1(N),\ \text{By modularity}\ f\left(-\frac{1}{Nz}\right)=CN^{-k/2}(-Nz)^k f(z)$$

$$\int_0^{i\infty}f(z)z^s\frac{dz}{z}=\int_0^{i\infty}\sum_{n=1}^{\infty}a_n e^{2\pi inz}z^s\frac{dz}{z}=\int_0^{i\infty}\theta(z)z^s\frac{dz}{z}=\sum_{n=1}^{\infty}a_n\int_0^{i\infty}z^s e^{2\pi inz}\frac{dz}{z}$$

$$[\ \text{where}\ t=-2\pi inz,\ \phi(t)=e^{-2\pi t},\ \theta(z)=\sum_{n=1}^{\infty}a_n\phi(iz)\ ]$$

$$=\sum_{n=1}^{\infty}a_n\left(\frac{-1}{2\pi n}\right)^s\int_0^{\infty}e^{-t}t^s\frac{dt}{t}=(-2\pi i)^{-s}\Gamma(s)\sum_{n=1}^{\infty}\frac{a_n}{n^s}=(-2\pi i)^{-s}\Gamma(s)L(f,s)=(2\pi)^{-s}\Gamma(s)L(f,s)$$

$$\int_0^{i\infty}f(z)z^s\frac{dz}{z}=\int_0^{i/\sqrt{N}}f(z)z^s\frac{dz}{z}+\int_{i/\sqrt{N}}^{i\infty}f(z)z^s\frac{dz}{z}=\int_{i/\sqrt{N}}^{i\infty}\left(f(z)z^s+i^kCN^{-k/2}f(z)\left(-\frac{1}{Nz}\right)^{s-k}\right)\frac{dz}{z}$$

$$=\int_{1/\sqrt{N}}^{\infty}\left(i^s f(iy)y^s+i^kCN^{-k/2}f(iy)\left(-\frac{1}{Niy}\right)^{s-k}\right)\frac{dy}{y}=\int_{1/\sqrt{N}}^{\infty}\left(i^s y^s+i^kCN^{-k/2}i^{s-k}N^{k-s}y^{k-s}\right)f(iy)\frac{dy}{y}$$

$$=i^s\int_{1/\sqrt{N}}^{\infty}\left(y^s+CN^{k/2-s}y^{k-s}\right)f(iy)\frac{dy}{y}=i^s\int_{1/\sqrt{N}}^{\infty}\left(y^s+CN^{k/2-s}y^{k-s}\right)\sum_{n=1}^{\infty}a_n e^{-2\pi ny}\frac{dy}{y}$$

$$L(f,s)=(2\pi)^s/\Gamma(s)\int_{1/\sqrt{N}}^{\infty}\left(y^s+CN^{k/2-s}y^{k-s}\right)\sum_{n=1}^{\infty}a_n e^{-2\pi ny}\frac{dy}{y}$$

$$\Lambda(f,s)=N^{s/2}(2\pi)^{-s}\Gamma(s)L(f,s),\ \Lambda(f,s)=i^k w\Lambda(f,k-s),\ w=\pm1$$

Research Connected with the Dark Heart Package

1. **Exploding the Dark Heart of Chaos** http://dhushara.com/DarkHeart/DarkHeart.htm *An exploration of the universality of the cardioid at the centre of the Mandelbrot set extended to the diversity of complex analytic functions with Mac XCode applications and Quicktime movies illustrating each example.*
2. **Fractal Geography of the Zeta Function** http://dhushara.com/DarkHeart/geozeta/zetageo.htm *The quadratic Mandelbrot set has been referred to as the most complex and beautiful object in mathematics and the Riemann Zeta function takes the prize for the most complicated and enigmatic function. Here we elucidate the spectrum of Mandelbrot and Julia sets of Zeta, to unearth the geography of its chaotic and fractal diversities, combining these two extremes into one intrepid journey into the deepest abyss of complex function space.*
3. **Experimental Observations on the Riemann Hypothesis and the Collatz Conjecture** http://dhushara.com/DarkHeart/RH2/RH.htm *This paper seeks to explore whether the Riemann hypothesis falls into a class of putatively unprovable mathematical conjectures, which arise as a result of unpredictable irregularity and to provide an experimental basis to discover some of the mathematical enigmas surrounding these conjectures.*
4. **A Dynamical Key to the Riemann Hypothesis** http://dhushara.com/DarkHeart/key/key2.htm *This sets out a dynamical basis for the non-trivial zeros of the Riemann zeta function being on the critical line x = 1/2. It does not prove the Riemann Hypothesis (RH), but it does give a dynamical explanation for why zeta and the Dirichlet L-functions do have their non-trivial zeros on the critical line and why other closely related functions do not. It suggests RH is an additional unprovable postulate of the number system, similar to the axiom of choice, associated with the limiting behavior of the primes as* $n \to \infty$.
5. **The Physics and Computational Exploration of Zeta and L-functions** http://dhushara.com/DarkHeart/dynamical/dynamical.htm *This article presents a spectrum of 4-D global portraits of a diversity of zeta and L-functions, using currently devised numerical methods and explores the implications of these functions in enriching the understanding of diverse areas in physics, from thermodynamics, and phase transitions, through quantum chaos to cosmology. The Riemann hypothesis is explored from both sides of the divide, comparing cases where the hypothesis remains unproven, such as the Riemann zeta function, with cases where it has been proven true, such as Selberg zeta functions.*

Research References

1. Aspenberg M, Yampolsky M (2009) Mating Non-Renormalizable Quadratic Polynomials Commun. Math. Phys. 287 1-

40 toi:10.1007/s00220-008-0598-y
2. Boyd Suzanne, Henriksen Christian (2012) The Medusa Algorithm For Polynomial Matings Conformal Geometry And Dynamics 16, 161–183 arXiv:1102.5047. http://www.math.cornell.edu/~dynamics/Matings/
3. Brown D, Halstead M (2007) Super-attracting cycles for the cosine-root family Chaos, Solitons and Fractals 31 1191-1202.
4. Buff X, Henriksen C (2001) Julia Sets in Parameter Spaces Communications in Mathematical Physics https://www.math.univ-toulouse.fr/~buff/Preprints/JuliaCubic/Copies.pdf .
5. Devaney R et al. (2013) Sierpinski curve Julia sets for quadratic rational maps arXiv: 1109.0368.
6. Devaney R et al. (2015) Generalized Baby Mandelbrot Sets Adorned with Halos in Families of Rational Maps https://pdfs.semanticscholar.org/6b13/a9d293f20dd01ef29fc96426be7f1a71c62b.pdf
7. Douady A Hubbard J (1985) On the dynamics of polynomial-like mappings Annales scientifiques de l'ENS 18/2 287-343.
8. Durkin M. (1998) Observations on the dynamics of the complex cosine-root family J. Differenc Equat Appl 4 215-28.
9. Epstein A., Yampolsky, M. (1996) Geometry of the Cubic Connectedness Locus I: Intertwining Surgery arXivMath/9608213v1
10. Jung Wolf (2014) Mandel http://mndynamics.com/indexp.html
11. Lei T (1992) Matings of quadratic polynomials Ergod. Th. & Dynam. Sys. 12 589-620.
12. Milnor J (1993) Geometry and Dynamics of Quadratic Rational Maps Expr. Math. 2/1 37-83.
13. Milnor J (1992) Remarks on Iterated Cubic Maps Expr. Math. 1/1 5-24.
14. Pérez-Marco R (1997) Fixed points and circle maps Acta Mathematica 179/2 243-294.
15. Riemann B (1859) On the Number of Prime Numbers less than a Given Quantity. http://www.maths.tcd.ie/pub/HistMath/People/Riemann/Zeta/EZeta.pdf
16. Romera M et al. (2004) External arguments of Douady cauliflowers in the Mandelbrot set Computers & Graphics 28/3 437-449.
17. Romera M, Pastor G, Alvarez G, Montoya F (2006) External arguments in the multiple-spiral medallions of the Mandelbrot set Computers & Graphics 30 460-469.
18. Schleicher D. Zakeri S.(2000) "On biaccessible points in the Julia set of a Cremer quadratic polynomial." Proc. AMS 128/3 933-937.
19. Siegel C (1942) Iterations of analytic functions Ann. Math. 43 607-612.
20. Shishikura M (1991) The Hausdorff Dimension Of The Boundary Of The Mandelbrot Set And Julia Sets Annals of Mathematics 147/2 225-267 arXiv:math/9201282.
21. Shishikura M (2014) Dynamical charts for irrationally indifferent fixed points of holomorphic functions http://math.bu.edu/keio2014/talks/Shishikura.pdf.
22. Woon S (1998) Fractals of the Julia and Mandelbrot sets of the Riemann Zeta Function arXiv:chao-dyn/9812031v1

Three Sample Dark Heart & Riemann Zeta C-script Movie Files

Movie frames are generated as tiff images, which can be turned into Quicktime movies with Quicktime Player pro 7's "open image sequence" option, or loading them collectively as files using Mpeg Stream clip, which is included with the package. If terminal doesn't recognize the gcc command, open an Apple Developer account (free) and install Mac OSX Command Line Tools for your system from https://developer.apple.com/download/more.

You need to make sure the correct parameters are put in the script. You can easily save a confirguration and look at the text file to check against the file structure. For example note that some variables are multiplexed specs[8] in Dark Heart and [24] and [25] in Riemann Zeta. For extreme floating point values, replace the fprintf("%f") command by "%e" to get scientific precision.

```
//generates a movie of a Julia journey around the Mandelbrot set of z^d+c using DHViewer
//save as djulia.c
//To run this file from terminal put it in a folder, cd to the folder and input
//gcc -o djuliao djulia.c -lm && ./djuliao   To run successive compiled versions type ./djuliao

#include <stdio.h>
#include <math.h>
#import <complex.h>
double pi=3.14159;
int frames = 41; //number of movie frames - normally use 500-1000!
const char base[] = "Params";

void WriteParamFile(int frameno, double param1, double param2, double param3);

int main(void)
{
FILE *mf;
char filename [ FILENAME_MAX ];
int filetyp = 3;
int k;
double d=6; //degree d of x^d+c
double astt = 0; //angle position
```

```
double aend = 2*(d-1)*pi;
double apos,xpos,ypos;
double _Complex zpos;
sprintf(filename, "%s.txt", base);
mf=fopen(filename,"w");
fprintf(mf,"%f %f \n",(float)filetyp, (float)frames);
fclose(mf);
for(k=0;k<frames;k++)
        {
        apos=astt+(aend-astt)*k/(frames-1);
        zpos=1.01*pow(d,-d/(d-1))*(d*cexp(I*apos/(d-1))-cexp(d*I*apos/(d-1)));
        xpos=creal(zpos);
        ypos=cimag(zpos);
        WriteParamFile(k, xpos, ypos, (double)d);
        }
return 0;
}

void WriteParamFile(int frameno, double param1, double param2, double param3)
{
FILE *mf;
char filename [ FILENAME_MAX ];
int j;

double specs[37];
double mandel=0;
double scale=3.5;
double screenX=0;
double screenY=0;
double cx=param1;
double cy=param2;
double thisfn=1;
double escType=0;
double orbitTrapE=0;
double escapeOnly=0;
double colorScheme=4;
double escapeBoundExp=1.666667;
double attractorEscBd=-4;
double maxIterations=1024;
double kx=param3;
double ky=0;
double oldfn=thisfn;

specs[0]=mandel;
specs[1]=scale;
specs[2]=screenX;
specs[3]=screenY;
specs[4]=cx;
specs[5]=cy;
specs[6]=thisfn;
specs[7]=escType; // abs, real, or imag
specs[8]=orbitTrapE; //orbit trap + 2*dF
specs[9]=escapeOnly;
specs[10]=colorScheme;
specs[11]=escapeBoundExp; //escape bound exponent
specs[12]=attractorEscBd; //attractor escape bound 10^-k
specs[13]=maxIterations; //iterations
specs[14]=kx; //real k
specs[15]=ky; //imag k
specs[16]=oldfn;
specs[17]=987.654321;

sprintf(filename, "%s%d.txt", base, frameno);
//printf("filename = \"%s\"\n", filename);
mf=fopen(filename,"w");
for (j=0;j<37;j++)
    fprintf(mf,"%f ",specs[j]);
fclose(mf);
}

//generates a movie of separation of mandelbrot sets of (z^4-p)(z+c) using DHViewer
//save as quintic.c
//To run this file from terminal put it in a folder, cd to the folder and input
//gcc -o quintico quintic.c -lm && ./quintico    To run successive compiled versions type ./quintico
```

```
#include <stdio.h>

double pi=3.14159;
int frames = 121; //number of movie frames - normally use 500-1000!
const char base[] = "Params";

void WriteParamFile(int frameno, double param1, double param2);

int main(void)
{
FILE *mf;
char filename [ FILENAME_MAX ];
int filetyp = 3;
int k;
double xstt = 0;
double xend = 3;
double xpos;
double ypos = 0;
sprintf(filename, "%s.txt", base);
mf=fopen(filename,"w");
fprintf(mf,"%f %f \n",(float)filetyp, (float)frames);
fclose(mf);
xpos=xstt;
for(k=0;k<frames;k++)
        {
        xpos=xstt+(xend-xstt)*k/(frames-1);
        WriteParamFile(k, (double)xpos, (double)ypos);
        }
return 0;
}

void WriteParamFile(int frameno, double param1, double param2)
{
FILE *mf;
char filename [ FILENAME_MAX ];
int j;

double specs[37];
double mandel=1;
double scale=10;
double screenX=0;
double screenY=0;
double cx=0;
double cy=0;
double thisfn=22;
double escType=0;
double orbitTrapE=0;  // orbittrap + 2*dF
double escapeOnly=1;
double colorScheme=0;
double escapeBoundExp=1.666667;
double attractorEscBd=-4;
double maxIterations=128;
double kx=4;
double ky=0;
double oldfn=thisfn;

specs[0]=mandel;
specs[1]=scale;
specs[2]=screenX;
specs[3]=screenY;
specs[4]=cx;
specs[5]=cy;
specs[6]=thisfn;
specs[7]=escType; // abs, real, or imag
specs[8]=orbitTrapE; //orbit trap and dF
specs[9]=escapeOnly;
specs[10]=colorScheme;
specs[11]=escapeBoundExp; //escape bound exponent
specs[12]=attractorEscBd; //attractor escape bound 10^-k
specs[13]=maxIterations; //iterations
specs[14]=kx; //real k
specs[15]=ky; //imag k
specs[16]=oldfn;
specs[17]=987.654321;
specs[18]=1;
```

```
specs[20]=1;
specs[26]=-param1; // function parameters in quintic equation
specs[28]=-param1;
specs[31]=1;
specs[35]=1;
specs[36]=0;

sprintf(filename, "%s%d.txt", base, frameno);
//printf("filename = \"%s\"\n", filename);
mf=fopen(filename,"w");
for (j=0;j<37;j++)
   fprintf(mf,"%f ",specs[j]);
fclose(mf);
}
```

A Sample Riemann Zeta Movie Script

```
//Generates a movie parameter file set of zeta Julia sets from c=-20 to c=2 using RZViewer to be run with RZViewer
//To run this file from Mac Terminal put it in a folder, cd to the folder and input
//gcc -o rzmovieo rzjulia.c -lm && ./rzmovieo  To run successive compiled versions type ./rzmovieo

#include <stdio.h>
#include<complex.h>
const double pi=3.1415926535;
const int frames = 5; //number of movie frames - normally use 500-1000!
const int spcno = 29;
const char base[] = "Params";

void WriteParamFile(int frameno, double param);

int main(void)
{
FILE *mf;
char filename [ FILENAME_MAX ];
int filetyp = 3;
int k;
double xstt =-20;
double xend = 2;
double xpos;
sprintf(filename, "%s.txt", base);
mf=fopen(filename,"w");
fprintf(mf,"%f %f \n",(float)filetyp, (float)frames);
fclose(mf);
xpos=xstt;
for(k=0;k<frames;k++)
        {
        if(k==0)
                xpos=xstt;
        else
                xpos=xstt+(xend-xstt)*k/(frames-1);
        WriteParamFile(k, (double)xpos);
        }
return 0;
}

void WriteParamFile(int frameno, double param)
{
FILE *mf;
char filename [ FILENAME_MAX ];
int j;

double specs[spcno];
double mandel=0;
double scale=80;
double screenX=0;
double screenY=0;
double cx=param;
double cy=0;
double altgamma=0;
double thisfn=1;
double split=1;
double orbitTrapE=0;
double addc=1;
double escapeonly=0;
double zetaterms=100;
```

```
double colsch=0;
double escapeboundExp=1.666667;
double attractorEscBd=-2;
double maxIterations=64;
double dolog=0;
double sang=1;
double domoib=0;
double cval=0;
double oldfn=thisfn;
double realk=0;
double imagk=0;
double crval=0;
double fullt=0;
double xm=1;
double xn=1;
double flip=0;

specs[0]=mandel;
specs[1]=scale;
specs[2]=screenX;
specs[3]=screenY;
specs[4]=cx;
specs[5]=cy;
specs[6]=altgamma;
specs[7]=thisfn;
specs[8]=split;
specs[9]=orbitTrapE; //orbit trap epsilon
specs[10]=addc; //additive c/ mult c
specs[11]=escapeonly;
specs[12]=colsch;
specs[13]=escapeboundExp; //escape bound exponent
specs[14]=zetaterms;
specs[15]=attractorEscBd; //attractor escape bound 10^-k
specs[16]=maxIterations; //iterations
specs[17]=dolog; //take log of the function
specs[18]=sang; //angle ploting
specs[19]=domoib; //mobius
specs[20]=cval;
specs[21]=oldfn;
specs[22]=realk;
specs[23]=imagk;
specs[24]=crval; // crval+2*Xi
specs[25]=fullt; // full terms+2*dZ+4*Mellin crval+2*Xi
specs[26]=xm;
specs[27]=xn;
specs[28]=flip;

sprintf(filename, "%s%d.txt", base, frameno);
//printf("filename = \"%s\"\n", filename);
mf=fopen(filename,"w");
for (j=0;j<spcno;j++)
    fprintf(mf,"%f ",specs[j]);
fclose(mf);
}
```